ENHANCED RADIATION FROM E. M. SOURCES SURROUNDED BY AN AXIALLY MAGNETIZED PLASMA COLUMN

A Thesis

Submitted in partial fulfilment
of the requirements for the degree of
DOCTOR OF PHILOSOPHY
IN THE FACULTY OF SCIENCE

by

NARENDRA KUMAR JOSHI

DEPARTMENT OF PHYSICS

BIRLA INSTITUTE OF TECHNOLOGY AND SCIENCE

PILANI-RAJASTHAN-INDIA

February, 1974.

TO MY PARENTS

BIRLA INSTITUTE OF TECHNOLOGY AND SCIENCE
PILANI (RAJASTHAN) INDIA

CERTIFICATE

The study and work on 'ENHANCED RADIATION FROM E. M. SOURCES SURROUNDED BY AN AXIALLY MAGNETIZED PLASMA COLUMN', carried out and presented herein, by Mr. Narendra Kumar Joshi, embodies original investigations, and was carried out under my supervision and guidance during the period December, 1970 to February 1974. It is recommended that the thesis be accepted for the award of the degree of Doctor of Philosophy in the Department of Physics, Faculty of Science, Birla Institute of Technology and Science, Pilani (Rajasthan).

(J. S. Verma)
Associate Professor,
Head, Deptt. of Physics.

ACKNOWLEDGEMENTS

It gives me great pleasure to place on record my heartfelt thanks to Dr. J. S. Verma, Professor and Head, Dept. of Physics, B.I.T.S., Pilani (Rajasthan), for his able and inspiring guidance during the entire course of this work.

I wish to express my thanks to Dr. Dhani Ram, Post Doctoral Research Fellow, B.I.T.S., Pilani and Dr. K.C. Gupta, Assistant Professor, Dept. of Electrical Engineering, I.I.T., Kanpur, for several useful discussions during the course of study.

Thanks are also due to Dept. of Information Processing Center, Pilani for providing computational facilities. Assistance of Mr. A. P. Mathur, Dr. Praveen Dhyani and Mr. S. S. Negi in running computer programmes is gratefully acknowledged.

I would like to express my thanks to my friends Dr. V. Sharma, Mr. B. K. Kaushik, Mr. Chandra Shekhar, Mr. D. C. Tiwari, Mr. P. K. Banerjee, Mr. D. C. Kashayap, Mr. M. C. Gupta and Mr. G. R. Rao for their whole hearted cooperation and timely help.

I thank Mr. [illegible]. K. Sinha for typing the manuscript and Mr. S. D. Dewan for drawing work.

I express my gratitude to my parents, wife Vidya and other members of my family for their forbearance and confidence in me.

I am thankful to the Director, B.I.T.S. and the Dean, Faculty of Science for providing available facilities during this research work. I wish to express my gratitude to U.G.C. for awarding Junior Research Fellowship for the period of three years.

(N. K. Joshi)

✓

TABLE OF CONTENTS

Certificate ii

Acknowledgements iii

List of Figures viii

List of Symbols xiv

Chapter I. INTRODUCTION I

Chapter 2. EXCITATION OF AXIALLY MAGNETIZED PLASMA COLUMN BY A MAGNETIC RING SOURCE.

2.I Introduction IO

2.2 Analysis II

2.3 Characteristics of the radiation field I4

2.4 Conclusions 24

Chapter 3. EXCITATION OF AXIALLY MAGNETIZED PLASMA COLUMN HAVING CENTRAL CONDUCTOR ALONG ITS AXIS

3.I Excitation by magnetic ring source 28

3.2 Excitation by open ended coaxial line 5I

Chapter 4. EXCITATION OF ANNULAR AXIALLY MAGNETIZED PLASMA COLUMN SURROUNDING AN AIR CORE HAVING CENTRAL CONDUCTOR

4.I Excitation by magnetic ring source 74

4.2 Excitation by open ended coaxial line I04

Chapter 5. RADIATION FIELD OF A MAGNETIC RING SOURCE SURROUNDED BY INHOMOGENEOUS ANISOTROPIC PLASMA COLUMN

5.I Introduction I3I

5.2 Radiation field in case of axially magnetized inhomogeneous plasma column. I33

5.3 Radiation field in case of axially magnetized inhomogeneous plasma column having central conductor along its axis I40

5.4 Radiation field in case of an air core having central conductor and surrounded by annular axially magnetized inhomogeneous plasma column I47

5.5 Conclusion I55

Chapter 6. SUMMARY, CONCLUDING REMARKS AND SUGGESTIONS FOR FURTHER WORK

6.1 Summary 158
6.2 Concluding remarks 163
6.3 Suggestions for further work 165

Appendices

Appendix A Analysis of the axially magnetized plasma column 169

Appendix B Analysis of the axially magnetized plasma column having central conductor 178

Appendix C Analysis of an air core having central conductor and surrounded by annular axially magnetized plasma column 181

Appendix D Saddle point integration method 184

List of References 190

List of Publications 197

***

LIST OF FIGURES

Fig. 2.I Geometry of configuration analysed.

Fig. 2.2 Radiation patterns with $w/w_p = 1.06$ (high density plasma) for different values of w_c/w_p ($w_c/w_p = 0.1, 0.2, 0.3, 0$).

Fig. 2.3 Radiation pattern with $w/w_p = 1.06$ (high density plasma) for the value of $w_c/w_p = 0.5$.

Fig. 2.4 Radiation patterns with $w/w_p = 1.06$ (high density plasma) for the different values of w_c/w_p ($w_c/w_p = 2.0, 5.0, \infty$).

Fig. 2.5 Radiation patterns with $w/w_p = 3.3$ (low density plasma) for the different values of w_c/w_p ($w_c/w_p = 2.5, 3.2, 4.0$).

Fig. 2.6 Variation of peak amplitude with $k_o a$.

Fig. 3.I Geometry of configuration analysed.

Fig. 3.2 Radiation patterns with $w/w_p = 1.06$ (high density plasma) for different values of w_c/w_p ($w_c/w_p = 0.1, 0.3$).

Fig. 3.3 Radiation patterns with w/w_p = 3.3 (low density plasma) for different values of w_c/w_p (w_c/w_p = 0.9, 2.5).

Fig. 3.4 Detailed structure of radiation peaks.

Fig. 3.5 Radiation patterns with w/w_p = I.06 (high density plasma) for different values of w_c/w_p (w_c/w_p = 0.5, 5.0).

Fig. 3.6 Radiation pattern with w/w_p = I.06 and $w_c/w_p = \infty$ (i.e. ϵ_I = I, uniaxial plasma column).

Fig. 3.7 Radiation patterns with w/w_p = 3.3 (low density plasma) for different values of w_c/w_p (w_c/w_p = 3.2, 4.0).

Fig. 3.8 Radiation pattern with w/w_p = 3.3 and $w_c/w_p = \infty$ (i.e. ϵ_I = I, uniaxial plasma column).

Fig. 3.9 Variation of peak amplitude with $k_o a$.

Fig. 3.10 Geometry of configuration analysed.

Fig. 3.II Radiation patterns with w/w_p = I.06 (high density plasma) for different values of w_c/w_p (w_c/w_p = 0.I, 0.3).

Fig.3.12 Radiation patterns with $w/w_p = 3.3$ (low density plasma) for different values of w_c/w_p ($w_c/w_p = 0.9,\ 2.5$).

Fig.3.13 Detailed structure of radiation peaks.

Fig.3.14 Radiation patterns with $w/w_p = I.06$ (high density plasma) for different values of w_c/w_p ($w_c/w_p = 0.5,\ 5.0$).

Fig.3.15 Radiation pattern with $w/w_p = I.06$ and $w_c/w_p = \infty$ (i.e. $\epsilon_I = I$, uniaxial plasma column).

Fig.3.16 Radiation patterns with $w/w_p = 3.3$(low density plasma) for different values of w_c/w_p ($w_c/w_p = 3.2,\ 4.0$).

Fig.3.17 Radiation pattern with $w/w_p = 3.3$ and $w_c/w_p = \infty$ (i.e. $\epsilon_I = I$, uniaxial plasma column).

Fig.3.18 Variation of peak amplitude with $k_o a_3$.

Fig.4.I Geometry of configuration analysed.

Fig.4.2a Radiation patterns with $w/w_p = I.06$ (high density plasma) for different values of w_c/w_p ($w_c/w_p = 0.I,\ 0.3$).

Fig.4.2b Detailed structure of radiation peaks .

Fig.4.2c Detailed structure of radiations peaks.

Fig.4.3a Variation of denominator of $F(\theta)$ with θ.

Fig.4.3b Variation of denominator of $F(\theta)$ with θ.

Fig.4.4 Radiation patterns with w/w_p = I.06 (high density plasma) for different values of w_c/w_p (w_c/w_p = 0.5, 5.0).

Fig.4.5 Radiation pattern with w/w_p = I.06 and $w_c/w_p = \infty$ (i.e. $\epsilon_I = I$, uniaxial plasma column).

Fig.4.6 Radiation patterns with w/w_p = 3.3 (low density plasma) for different values of w_c/w_p (w_c/w_p = 0.9, 2.5).

Fig.4.7 Radiation patterns with w/w_p = 3.3 (low density plasma) for different values of w_c/w_p (w_c/w_p = 3.2, 4.0).

Fig.4.8 Radiation pattern with w/w_p = 3.3 and $w_c/w_p = \infty$ (i.e. $\epsilon_I = I$, uniaxial plasma column).

Fig.4.9 Variation of peak amplitude with $k_o b$.

Fig.4.I0 Variation of peak amplitude with $k_o a$.

Fig.4.II Geometry of configuration analysed.

Fig.4.I2a Radiation patterns with w/w_p = I.06 (high density plasma) for different values of w_c/w_p (w_c/w_p = 0.I, 0.3).

Fig.4.I2b Detailed structure of radiation peaks.

Fig.4.I3a Variation of denominator of F(θ) with θ.

Fig.4.I3b Variation of denominator of A(θ) with θ.

Fig.4.I4 Radiation patterns with w/w_p = I.06 (high density plasma) for different values of w_c/w_p (w_c/w_p = 0.5, 5.0).

Fig.4.I5 Radiation patterns with w/w_p = I.06 and w_c/w_p = ∞ (i.e. ϵ_I = I, uniaxial plasma column).

Fig.4.I6 Radiation patterns with w/w_p = 3.3 (low density plasma) for different values of w_c/w_p (w_c/w_p = 0.9, 2.5).

Fig.4.I7 Radiation patterns with w/w_p = 3.3 (low density plasma) for different values of w_c/w_p (w_c/w_p = 3.2, 4.0).

Fig.4.I8 Radiation pattern with w/w_p = 3.3 and $w_c/w_p = \infty$ (i.e. ε_I= I, uniaxial plasma column).

Fig.4.I9 Variation of peak amplitude with $k_o b$.

Fig.4.20 Variation of peak amplitude with $k_o a_3$.

Fig.5.I Geometry of configuration analysed.

Fig.5.2 Geometry of configuration analysed.

Fig.5.3 Geometry of configuration analysed.

Fig.D.I ξ - plane representation.

Fig.D.2 β-plane representation.

***

LIST OF SYMBOLS

a - radius of the ring source

a_I - radius of the central conductor or the outer radius of the inner conducor of open ended coaxial line.

a_2 - inner radius of the annular plasma column.

a_3 - inner radius of the outer conductor of open ended coaxial line.

b - radius of the plasma column or outer radius of the annular plasma column.

I - For numeral one.

w - source frequency in radians

w_p - electron plasma frequency in radians.

w_c - electron cyclotron frequency in radians.

$\tilde{\epsilon}$ - permittivity tensor of the cold, anisotropic plasma medium.

$\epsilon_I, \epsilon_2, \epsilon_3$ - transverse, cross and longitudinal component of $\tilde{\epsilon}$.

$\tilde{\varepsilon}(\rho)$ - permittivity tensor of the cold, inhomogeneous and anisotropic plasma medium.

$\varepsilon_I(\rho), \varepsilon_2(\rho), \varepsilon_3(\rho)$ - transverse, cross and longitudinal component of $\tilde{\varepsilon}(\rho)$.

n_e - free electron density.

$n(\rho)$ - free electron density of radially inhomogeneous plasma column.

m_e - mass of the electron

ε_0, μ_0 - free space permittivity and permeability.

ε_a - permittivity of the air.

k_0 - propagation constant in free space.

$J_I(\ ), J_0(\ )$ - Bessel's functions of first kind and of first and zeroth order respectively.

$Y_I(\ ), Y_0(\ )$ - Bessel's functions of second kind and of first and zeroth order respectively.

$H_I(), H_0()$ - Hankel's functions of first kind and of first and zeroth order respectively.

H_ϕ - the ϕ - component of the magnetic field.

$F(\theta)$	- a function of θ describing radiation field distribution.
HPBW	- half power beam width.
equ.	- equation
chap.	- chapter.
*	- sign of multiplication.

...

CHAPTER I

INTRODUCTION

CHAPTER I.

INTRODUCTION:

A popular cliche is that more than 99.9% of the matter in our universe exists in the plasma state. This is not surprising if one looks at the amount of plasma in the geophysical and astrophysical environment. The word plasma as used here denotes an assembly of charged particles in which the time average charge density is zero. An ionized and neutral stationary plasma in a weak electromagnetic field can be represented as an equivalent dielectric medium. However, in presence of a static magnetic field, the plasma becomes anisotropic so that its equivalent dielec-tric 'constant' behaves as a 'tensor'.

The study of e.m. wave propagation through an anisotropic plasma medium is of considerable interest due to its relevance to space exploration, re-entry physics, plasma diagonostics, radio astronomy and ionospheric physics. Ionospheric anisotropy is due to the presence of earth's magnetic field.

The 'black-out' suffered by the space vehicle while it re-enters the earth's atmosphere , the transmission and reception of radio waves by aerials carried on rockets or satellites and wave guide like properties of ionosphere have focussed attention on the problems associated with the existence of a localized source immersed in an anisotropic plasma medium. Pattern distortion due to an anisotropic plasma sheath surrounding an antenna has been studied by many workers[1-6]. The presence of multiple narrow radiation peaks in the computation of the radiation pattern of an antenna on models of re-entry vehicles[7-8], excitation of leaky waves on anisotropic plasma geometry[9], and emergence of radiation peaks from cylindrical plasma geometries [-12] excited by a magnetic ring source have motivated the research work reported here.

The radiation characteristics of e.m. sources surrounded by anisotropic plasma medium have received considerable attention in the literature[13-16]. The reviews and bibliographies for sources in plasma have been reported by Felsen[17], Bachyanski[18] and Wait and Brackett[19]. Various plasma geometries for the study of radiation field have been analysed.

Newstin and Lurye[20] have dealt with the radiation field of an isotropic plasma slab of finite thickness , they have however disregarded the presence and significance of both surface and complex waves. Tamir and Oliner[21] have calculated the radiation field of an isotropic plasma slab excited by a line source via a steepest descent method and then have shown that geometrical optical considerations involving the critical angle agrees with this result. Then he has shown that near field is given mainly by contribution from complex waves, and calculated radiation field by means of a Kirchhoff - Huygen's integration along the plasma air interface assuming the presence of this near field only. The pattern calculated by both methods are in agreement with each other. In the transparent region ($w > w_p$), both these methods predict the presence of radiation peaks before the critical angle. Harris[22] studied the radiation patterns of an infinite magnetic line source in air gap between the ground plane and plasma slab and predicted the presence of well enhanced and sharp narrow radiation peaks beyond the critical angle.

Magnetized plasma slabs have been analysed by Wait[23] and by Meltz and Shore[5]. Wait[23] has analysed an extremely thin plasma slab with a major emphasis on the radiation field. Meltz and Shore[5] have shown that leaky waves are supported by uniaxial plasma layers and obtained radiation peaks.

Radiation from axially magnetized plasma[24-25] column having an electric dipole along and perpendicular to the axis for symmetric and dipolar mode have been studied. Gupta and Singh[26-27] have studied the guided wave field and radiation field of a magnetic ring source placed outside the plasma column (isotropic plasma column, axially magnetized plasma column). Samaddar and Yildiz[28] have studied the coupled electroacoustic waves on an isotropic plasma column excited by a ring source of electromagnetic waves. But these studies are concerned mostly with surface waves.

Samaddar[29] has also studied the wave propagation along an anisotropic column surrounded by a metallic wave guide with a ring source placed outside the anisotropic column. In this analysis, the dyadic Green's function for a point source is constructed in a formal way from the source- free solution of the appropriate Maxwell's equations. In this configuration the plasma column is surrounded by a metallic waveguide and there is no space wave radiating out. This method cannot be conveniently applied for the case of open plasma columns, in which case a part of the electromagnetic power goes into the radiation fields.

Gupta[9] has studied the radiation pattern of a magnetic ring source in plasma column and predicted the presence of radiation peaks. Dhani Ram and Verma[11] studied the radiation pattern of a magnetic ring source in a plasma column having central conductor along its axis and predicted the presence of radiation peaks near or before the critical angle. They[12] also studied the radiation patterns of a magnetic ring source in an air core having central conductor and surrounded by an annular plasma column and shown that sharp radiation peaks are obtained beyond the critical angle.

The work reported by these authors show that radiation peaks are obtained from various cylindrical plasma geometries excited by a magnetic ring source. The direction of these peaks can be changed by changing the plasma density. Number of radiation peaks can be controlled by suitably adjusting the parametric values of the configurations. Based upon these results they have suggested to develop an electronically scannable narrow beam plasma antenna system. In all these geometries, plasma has been considered to be an isotropic, lossless, incompressible and homogeneous medium characterized by a relative permittivity given by $\epsilon_p = 1 - (w_p^2/w^2)$, where w_p is the plasma frequency and w is the operating frequency.

In this thesis, three plasma geometries [(i) axially magnetized plasma column (ii) axially magnetized plasma column with central conductor (iii) an air core having a central conductor and surrounded by an annular axially magnetized plasma column] excited by circular symmetric e.m. source or sources have been analysed. Enhanced radiation peaks are obtained in all the cases. The radiation patterns for the case of uniaxial plasma (i.e. infinite magnetic field) have also been studied. The plasma here is anisotropic dielectric medium by virtue of an impressed magneto-static field in the axial direction and its permittivity is given by the permittivity tensor. Thermal effects and losses are neglected and the plasma density is assumed to be uniform over the cross-section of the column.

In chapter 2, the radiation patterns of a magnetic ring source surrounded by an axially magnetised plasma column have been studied. The radiation patterns with a radiation peak or radiation peaks are obtained. The direction and number of radiation peaks depend upon the value of applied magnetic field, plasma column diameter and plasma density. The direction of radiation peak can be scanned by varying the plasma density as well as the magnetic field and thus increases the range of angles through which beam can be scanned as compared to the isotropic plasma column.

In chapter 3, the radiation patterns of a magnetic ring source in an axially magnetised plasma column having central conductor along its axis have been discussed. Due to the presence of central conductor, it has been found that more enhanced radiation peaks are obtained than in the previously analysed geometry. The applied magnetic field here also does an additional scanning function. The case of more practically feasible source of electromagnetic wave such as an open ended co-axial line excited in TEM mode have also been discussed.

Chapter 4 is concerned with the radiation patterns of a magnetic ring source in an air core having central conductor and surrounded by an axially magnetized annular plasma column. This geometry gives the most enhanced radiation peaks with a very small value of half power beam width. The applied magnetic field increases the range of scanning angle. The radiation patterns for an open ended coaxial line excited in TEM mode have also been studied. In this case, the main radiation peak is obtained in the end fire direction.

In chapter 5, the radiation fields of a magnetic ring source in the three geometries described above considering the plasma column to be inhomogeneous have been obtained. The method of analysis involves the technique of the Fourier- Transform and contour integration for solution of the inhomogeneous wave equation. It has been assumed that the free electron density within the plasma cylinder is inhomogeneous in the radial direction and the density profile is parabolic.

Finally, chapter 6 summarises and discusses results presented here and proposes areas for the further work.

***

CHAPTER 2.

EXCITATION OF AXIALLY MAGNETIZED PLASMA COLUMN BY A MAGNETIC RING SOURCE

2.I Introduction IO

2.2 Analysis II

2.3 Characteristics of the radiation field I4

2.4 Conclusions 24

CHAPTER 2.

EXCITATION OF AXIALLY MAGNETIZED PLASMA COLUMN BY A MAGNETIC RING SOURCE:

2.I INTRODUCTION:

The radiation field of a ring of electromagnetic waves placed inside a cylindrical isotropic plasma column has been studied[9-10]. It has been found that radiation patterns possess one or more sharply peaked beams. The direction of these beams could be varied by varying the plasma density and column diameter. In this chapter, it is shown that a system consisting of a magnetic ring source surrounded by an axially magnetized plasma column may give rise to a radiation pattern with single or multiple beams. Here the direc-tion of beam can be scanned by varying the plasma density, column diameter and magnetic field. Since this geometry has one more scanning function (i.e. magnetic field) the beam can be scanned over a considerably wider range of angles. For very high magnetic fields the peak shifts towards the end fire direction.

In the analysis carried out, the plasma is considered to be a lossless and anisotropic dielectric medium with the permittivity given by the permittivity tensor. Thermal effects are neglected and the plasma density is considered to be uniform over the cross-section of the column. The existence of a circular symmetric E-mode is assumed. It has been shown[30] that the E-mode can be considered to exist independently when the operating frequency is away from the cyclotron frequency. The inhomogeneous wave equations are solved by the method of Fourier Transform. This yields the solution for the field in the form of a definite integral. The radiation field is obtained from the asymptotic evaluation of the integral by saddle point integration. The method of saddle point integration is given in Appendix D.

2.2 ANALYSIS:

The geometry of the configuration analysed is illustrated in fig. 2.1. An infinitely long column of plasma, radius 'b' is oriented with its axis along the z-axis of the cylindrical coordinate system (ρ, ϕ , z). The medium surrounding the plasma column and extending to infinity is free space, with permittivity and permeability ϵ_0 and μ_0. The source of electromagnetic radiation is a ring of magnetic current of radius 'a' (a < b), concentric with the plasma column and situated in the z = 0 plane. The source field distribution is mathematically represented by

$$\bar{K} = \bar{\phi}\, \delta (\rho - a) \, \delta (z) \qquad (2.1)$$

where δ represents Kronecker's delta function and $\bar{\phi}$ is a unit vector in the ϕ - direction.

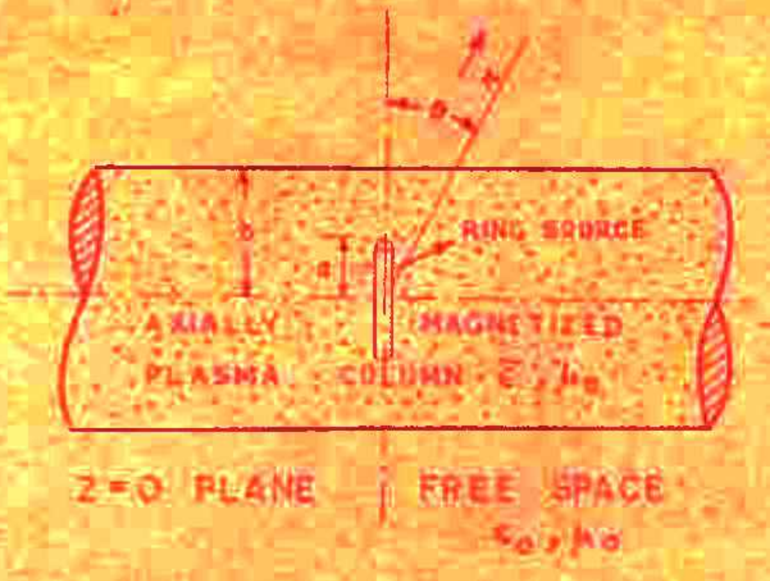
R
θ
b
a
RING SOURCE
AXIALLY MAGNETIZED PLASMA COLUMN $\bar{\epsilon}, \mu_0$
Z=0 PLANE
FREE SPACE
ϵ_0, μ_0

FIG. 2

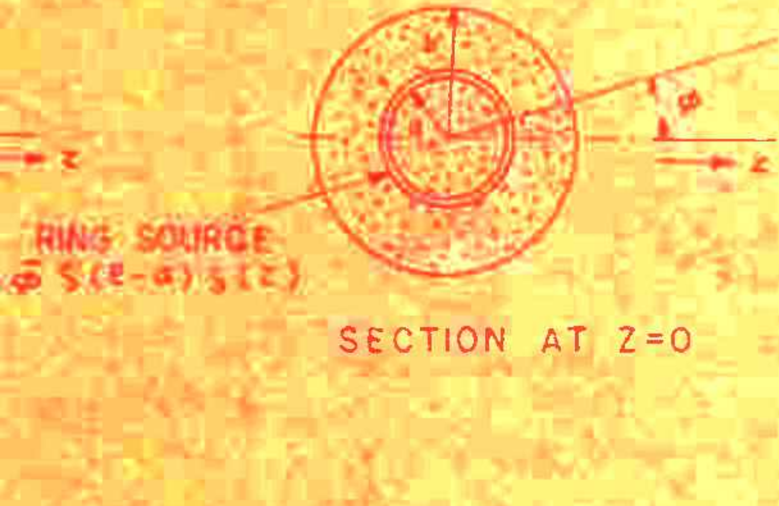

r
φ
z
z
RING SOURCE
φ δ(r-a) δ(z)

SECTION AT Z=0

Due to the choice of the source of excitation, the electromagnetic fields will be independent of the angular coordinate (i.e. $\frac{\partial}{\partial \phi} = 0$). For the circular symmetric TM_{01} mode, the inhomogeneous wave equation for H_ϕ (the ϕ - component of the magnetic field) may be written as

$$\frac{\partial^2 H_\phi}{\partial \rho^2} + \frac{I}{\rho} \frac{\partial H_\phi}{\partial \rho} - \frac{I}{\rho^2} H_\phi + \frac{\epsilon_3}{\epsilon_I} \frac{\partial^2 H_\phi}{\partial z^2} + k_o^2 \epsilon_3 H_\phi$$

$$= - j\omega\epsilon_o\epsilon_3 \delta \; (\rho - a) \; \delta \; (z) \qquad (2.2)$$

where $k_o^2 = \omega^2 \mu_o \epsilon_o$ and ϵ_I and ϵ_3 are the components of the dielectric tensor as given in Appendix A.

In order to solve equation (2.2) for H_ϕ, it is reduced to an homogeneous ordinary differential equation by method of Fourier- Transform. It is solved in terms of Bessel functions with particular reference to the radiation field, by essentially the same procedure as outlined by Duncan[3I] and Gupta and Singh[27], with appropriate boundary conditions at the junctions of different radial zones. The detail of analysis is given in Appendix A. The solution of the radiation field in spherical coordinate system (r, θ, ϕ) can be put in the form,

$$H_\phi = -j(\frac{\epsilon_o}{\mu_o}) \; \frac{k_o a}{\pi} \; \epsilon_3 \; F(\theta) \; \frac{e^{jk_o r}}{r} \qquad (2.3)$$

where

$$F(\theta) = \frac{J_1(k_0 a v)}{\left\{(k_0 b v) J_0(k_0 b v) H_1(k_0 b \cos\theta) - \epsilon_3 (k_0 b \cos\theta) J_1(k_0 b v) H_0(k_0 b \cos\theta)\right\}} \qquad (2.4)$$

$$v = \sqrt{\left(\epsilon_3 - \frac{\epsilon_3}{\epsilon_1} \sin^2\theta\right)} \qquad (2.5)$$

k_0 is the free space propagation constant. Angle θ is measured from the normal to the z-axis. ϵ_1 and ϵ_3 are the components of the permittivity tensor. J_n and H_n are the Bessel function of the first kind and Hankel function of first kind and of nth order respectively, and $F(\theta)$ is the factor which determines the variation of field with θ.

2.3 CHARACTERISTICS OF THE RADIATION FIELD:

The radiation patterns (variation of $F(\theta)$ with θ) have been computed with the help of an IBM-1130 computer for parametric values $k_0 b = 15.0$, $k_0 a = 7.5$, $\epsilon_3 = .1100$ and $\epsilon_3 = .0081$. When plasma frequency is much lower than the source frequency, ϵ_3 is only slightly less than unity and we shall call it low plasma density case. On the other hand when w_p is only slightly lower than the source frequency, ϵ_3 is near zero and we shall call it a high plasma density case. For given values of w/w_p, the value of ϵ_1 changes with ν_c/w_p

and may be divided into three sets as (i) $\epsilon_1 \leq \epsilon_3$ (ii) ϵ_1 is negative (iii) $\epsilon_1 \geq 1$. The effects of various parameters on the shape of the radiation pattern are discussed below:

Effect of magnetic field in high density plasma ($\epsilon_3 = .1100$).

When $\epsilon_1 \leq \epsilon_3$, the radiation pattern has a peak as shown in fig. 2.2. The radiation pattern for the isotropic case ($\epsilon_1 = \epsilon_3$) is also plotted in the fig. 2.2. The peak of the radiation pattern corresponds to minimum of the denominator given by equ. (2.4). For $\epsilon_1 = 0.1100$, 0.1020, 0.0711 and 0.0325, the peaks occur at 16.3°, 15.7°, 13.6° and 8.7° respectively. The half power beam width for these peaks is 3.0°, 3.4°, 3.2° and 1.85° respectively. The minima of denominator occur at $k_o bv = 2.6481$, 2.6622, 2.664 and 2.6694 for which $J_o(k_o bv)$ is nearly equal to zero. Parameter $k_o bv$ is real for $\epsilon_3 > \frac{\epsilon_3}{\epsilon_1} \sin^2 \theta$ and for other values it is imaginary. For imaginary argument the ordinary Bessel function in equ. (2.4) changes to modified Bessel functions.

When ϵ_1 is negative, the value of v becomes large, so $k_o bv$ is large and thus the denominator of $F(\theta)$ will pass through a greater number of zeros as θ varies from 0 to 90°.

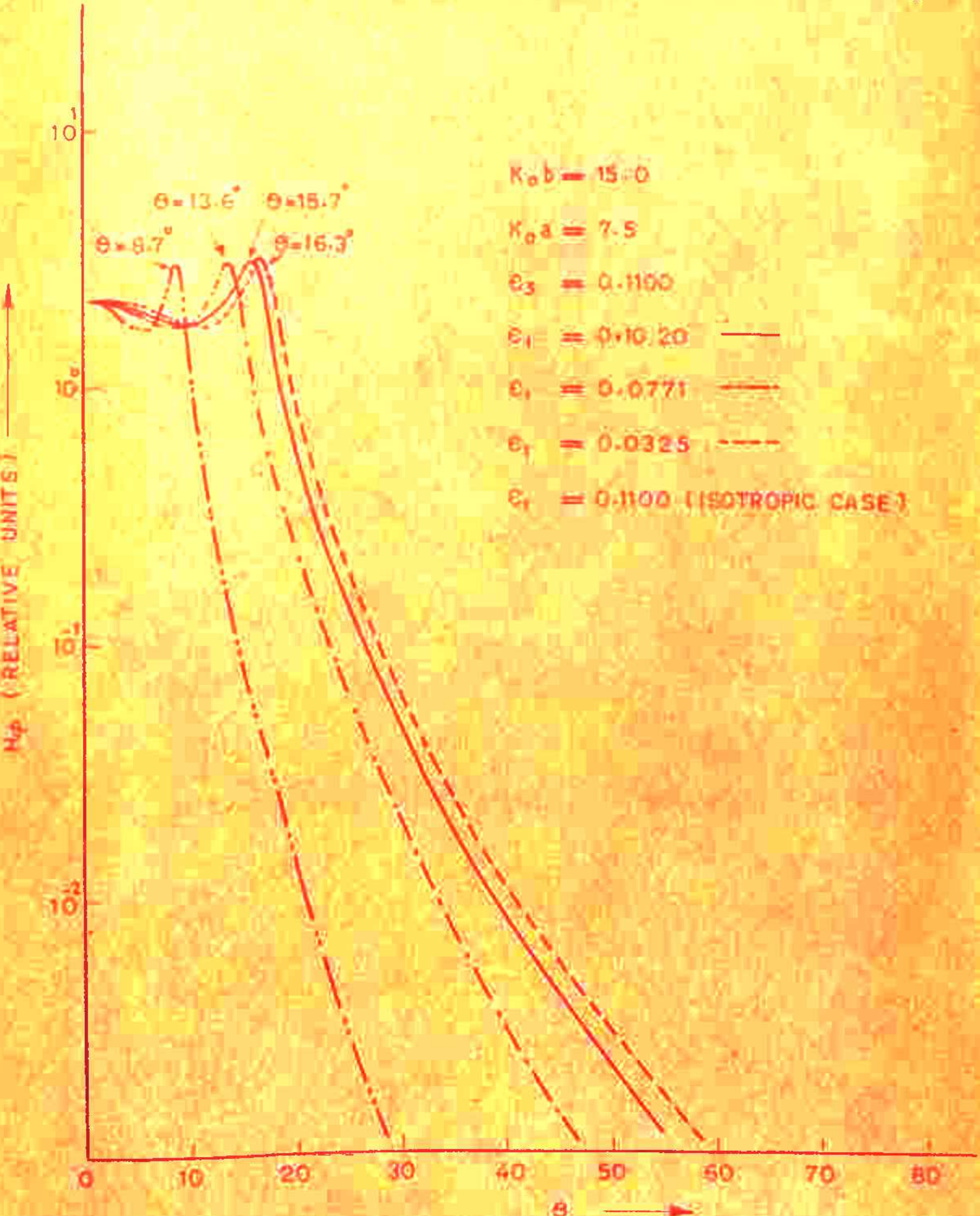
10^1
10^0
10^{-1}
10^{-2}
H_p (RELATIVE UNITS)
$\theta = 8.7°$
$\theta = 13.6°$
$\theta = 15.7°$
$\theta = 16.3°$
$K_0 b = 15.0$
$K_0 a = 7.5$
$\epsilon_3 = 0.1100$
$\epsilon_1 = 0.1020$
$\epsilon_1 = 0.0771$
$\epsilon_1 = 0.0325$
$\epsilon_1 = 0.1100$ (ISOTROPIC CASE)
0
10
20
30
40
50
60
70
80
θ

FIG. 2.2

For ϵ_1 = − 0.1446, three peaks are obtained at θ equal to 10.3°, 32.9° and 54.8° with half power width of the peak equal to 16.5° , 1.69° and 1.60° respectively as shown in fig. 2.3. These peaks occur for the corresponding values of $k_o bv$ equal to 5.4920, 8.6906 and 11.8109 which in turn corresponds to zeros of J_o ($k_o bv$). When $\epsilon_1 \geq 1$, the radiation peak is obtained in end fire direction as shown in fig. 2.4. For ϵ_1 = 1.0000, 1.0418, 1.3476 the peaks occur at 61°, 63° and 63.3° with half power widths of the peaks equal to 9.9° , 10.0° and 15.0° respectively. The corresponding values of $k_o bv$ are equal to 2.4101, 2.4255 and 2.5739 for which J_o (k_o bv) is nearly equal to zero. We note that in the case of highly dense plasma, the radiation pattern is governed by the denominator of F (θ) and peaks correspond to zeros of J_o($k_o bv$).

Effect of magnetic field in low density plasma(ϵ_3 = .9001):

In this case, the radiation pattern has nulls and peaks as shown in fig. 2.5. For ϵ_1 = 0.7844 (i.e. when $\epsilon_1 < \epsilon_3$), the nulls are obtained at 10° and 48° and peaks at 37° and 58.6° with half power widths equal to 15.5° and 2.15° respectively. The nulls correspond to the minima of the numerator. The minima of numerator occur at $k_o av$ = 7.0085, 3.8859 for which J_1($k_o av$) is nearly equal to zero. The peaks are

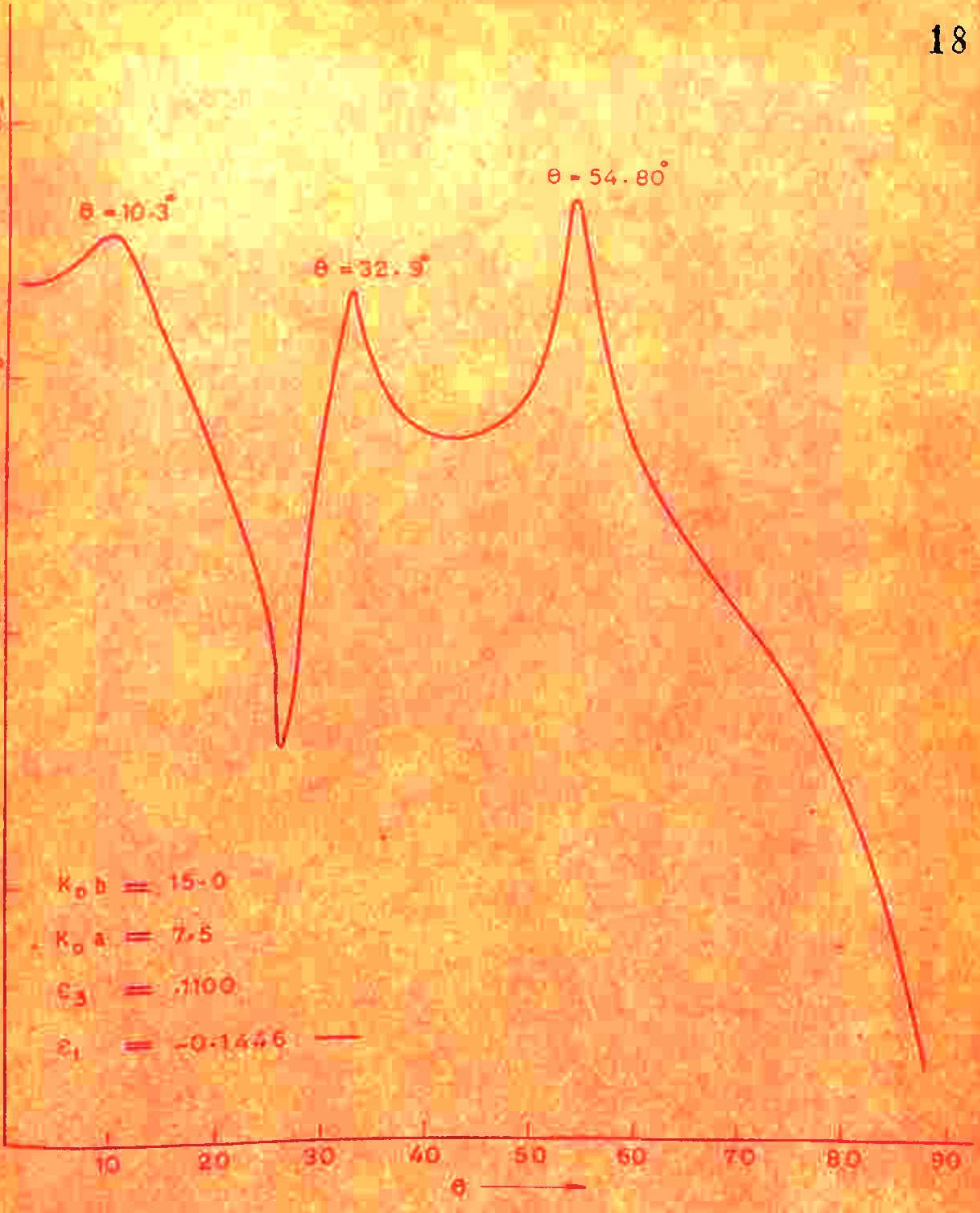
θ = 10.3°
θ = 32.9°
θ = 54.80°
K₀ b = 15·0
K₀ a = 7·5
ε₃ = ·1100
ε₁ = −0·1446
10
20
30
40
50
60
70
80
90
θ →

FIG. 2.3

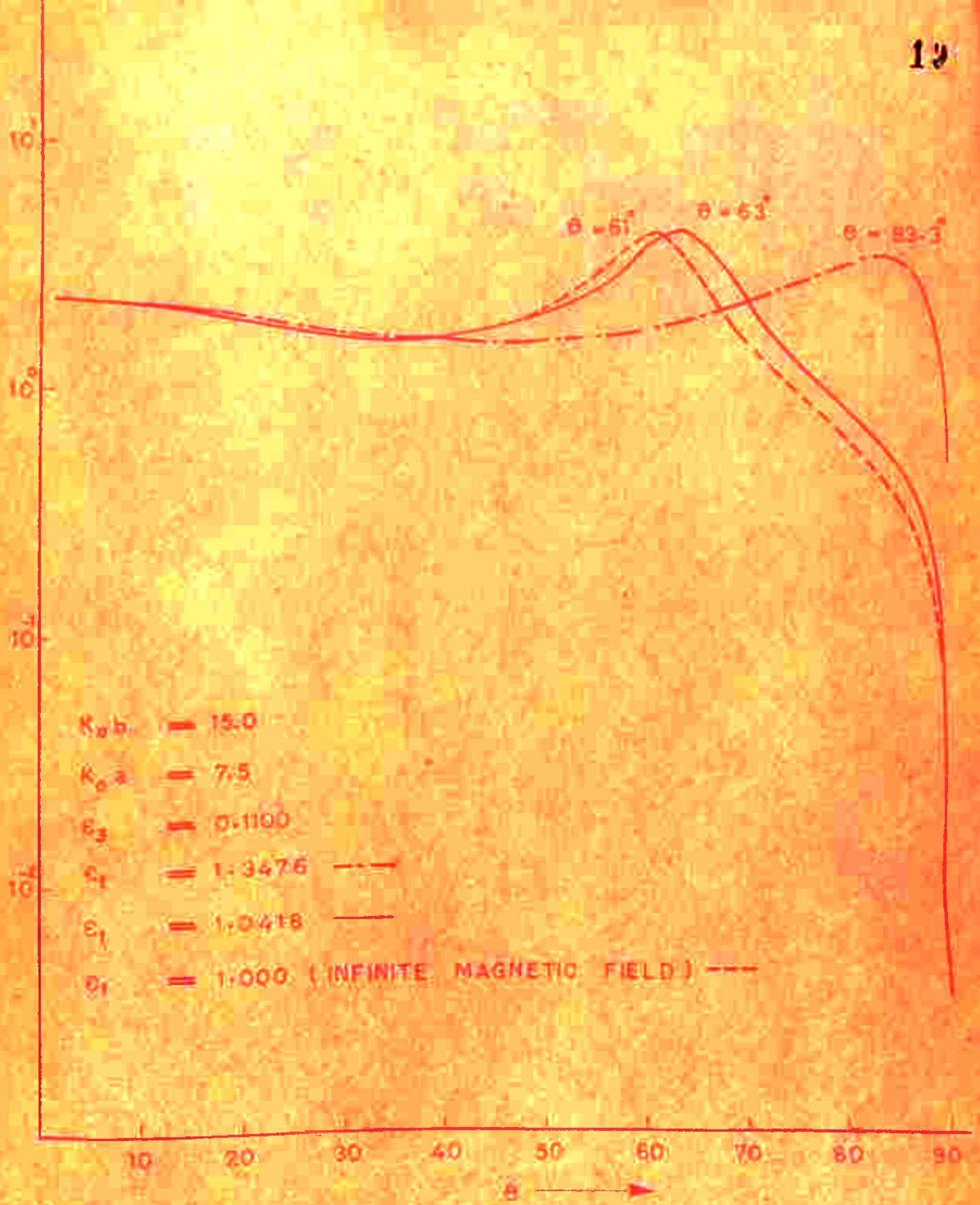

10^{1}
10^{0}
10^{-1}
10^{-2}
θ = 61°
θ = 63°
θ = 83.3°
$K_0 b = 15.0$
$K_0 a = 7.5$
$\varepsilon_3 = 0.1100$
$\varepsilon_1 = 1.3476$ - · -
$\varepsilon_1 = 1.0418$ —
$\varepsilon_1 = 1.000$ (INFINITE MAGNETIC FIELD) - - -
10
20
30
40
50
60
70
80
90
θ →

FIG. 2. 4

obtained when denominator is minimum. The minima of denominator occur at $k_o bv$ = I0.4530 and 3.7703 for which J_I ($k_o bv$) is nearly equal to zero.

When ϵ_I is negative, the value of v becomes large so $k_o bv$ is large and thus the denominator of F(θ) will pass through a greater number of zeros as θ varies from 0 to 90°. For ϵ_I = -0.5384, the radiation pattern has a null at 48° and three peaks at 34° , 56° and 84° with half power beam widths equal to I5.5° , 7.5° and I2.5° respectively. The null occurs at the corresponding value of $k_o av$ = I0.I739 for which J_I (k_o av) is nearly equal to zero. These peaks occur for the corresponding values of $k_o av$ = I7.9745, 2I.4268 and 24.0774 for which J_o($k_o bv$) is nearly equal to zero. When ϵ_I = I, the radiation pattern has nulls at θ = I2° and 67° and peaks at 43° and 85.5° with half power beam widths equal to 25° and 9.5°. The nulls occur at the corresponding values of $k_o av$ = 7.0168 and 6.656I for which J_I($k_o av$) is nearly equal to zero. The peaks occur at the corresponding values of $k_o bv$ equal to II.I715, 5.8927 for which J_o($k_o bv$) is nearly equal to zero. We note in this case that the nulls are obtained when J_I($k_o av$) is minimum and peaks are obtained when denominator is minimum , i.e., either J_I($k_o bv$) or J_o ($k_o bv$) is nearly equal to zero.

Effect of plasma density:

The ϵ_3 is given by $\epsilon_3 = I - \frac{\omega_p^2}{\omega^2}$ which in turn depends upon the plasma density ($\omega_p \propto \sqrt{n_e}$). The direction of the radiation peak depends upon the plasma density. Since the value of $k_o bv$ at the peak is fixed [near zero of $J_0(k_o bv)$ or $J_I(k_o bv)$] and $k_o bv$ is given by the relationship

$$k_o bv = k_o b \sqrt{(\epsilon_3 - \frac{\epsilon_3}{\epsilon_I} \sin^2 \theta)}$$

When plasma density is increased or decreased the value of ϵ_3 varies and hence the value of $k_o bv$. The value of $k_o bv$ can vary from $k_o b \sqrt{\epsilon_3}$ to zero. The radiation patterns for ϵ_3 = .II00 and ϵ_3 =.908I are shown in fig. (2.2), (2.3), (2.4) and (2.5). It may also be noted that the value of half power beam width is also affected by plasma density.

Effect of $k_o b$:

$k_o b$ affects the direction as well as the amplitude of the radiation peak formed. The radiation peak for ϵ_3=.II00, ϵ_I =.0325 is obtained near the zero of $J_0(k_o bv)$. For ϵ_3 =.908I and ϵ_I =0.7844 the nulls are obtained near the zeros of $J_I(k_o av)$ and peaks near the zeros of $J_I(k_o bv)$. It has also been found that number of peaks increases with the increase in value of $k_o b$ for some parameters. The direction and amplitude of the radiation peaks for two different values of $k_o b$ is given in Table 2.I.

TABLE - 2.I

Effect of varying $k_o b$ (i.e., for a fixed k_o, changing the diameter of the plasma column).

ε_3 = .II00 ε_I = .0328 $k_o a$ = 7.5

$k_o b$	$k_o bv$	$k_o av$	Direction of peaks (in degrees)	Amplitude of H_z (Relative units)
I8.75	5.5203	2.208I	4.8°	$0.4298x10^{I}$
	2.0475	I.I390	9.2°	$0.209Ix10^{I}$
22.50	5.5499	I.8409	6.9°	$0.4I3Ix10^{I}$

ε_3=0.908I ε_I=0.7844 $k_o a$ = 7.5

$k_o b$	$k_o bv$	$k_o av$	Direction of peaks and nulls (in degrees)	Amplitude of H_z (Relative units)
I8.75	I7.52I3	7.0085	$I0^{\circ}$	$0.3520x10^{-2}$
	I3.2357	5.2942	36.5°	$0.5799x10^{0}$
	9.7I49	3.8859	48°	$0.3747x10^{-I}$
	3.8089	I.5235	59.9°	$0.I397x10^{I}$
22.50	2I.0256	7.0085	$I0^{\circ}$	$0.3558x10^{-2}$
	I6.I263	5.3754	35.7°	$0.5768x10^{0}$
	II.6579	3.8859	48°	$0.3304x10^{-I}$
	3.8370	I.2790	60.6°	$0.I392x10^{I}$

Effect of $k_o a$:

The source radius 'a' occurs only in the numerator of equ. (2.4). Since , as discussed above, the position of the peak is governed by the denominator only, any variation in source radius will not change the direction of peak and only the amplitude of the peak will be affected. That means for a fixed value of k_o, the direction of the peak is independent of the magnetic ring source radius. The variation of peak amplitude for ϵ_3= .1100 and ϵ_1 = .0325 is as shown in fig. (2.6).

2.4 CONCLUSIONS:

From the results presented in the previous section, we note that a magnetic ring source surrounded by axially magnetized plasma column gives rise to a radiation peak or peaks. The direction of the peak depends upon the plasma density (through ϵ_3), magnetic field (through ϵ_1) and the column diameter (through $k_o b$). The direction of the peak is independent of the diameter of the magnetic ring source. The peaks are obtained when the denominator of $F(\theta)$ is minimum which in turn is governed by the value of $J_o(k_o bv)$ or $J_1 (k_o bv)$. The direction of the peak can be scanned by varying the plasma density as well as the

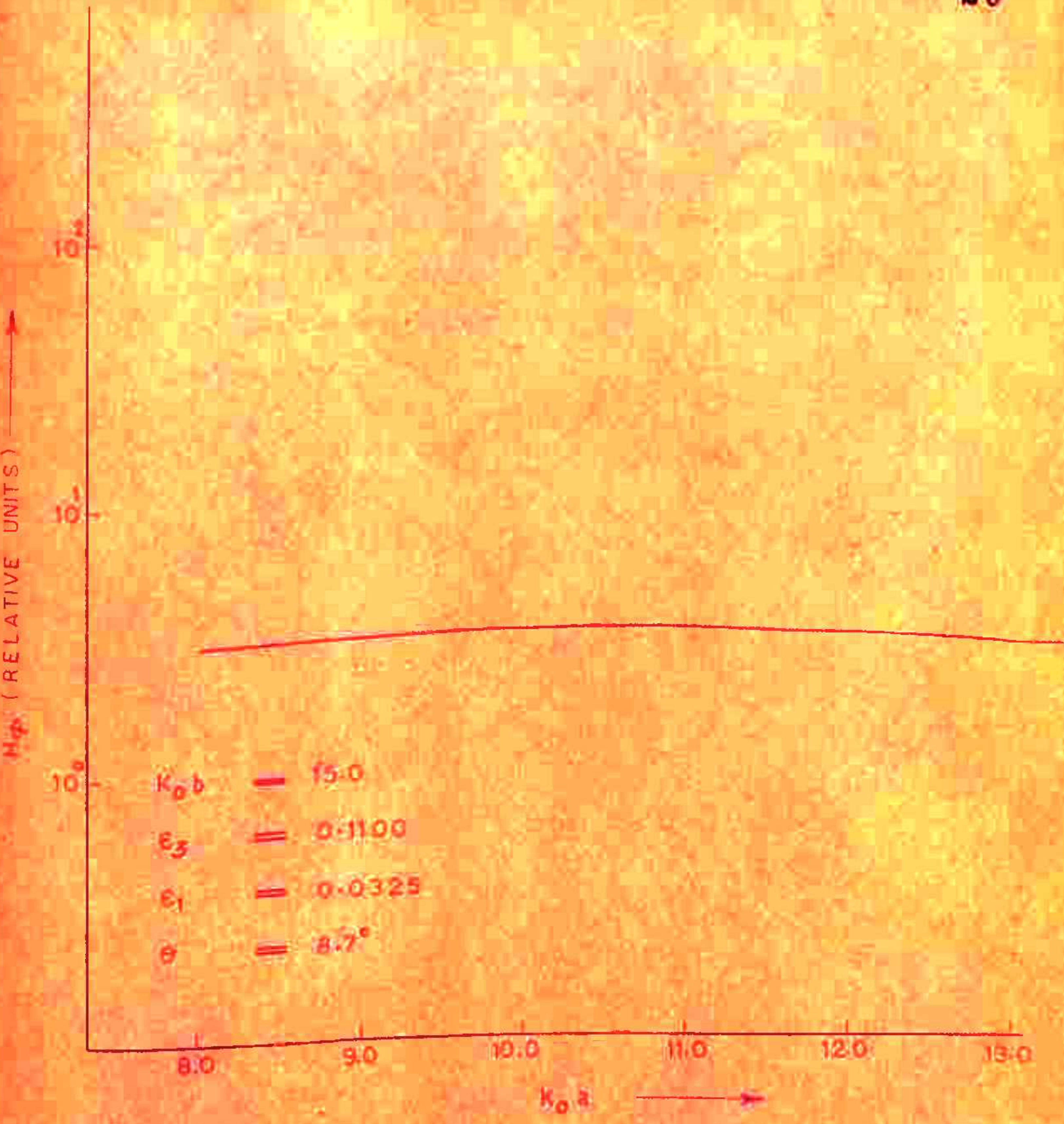
H_ϕ (RELATIVE UNITS) →
10^2
10^1
10^0
$K_o b$ = 15·0
ϵ_3 = 0·1100
ϵ_1 = 0·0325
θ = 8·7°
8.0
9.0
10.0
11.0
12.0
13.0
$k_o a$ →

FIG. 2.6

magnetic field and thus increases the range of angles through which the beam can be scanned as compared to the isotropic plasma column. It may also be noted that sharp peaks are obtained for the case of high plasma density. For very high magnetic fields the broad radiation peak is obtained in the end fire direction.

***

CHAPTER 3.

EXCITATION OF AXIALLY MAGNETIZED PLASMA COLUMN HAVING CENTRAL CONDUCTOR ALONG ITS AXIS

3.I Excitation by magnetic ring source

3.I.I Introduction 28
3.I.2 Analysis 29
3.I.3 Characteristics of the radiation field 33
3.I.4 Discussion 48

3.2 Excitation by open ended coaxial line

3.2.I Introduction 5I
3.2.2 Analysis 52
3.2.3 Characteristics of the radiation field 55
3.2.4 Discussion 70

CHAPTER 3.

EXCITATION OF AXIALLY MAGNETIZED PLASMA COLUMN HAVING CENTRAL CONDUCTOR ALONG ITS AXIS:

3.1 EXCITATION BY MAGNETIC RING SOURCE:

3.1.1 INTRODUCTION:

Tamir and Oliner[21] predicted the presence of radiation peaks near and before the critical angle in case of an infinite grounded plasma slab excited by an infinite magnetic line source. The corresponding cylindrical isotropic plasma geometry (plasma column having central conductor along the axis) excited by the magnetic ring source has been studied by Dhumi Ram and Verma[11]. They have also predicted the presence of narrow radiation peak formed near and before the critical angle. The direction of this beam could be varied by varying the plasma density, diameters of the plasma column and the central conductor.

In this chapter, the radiation patterns of a magnetic ring source surrounded by an axially magnetized plasma column having central conductor have been discussed. Enhanced radiation peak or peaks are obtained. The direction of these peaks or peak can be varied by changing the plasma density, applied magnetic field, column diameter and diameter of the central conductor. Since this geometry has one more scanning function (i.e. magnetic field) the beam can be varied over a considerably wider range of the angles than the previously analysed isotropic geometry. For uniaxial plasma, the peak is obtained at 90°.

In the analysis carried out, the plasma is considered to be a lossless and anisotropic dielectric medium with the permittivity given by the permittivity tensor. Thermal effects are neglected and the plasma density is assumed to be uniform over the cross-section of the column. The existence of a circular symmetric E-mode is assumed. It has been shown[30] that the E-mode can exist independently when the operating frequency is away from the cyclotron frequency. The inhomogeneous wave equations are solved by the method of Fourier Transform. This yields the solution for the field in form of definite integral. The radiation field is obtained from the asymptotic evaluation of the integral by saddle point integration. The method of saddle point integration is given in Appendix D.

3.1.2 ANALYSIS:

The geometry of the configuration analysed is shown in fig. 3.1. An infinitely long axially magnetized plasma column of radius 'b' and having a central conductor of radius 'a_I' along the axis is oriented with its axis along the z-axis of the cylindrical coordinate (ρ, ϕ , z) system. The medium surrounding the plasma column and extending to infinity is

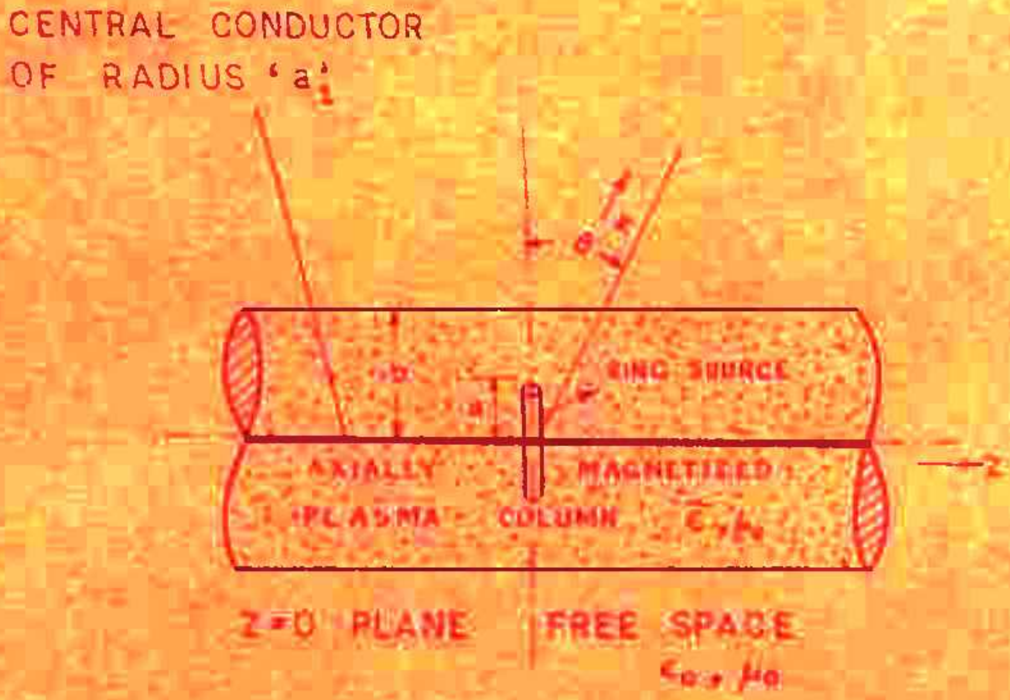
CENTRAL CONDUCTOR
OF RADIUS 'a'
d
b
a
RING SOURCE
AXIALLY MAGNETIZED
PLASMA COLUMN $\bar{\epsilon}, \mu_0$
z
Z=0 PLANE
FREE SPACE
ϵ_0, μ_0

FIG. 3.1

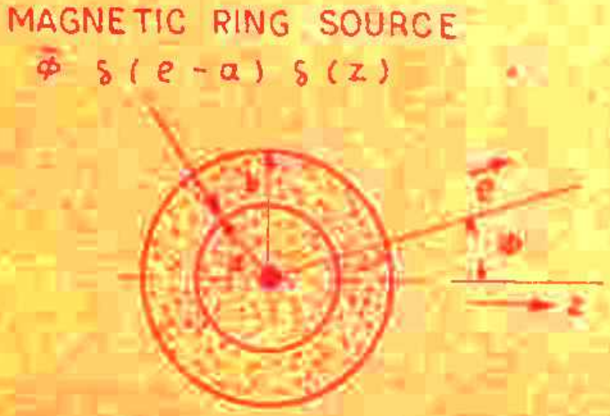
MAGNETIC RING SOURCE
$\bar{\Phi}\,\delta(\rho - a)\,\delta(z)$
b
a
ρ
φ
z

SECTION AT Z = 0

free space, with permittivity and permeability ϵ_0 and μ_0. The source of electromagnetic radiation is a ring of magnetic current of radius 'a' (a < b) concentric with the plasma column and situated at z = 0 plane. This source of electromagnetic radiation is mathematically represented by

$$\bar{K} = \bar{\phi} \ \delta (\rho - a) \delta (z) \qquad (3.I.I)$$

where δ represents Kronecker's delta function and $\bar{\phi}$ is a unit vector in the ϕ - direction.

Due to the choice of the source of excitation, the electromagnetic fields will be independent of the angular coordinate (i.e. $\partial/\partial\phi = 0$). For the circular symmetric TM_{01} mode, the inhomogeneous wave equation for H_ϕ (the ϕ - component of the magnetic field) may be written as

$$\frac{\partial^2 H_\phi}{\partial \rho^2} + \frac{I}{\rho^2} \frac{\partial H_\phi}{\partial \rho} - \frac{I}{\rho^2} H_\phi + \frac{\epsilon_3}{\epsilon_I} \frac{\partial^2 H_\phi}{\partial z^2}$$

$$+ k_0^2 \ \epsilon_3 H_\phi = -j\omega\epsilon_0\epsilon_3 \ \delta \ (\rho - a) \ \delta(z) \qquad (3.I.2)$$

where $k_0^2 = \omega^2\mu_0\epsilon_0$, and ϵ_I and ϵ_3 are the components of the dielectric tensor as given in Appendix A.

In order to solve equation (3.I.2) for H_ϕ , it is first reduced to a homogeneous ordinary differential equation by the method of Fourier-Transform. Then it can be solved in terms of Bessel function, with particular reference to the radiation field, by essentially the procedure outlined by Duncon[3I] and Gupta and Singh[27], with appropriate boundary conditions at the junctions of different radial zones. The detail of the analysis is given in Appendix B. The solution of the radiation field in spherical co-ordinate system (r, θ , φ) can be put in the form,

$$H_{\phi}(r,\theta) = - \frac{j\omega\epsilon_3}{\pi} F(\theta) \frac{e^{jk_o\bar{r}}}{\bar{r}} \qquad (3.I.3)$$

where

$$F(\theta) = F_I(\theta)\, F_2(\theta)$$

$$F_I(\theta) = a \left\{ J_o(k_o a_I v)\, Y_I(k_o a v) - Y_o(k_o a_I v) J_I(k_o a v) \right\}$$

$$F_2(\theta) = \frac{I}{\begin{array}{l}(k_o b v) H_I(k_o b \cos\theta) * \left\{ J_o(k_o a_I v) Y_o(k_o b v) \right. \\ \left. - Y_o(k_o a_I v)\, J_o(k_o b v) \right\} - \epsilon_3 (k_o b \cos\theta) H_o(k_o b \cos\theta) \\ * \left\{ J_o(k_o a_I v) Y_I(k_o b v) - Y_o(k_o a_I v) J_I(k_o b v) \right\}\end{array}}$$

$$v = \sqrt{\left(\epsilon_3 - \frac{\epsilon_3}{\epsilon_I} \sin^2\theta \right)} \qquad (3.I.4)$$

k_o is the free space propagation constant. Angle θ is measured from the normal to the z-axis. ϵ_I and ϵ_3 are the components of the permittivity tensor. J_n , Y_n and H_n are the Bessel function of first kind, second kind and Hankel function of first kind and of nth order respocively. F(θ) is the factor which determines the variation of field with θ.

3.I.3. CHARACTERISTICS OF THE RADIATION FIELD:

The radiation patterns (variation of F(θ) with θ) have been computed with the help of an IBM- II30 computer for parametric values $k_o b = 20.0$, $k_o a_I = 0.2$, $k_o a = 2.0$, $\epsilon_3 = .II30$ and $\epsilon_3 = .9081$. When plasma frequency is much lower than the source frequency, ϵ_3 is only slightly less than unity and we shall call it low plasma density case. On the other hand when w_p is only slightly lower than the source frequency, ϵ_3 is near zero and we shall call it a high plasma density case. Since F (θ) is an expression involving both the Bessel and Hankel function in a complicated way, it is difficult to express analytically the behaviour of F(θ) with various parameters. Therefore, computational results are presented first and then these results are analysed to give a qualitative relationship between the location of the peak and other parameters of the configuration. For given values of w/w_p, the value of ϵ_I changes with w_c/w_p and may be divided into three sets as (i) $\epsilon_I \leq \epsilon_3$ (ii) ϵ_I is negative (iii) $\epsilon_I \geq I$. The effects of various parameters on the shape of the radiation pattern are discussed below:

Effect of magnetic field in high density plasma ($\epsilon_3 = .1100$):

When $\epsilon_I \leq \epsilon_3$ the radiation peaks are obtained, one of them is a major radiation peak. The value of v in this case first decreases as θ increases and when $\epsilon_3 < \left(\frac{\epsilon_3}{\epsilon_I} \sin^2 \theta\right)$ it becomes negative and starts increasing. For negative value of v the ordinary Bessel function in equation (3.I.3) will change to modified form. For $\epsilon_I = .1020$ and $\epsilon_I = .0325$, the radiation patterns are plotted in fig. 3.2. The pattern is plotted only for the values of θ for which v is positive. For negative v, the pattern is governed by the values of modified Bessel function whose arguments are increasing as θ increases, so the pattern become oscillatory. For $\epsilon_I = .1020$, the radiation peaks at 7.6° and 18.6° are obtained with half power beam widths equal to 3.5° and $.031^\circ$ respectively. For $\epsilon_I = .0325$, the radiation peaks at 4.24° and 10.37° are obtained with half power beam widths equal to 1.9° and $.028^\circ$ respectively. The detailed structure of the major radiation peak for $\epsilon_I = .0325$ is shown in fig. 3.4. The major radiation peak is obtained when the value of v is minimum or the value of k_0bv, k_0a_Iv and k_0av is minimum as shown in Table 3.I. It may be noted that the major peak corresponds to the maxima of numerator and other peak is obtained for the minima of denominator.

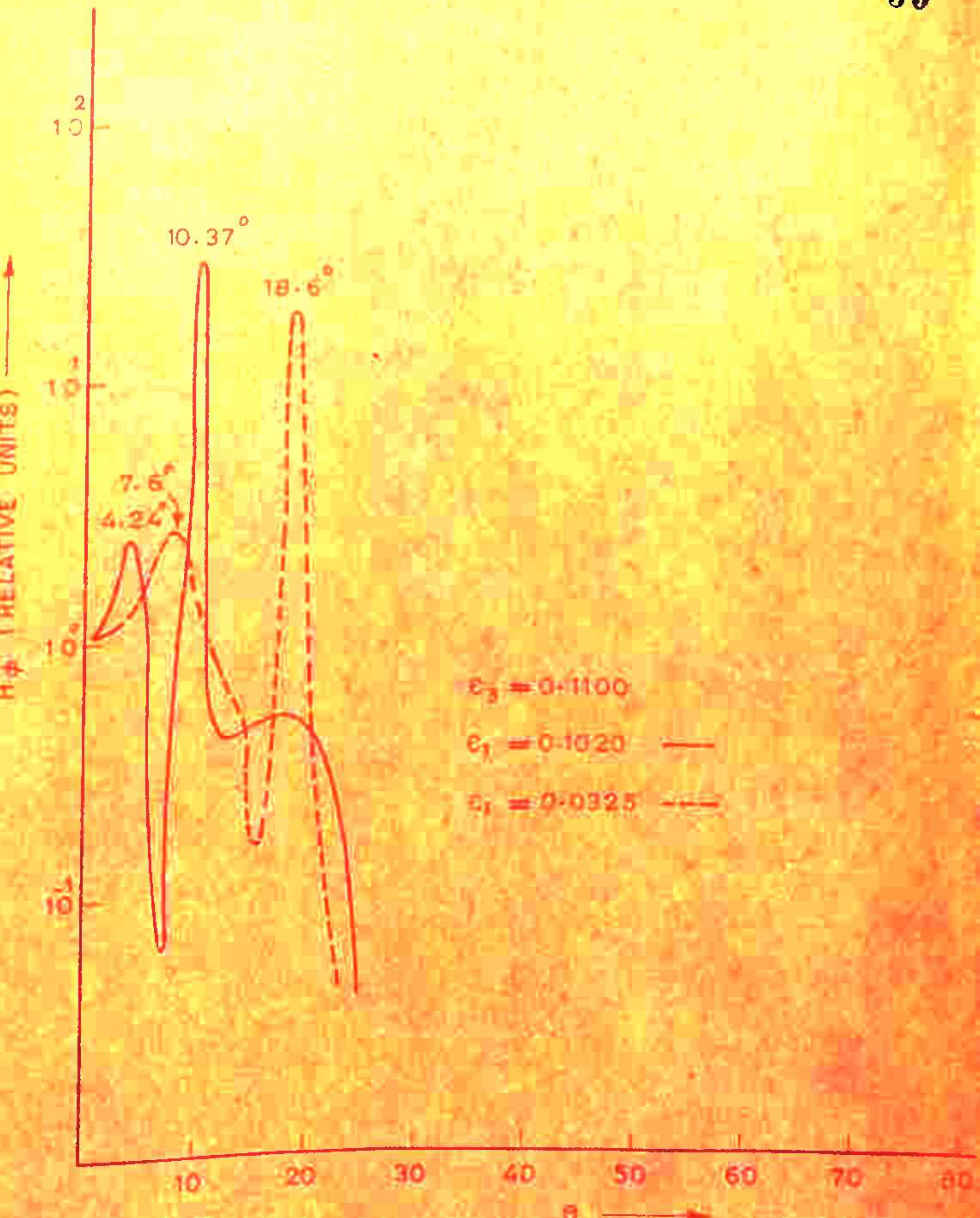
10^2
10^1
10^0
10^{-1}
H_ϕ (RELATIVE UNITS)
10.37°
18·6°
7·6°
4.24°
$\epsilon_3 = 0·1100$
$\epsilon_1 = 0·1020$ ——
$\epsilon_1 = 0·0325$ ----
10
20
30
40
50
60
70
80
θ

FIG. 3.2

When ϵ_1 is negative, the value of v increases as value of θ increases, so the value of $k_0 bv$, $k_0 a_1 v$ and $k_0 av$ also increases. For higher values of arguments, the Bessel functions are approximately equal to sine and cosine functions, so as θ varies from 0 to 90°, an oscillatory pattern is obtained. For $\epsilon_1 = -0.1446$, the radiation pattern is shown in fig. 3.5. When $\epsilon_1 > 1$, the value of v decreases as θ increases, no sharp radiation peaks are obtained in this case. For $\epsilon_1 = 1.0418$, the radiation pattern is shown in fig. 3.5. When $\epsilon_1 = 1$ (infinite magnetic field), the numerator has maximum value at 90°, so a sharp radiation peak is obtained at 90° as shown in fig. 3.6.

Effect of magnetic field in low density plasma ($\epsilon_3 = .9081$):

When $\epsilon_1 \leq \epsilon_3$, the radiation peaks are obtained, one of them is a major radiation peak. The value of v becomes negative for $\epsilon_3 < \left(\frac{\epsilon_3}{\epsilon_1} \sin^2 \theta\right)$ and ordinary Bessel function change to modified form. For negative values the patterns becomes oscillatory so it has been plotted only for those values of θ for which v is positive. The radiation patterns for $\epsilon_1 = .9007$ and $\epsilon_1 = .7844$ are plotted in fig. 3.3. For $\epsilon_1 = .9007$, the radiation peaks at 68.4° and 71.48° are obtained with half power beam widths equal to 3.54° and 0.081° respectively. For $\epsilon_1 = 0.7844$, the radiation peaks at 58.95° and 62.24°

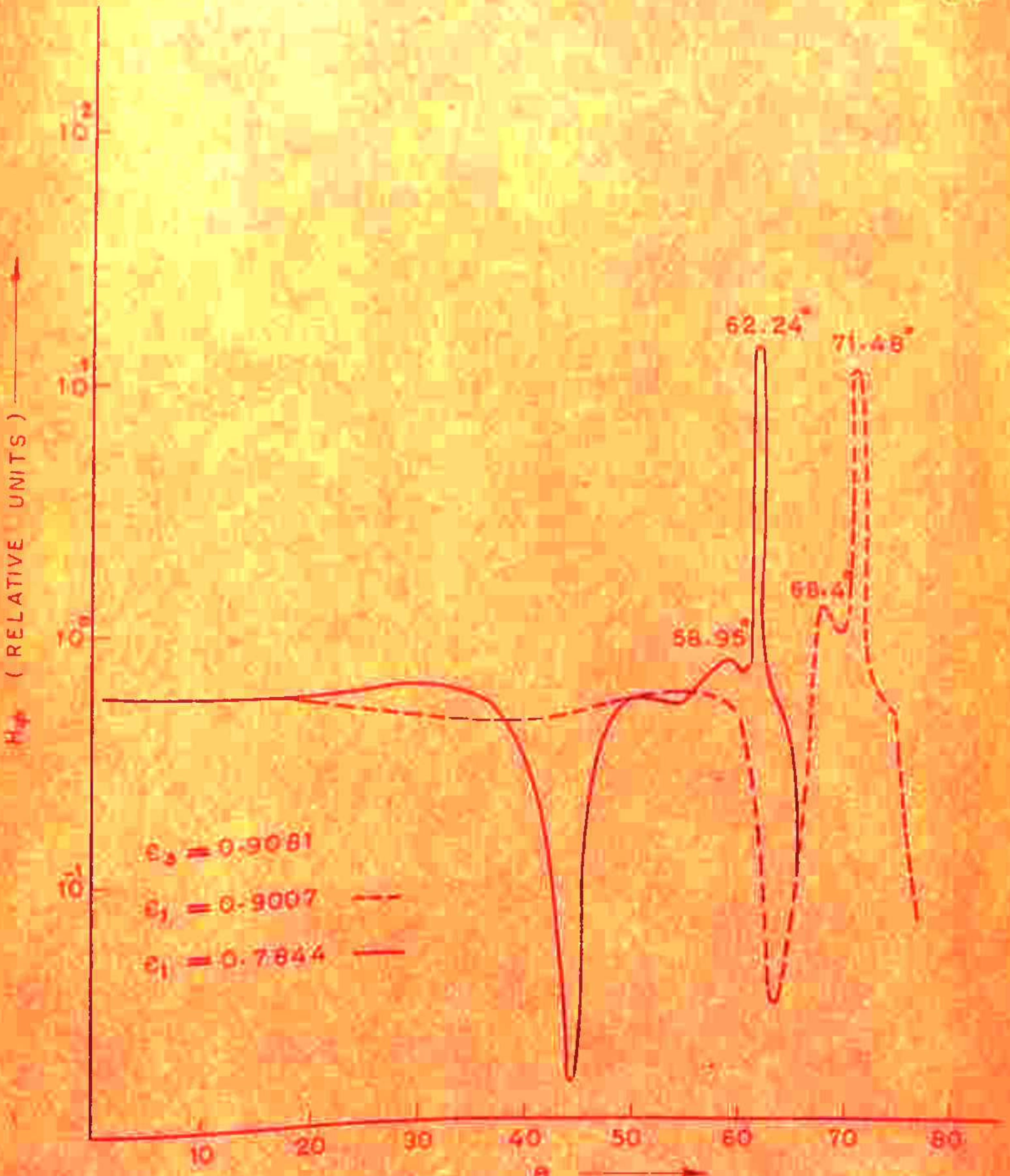
10^2
10^1
10^0
10^{-1}
H_ϕ (RELATIVE UNITS)
62.24°
71.48°
68.4°
58.95°
$\epsilon_s = 0{\cdot}9081$
$\epsilon_1 = 0{\cdot}9007$
$\epsilon_1 = 0{\cdot}7844$
10
20
30
40
50
60
70
80
θ

FIG. 3.3

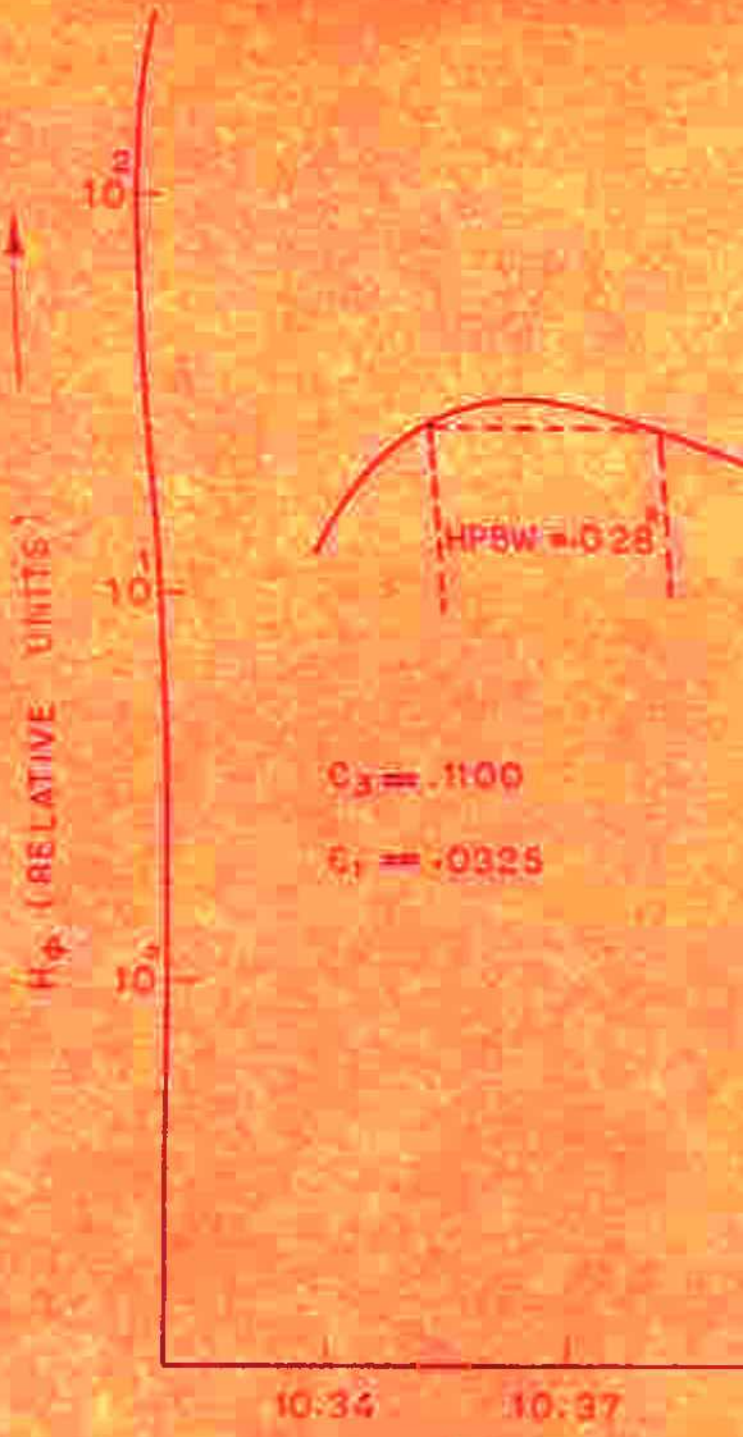
10^2
10^1
10^0
H_ϕ (RELATIVE UNITS)
HPBW = .028°
C_3 = .1100
C_1 = .0325
10:34
10:37

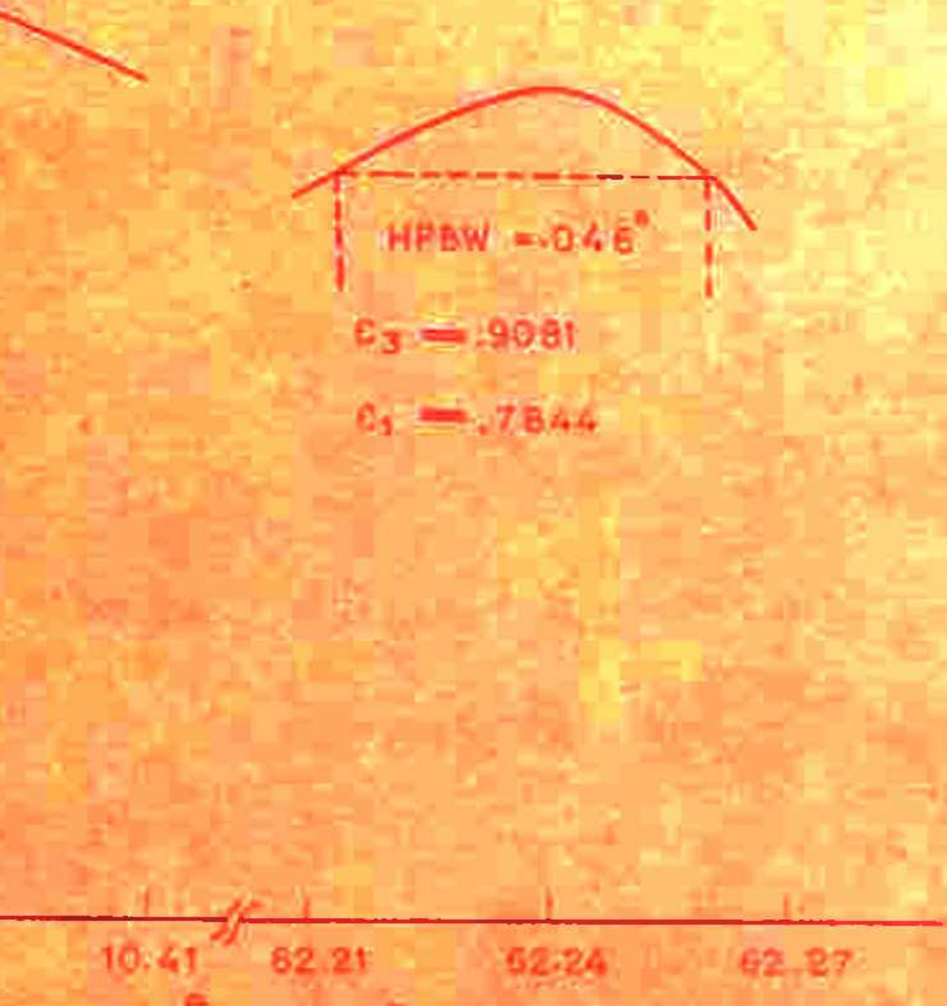

FIG 3.4

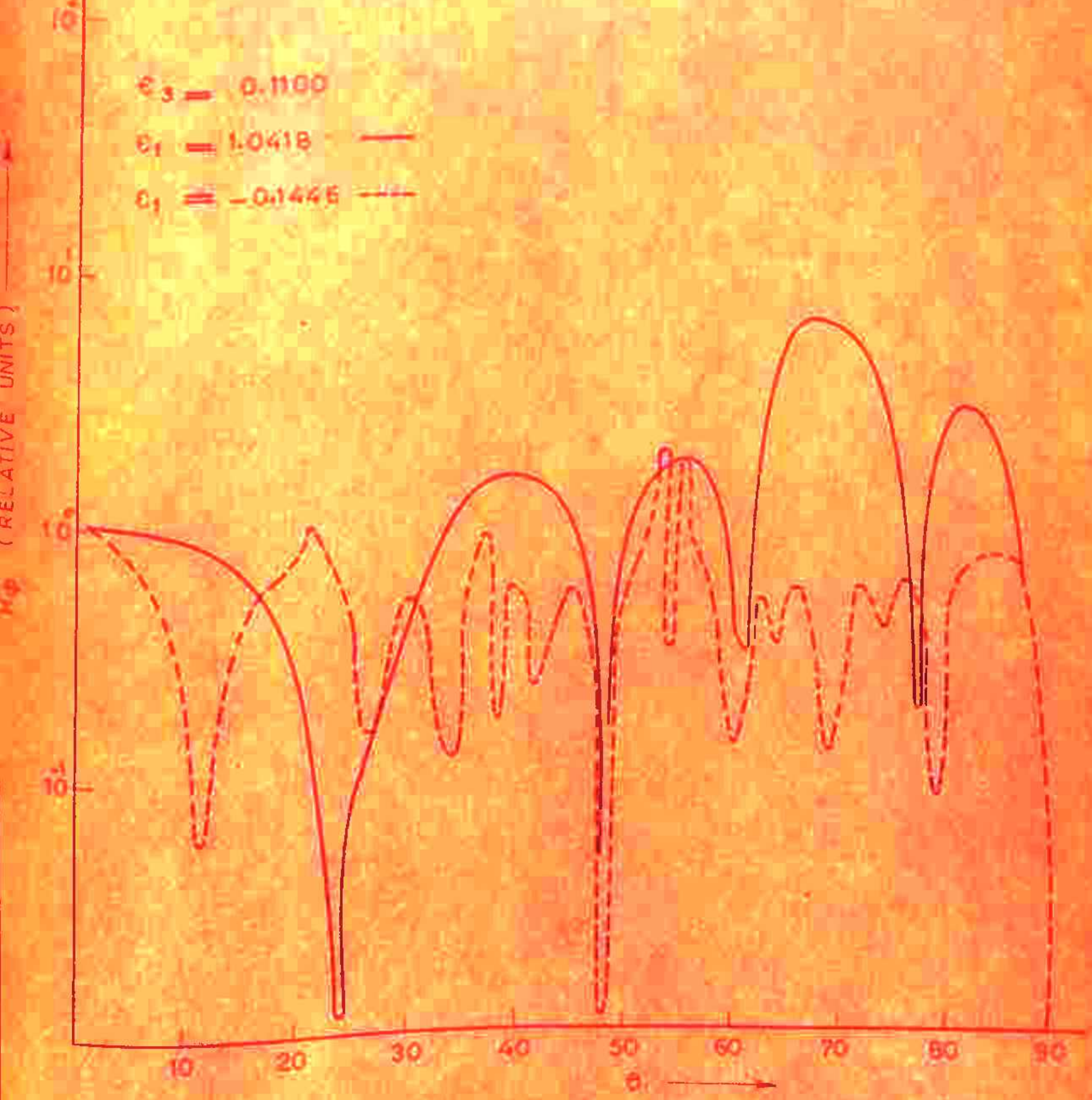
10^{2}
10^{1}
10^{0}
10^{-1}
M_ϕ (RELATIVE UNITS)
$\epsilon_3 = 0.1100$
$\epsilon_1 = 1.0418$
$\epsilon_1 = -0.1446$
10
20
30
40
50
60
70
80
90
θ

FIG. 3.5

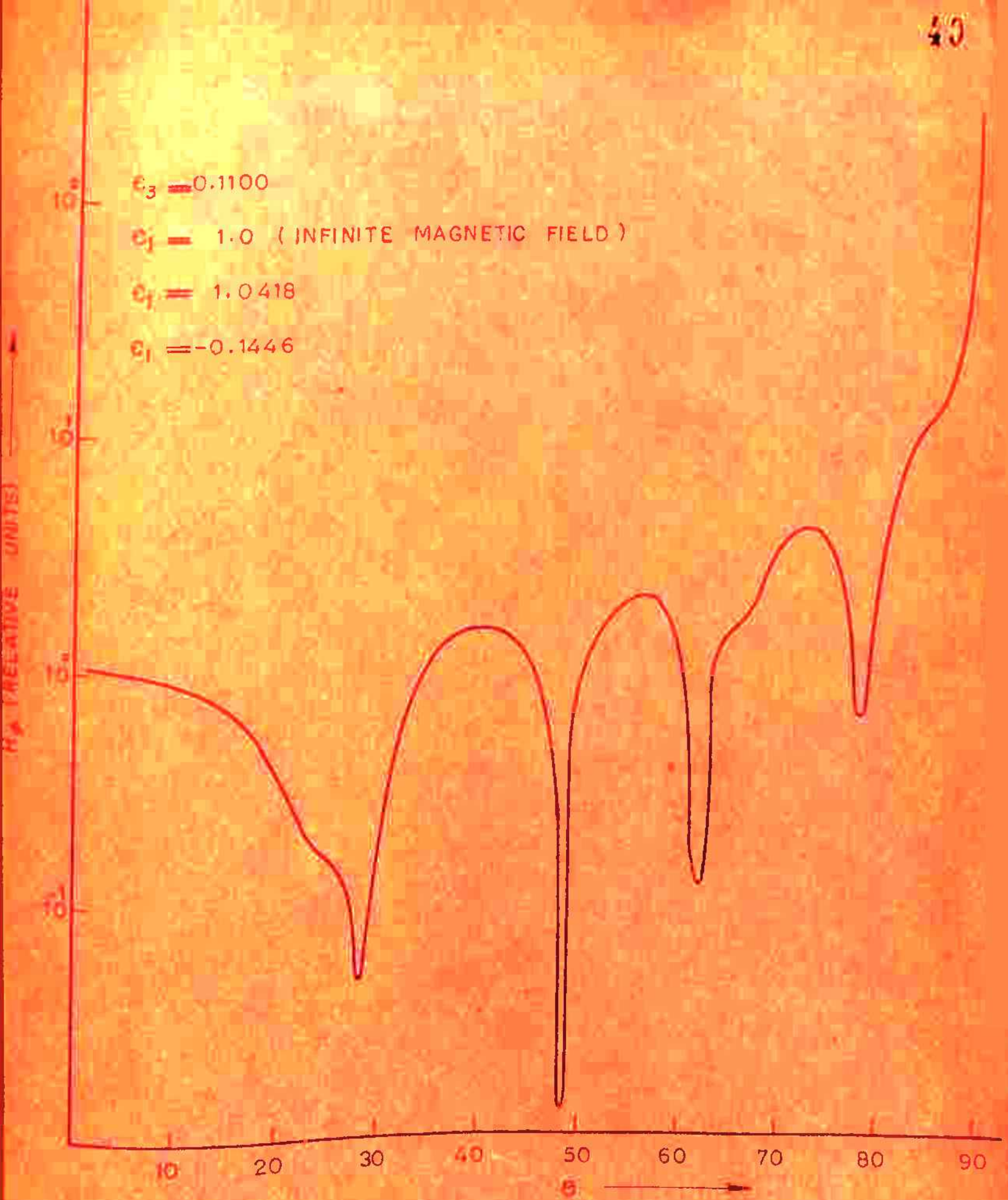
$\varepsilon_3 = 0.1100$
$\varepsilon_1 = 1.0$ (INFINITE MAGNETIC FIELD)
$\varepsilon_1 = 1.0418$
$\varepsilon_1 = -0.1446$
10^2
10^1
10^0
10^{-1}
H_a (RELATIVE UNITS)
10
20
30
40
50
60
70
80
90
θ

FIG. 3.6

are obtained with half power beam widths equal to 3.06° and 0.046° respectively. The detailed structure of the major radiation peak for $\varepsilon_I = 0.7844$ is shown in fig. 3.4. In this case also, the major radiation peak is obtained when the value of v is minimum or the value of $k_o bv$, $k_o a_I v$ and $k_o av$ is minimum as shown in Table 3.I. It may be noted that in this case also, the major peak corresponds to the maxima of numerator and other peak is obtained for the minima of denominator.

When ε_I is negative, the value of v increases as value of θ increases, so the pattern is governed by sine and cosine function therefore as θ varies from 0 to 90°, an oscillatory pattern is obtained. For $\varepsilon_I = -0.5384$, the radiation pattern is shown in fig. 3.7. For $\varepsilon_I = 1.1956$, the radiation pattern is plotted in fig. 3.7 and it can be seen that only shallow peaks are obtained. When $\varepsilon_I = I$ (i.e. uniaxial case), the numerator has maximum value at 90°, so a sharp radiation peak is obtained at 90° as shown in fig. 3.8.

Effect of $k_o b$:

$k_o b$ affects the direction as well as the amplitude of radiation peaks formed. For a fixed value of k_o, the higher values of $k_o b$ mean increasing the diameter of the plasma column. Three different values of $k_o b$ = 21.5, 23.0

Parameters for the radiation peaks

High density plasma(C_3=.I100)

C_I	Direction of radiation peaks (in degrees)	k_0bv	k_0a_1v	k_0av	Denominator of F(θ)	Numerator of F(θ)	Amplitude for H_φ (relative units)
0.1020	7.6^0	6.0374	0.0603	0.6037	0.7219xI0^{-1}	0.7166xI0^0	0.1653xI0^1
	18.6^0	0.2944	0.0029	0.0294	0.4926xI0^0	0.2I60xI0^2	0.I080xI0^2
0.0325	4.24^0	6.0495	0.0604	0.6049	0.7274xI0^{-I}	0.7I39xI0^0	0.260IxI0^0
	I0.37^0	0.3682	0.0036	0.0368	0.2708xI0^0	0.I726xI0^2	0.3089xI0^2

Low density plasma (C_y = .908I)

C_I	Direction of radiation peaks (in degrees)	k_0bv	k_0a_1v	k_0av	Denominator of F(θ)	Numerator of F(θ)	Amplitude for H_φ (relative units)
0.9007	68.4^0	3.8I00	0.038I	0.38I0	0.I647xI0^I	0.I454xI0^I	0.I075xI0^I
	71.48^0	0.7507	0.0075	0.0750	0.3373xI0^0	0.8437xI0^I	0.I042xI0^2
0.7844	58.95^0	4.8I88	0.048I	0.48I0	0.I576xI0^I	0.II48xI0^I	0.7246xI0^0
	62.24^0	0.7070	0.0070	0.0707	0.2470xI0^0	0.0963xI0^I	0.I244xI0^2

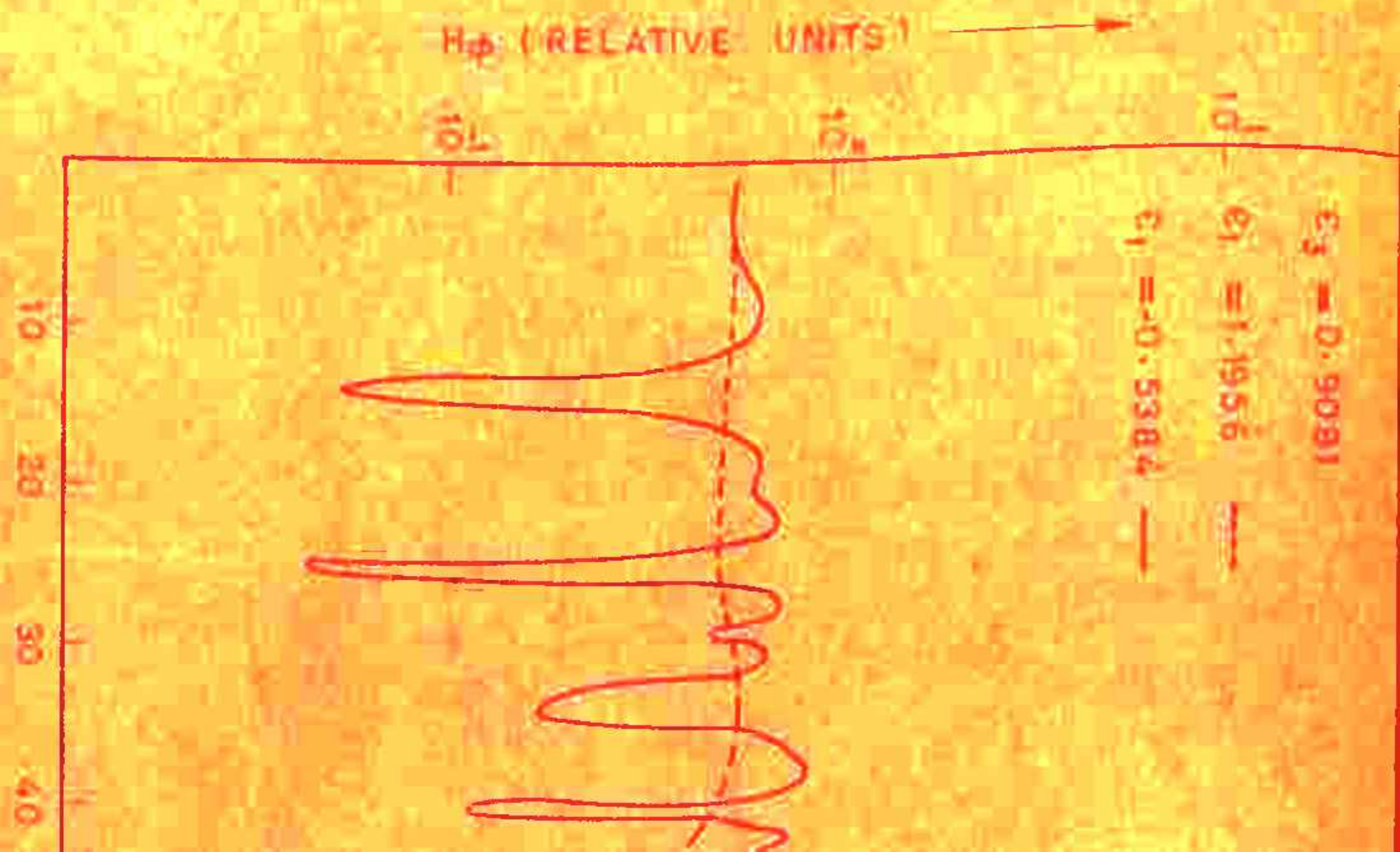
Hφ (RELATIVE UNITS)
10⁻¹
10⁰
10¹
ε₃ = 0.9081
ε₂ = 1.1956
ε₁ = 0.5384
10
20
30
40

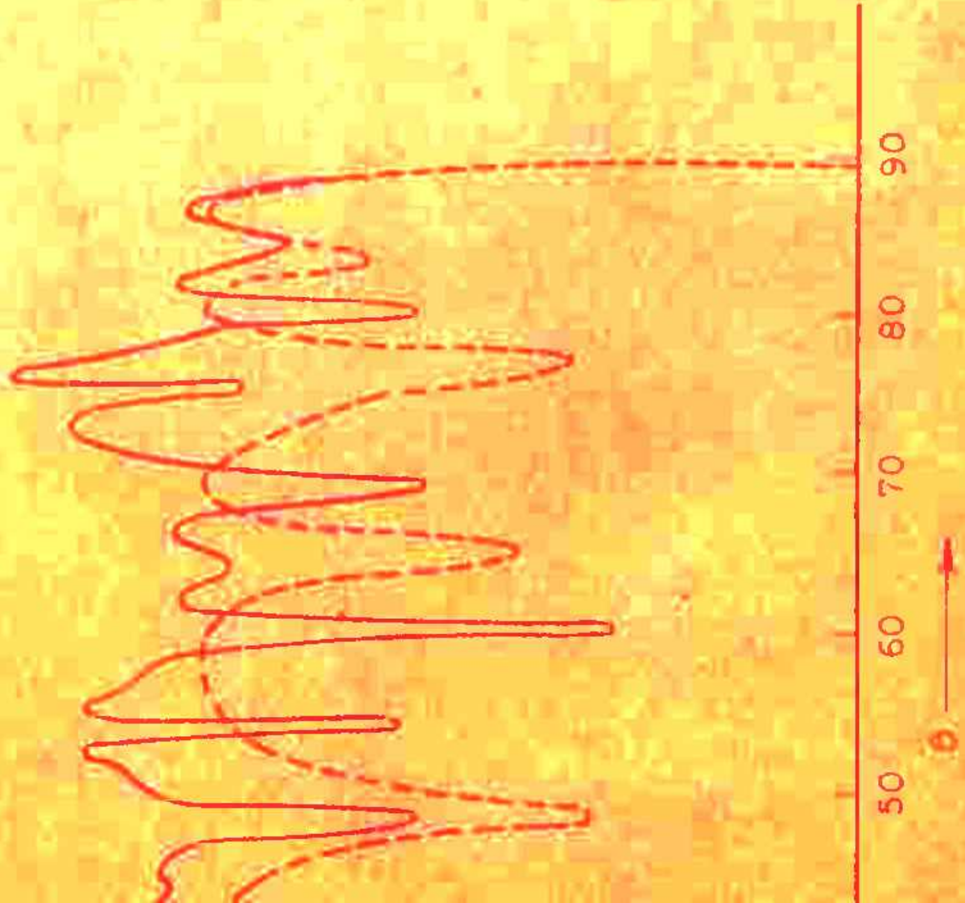

IG. 3.7

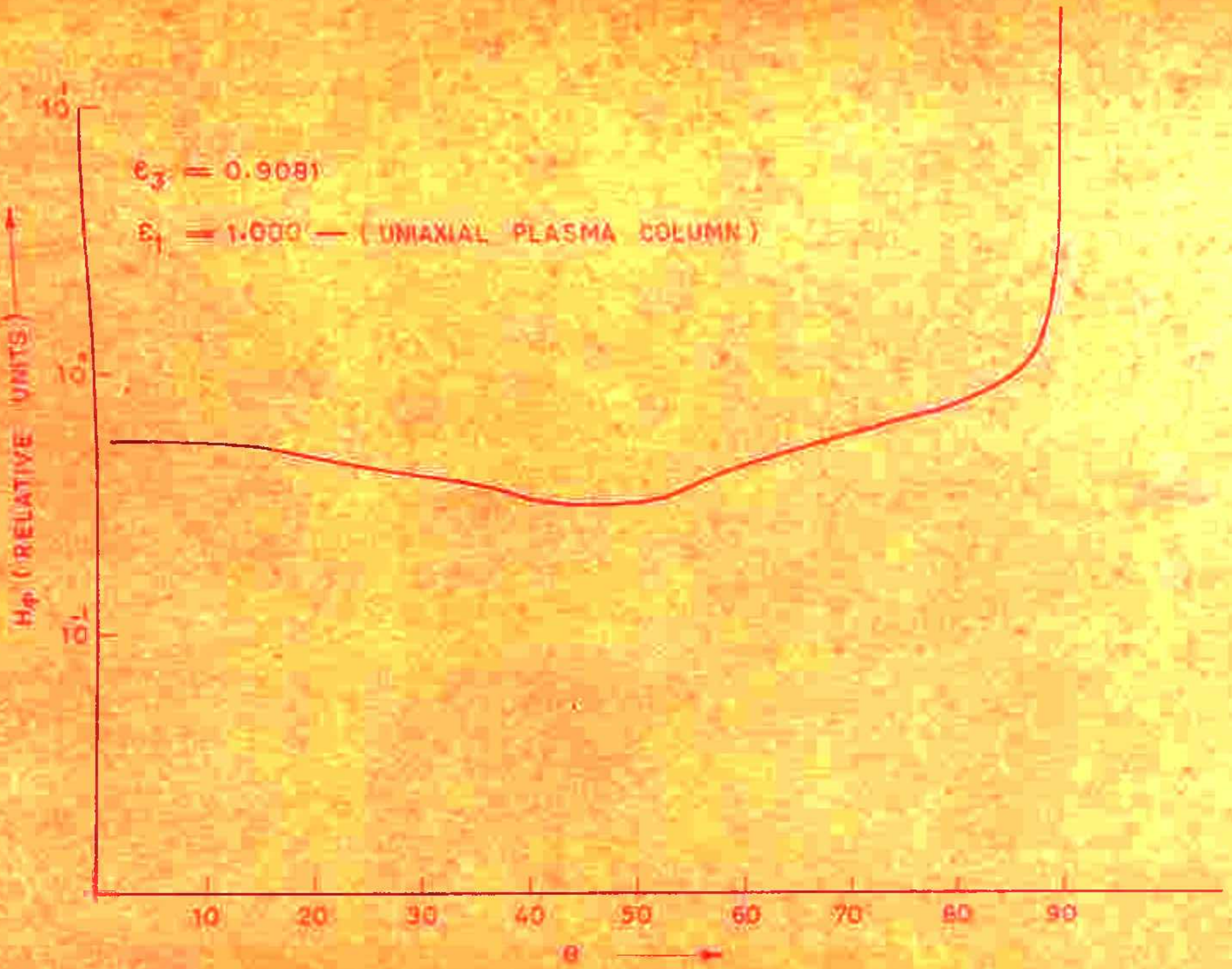
10^{1}
10^{0}
10^{-1}
H_ϕ (RELATIVE UNITS)
$\epsilon_3 = 0.9081$
$\epsilon_1 = 1.000$ — (UNIAXIAL PLASMA COLUMN)
10
20
30
40
50
60
70
80
90
θ

FIG-3-8

and 24.0 have been taken. The directions and amplitudes of the radiation peaks for ϵ_3 = .II00, ϵ_I = .0325 and ϵ_3=.9081, ϵ_1 = .7844 are given in Table 3.2 for these three different values of $k_o b$.

Effect of $k_o a_I$:

$k_o a_I$ affects the amplitude of the radiation peak and also the direction upto a small extent. For fixed value of k_o, the higher value of the diameter of central conductor gives rise to a stronger radiation peak. The direction of major peak is affected slightly but direction of the first peak is changed as given in Table 3.3. The directions and amplitudes of the radiation peaks for ϵ_3 = .II00, ϵ_I=.0325 and ϵ_3 = .9080, ϵ_I = .7844 are given in Table 3.3 for three different values of $k_o a_I$.

Effect of plasma density:

The direction of the peak is governed by the value of v (equ. 3.I.4). The ϵ_3 is given by $\epsilon_3 = (I-\omega_p^2/\omega^2)$ which, in turn, depends upon the plasma density. The value of v can vary from 0 to $\sqrt{\epsilon_3}$. For large values of ϵ_3, the peak will shift from broad side direction to end fire direction. The radiation patterns for ϵ_3 = .II00 and ϵ_3 = .908I are shown in fig. (3.2), (3.3), (3.4), (3.5), (3.6),

TABLE - 3.2.

Effect of varying $k_0 b$ (i.e. for a fixed k_0, changing the diameter of the plasma column)

$\epsilon_3 = 0.1100$, $\epsilon_1 = 0.0325$, $k_0 a_1 = 0.2$, $k_0 a = 2.0$

$k_0 b$	Direction of the peaks (in degrees)	Amplitude of H_z (Relative units)
21.5	4.35°	0.1261×10^1
	10.30°	0.1653×10^2
23.0	6.20°	0.3061×10^1
	10.38°	0.2685×10^2
24.5	6.40°	0.1744×10^1
	9.40°	0.3524×10^2

$\epsilon_3 = 0.0081$, $\epsilon_1 = 0.7844$, $k_0 a_1 = 0.2$, $k_0 a = 2.0$

$k_0 b$	Direction of the peaks (in degrees)	Amplitude of H_z (Relative units)
21.5	60.29°	0.1296×10^1
	62.30°	0.5840×10^1
23.0	60.40°	0.1634×10^1
	62.28°	0.1211×10^2
24.5	60.30°	0.1731×10^1
	64.80°	0.4979×10^1

TABLE - 3.3.

Effect of varying $k_o a_1$ (i.e. for a fixed k_o, changing the diameter of the plasma column).

$\epsilon_3 = 0.1100$, $\epsilon_1 = 0.0325$, $k_o b = 20.0$, $k_o a = 2.0$

$k_o a_1$	Direction of the peaks (in degrees)	Amplitude of H_z (Relative units)
0.08	4.66°	0.1659×10^{1}
	10.39°	0.2737×10^{2}
0.12	4.49°	0.2025×10^{1}
	10.38°	0.2746×10^{2}
0.16	4.36°	0.2331×10^{1}
	10.38°	0.2771×10^{2}

$\epsilon_3 = 0.0061$, $\epsilon_1 = 0.7844$, $k_o b = 20.0$, $k_o a = 2.0$

$k_o a_1$	Direction of the peaks (in degrees)	Amplitude of H_z (Relative units)
0.08	59.13°	0.6444×10^{0}
	62.26°	0.7653×10^{1}
0.12	59.09°	0.6752×10^{0}
	62.26°	0.1062×10^{2}
0.16	59.0°	0.7023×10^{0}
	62.25°	0.1132×10^{2}

(3.7) and (3.8). It may also be noted that the amplitude and value of half power beam width are also affected by the plasma density.

Effect of $k_o a$:

$k_o a$ does not affect the direction of radiation peak but affects its amplitude. Hence for a fixed value of k_o, the direction of the peak is independent of the magnetic ring source but the amplitude of the peak is dependent upon the diameter of the ring source. The variation of major peak amplitude for ϵ_3 = .008I and ϵ_I = .9007 is shown in fig. 3.9.

3.I.4 DISCUSSION:

The study of radiation patterns of a magnetic ring source in an axially magnetized plasma column having central conductor along its axis shows the presence of well enhanced radiation peaks. The main observation in the present study is that for the case of $\epsilon_I < \epsilon_3$ (i.e. $w_c < w < w_p$), two radiation peaks are observed. The first peak corresponds to the minima of denominator and major peak corresponds to the maxima of the numerator. When ϵ_I is negative or $\epsilon_I > I$, only shallow peaks are obtained. It may also be noted that stronger radiation peaks are obtained for the case of high

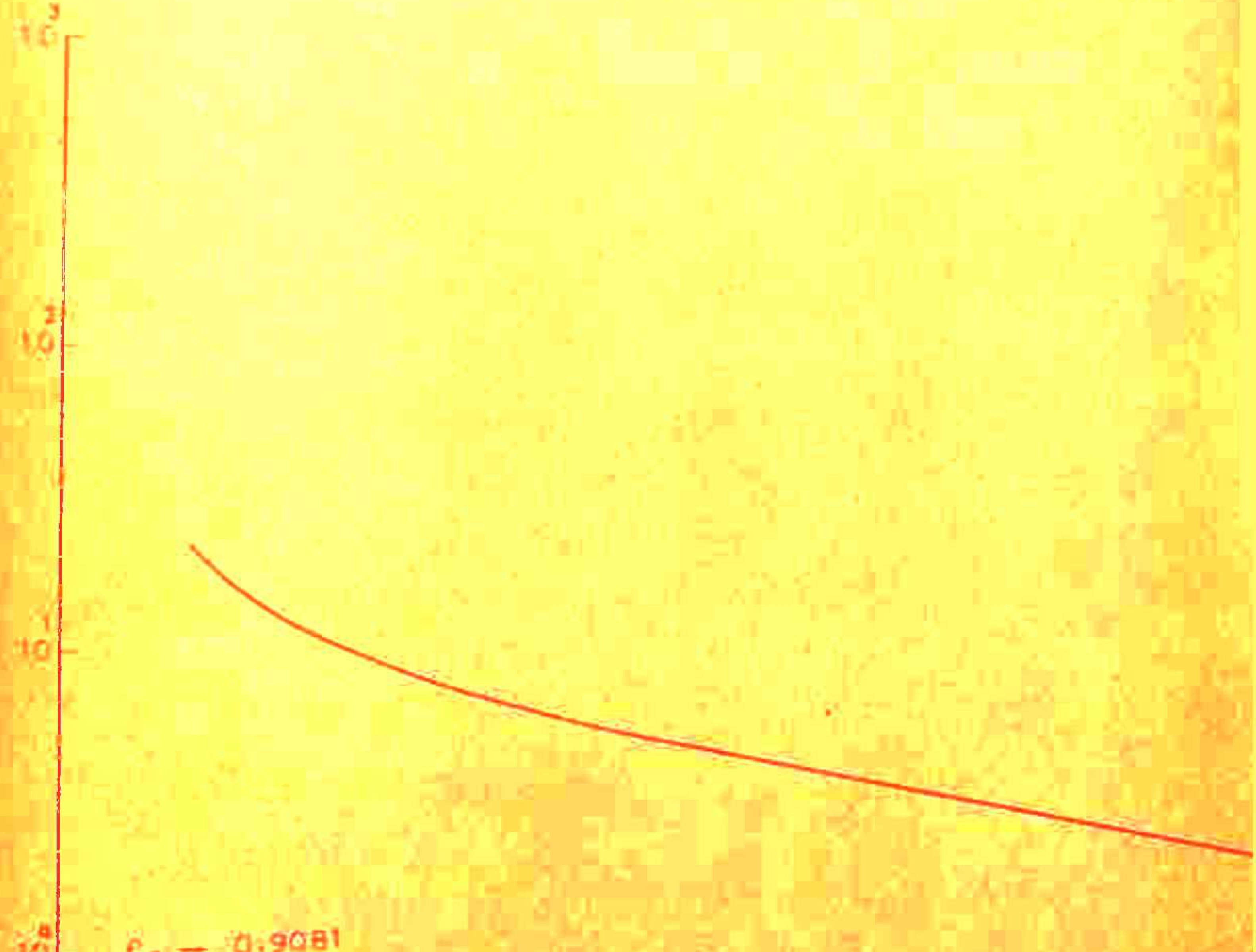
10^3
10^2
10^1
10^0
$\epsilon_3 = 0.9081$
$\epsilon_1 = 0.9007$
$\theta = 71.48^\circ$
1.0
2.0
3.0
4.0
5.0
6.0
7.0
8.0
9.0
$K_0 a$ →

FIG. 3.9

plasma density. For uniaxial plasma column, a sharp radiation peak at 90° corresponding to the maxima of numerator is obtained. The direction of the peak depends upon the plasma density (through ϵ_3), applied magnetic field (through ϵ_I), column diameter (through $k_o b$) and diameter of central conductor (through $k_o a_I$).

The expression for the radiation field of a magnetic ring source in axially magnetised plasma column in the absence of central conductor can not be deduced from that of magnetic ring source in axially magnetised plasma column having central conductor along its axis by merely putting the value of the diameter of central conductor equal to zero in it. It is because that very presence of the central conductor imposes forced boundary conditions on the fields of electromagnetic wave. The expression for the radiation field of the magnetic ring source in axially magnetised plasma column has been given in section 2.2. Comparing these two cases, we find that the very presence of the central conductor modifies the whole radiation pattern. This configuration gives rise to stronger radiation peaks with smaller value of half power beam width.

3.2 EXCITATION BY OPEN ENDED COAXIAL LINE:

3.2.I INTRODUCTION:

In section 3.I of this chapter, the radiation patterns of a magnetic ring source in an axially magnetized plasma column having central conductor along its axis have been discussed. In that case it is found that the diameter of magnetic ring source does not affect the direction of radiation peaks but affects only their amplitudes. The field distribution of a magnetic ring source is given by Kronecker's delta function. The physical realisation of such an ideal magnetic ring source is not very convenient. The study of the radiation pattern of an open ended coaxial line excited in TEM mode in an axially magnetized plasma column having central conductor along its axis is therefore made as an attempt in the direction of studying the case of more practically feasible source of electromagnetic waves.

The present study is concerned with the radiation patterns of an open ended coaxial line excited in an axially magnetized plasma column having central conductor along its axis. The field distribution at the open end cross-section of the coaxial line is assumed to be equivalent to the vector sum of magnetic current rings of various radii ranging from the outer radius of the inner conductor to the inner radius of the outer conductor of the coaxial line.

The radiation field is obtained as a vec-tor sum of field components due to individual rings of magnetic current.

This geometry gives rise to stronger radiation peaks with smaller value of half power beam- width. The direction of radiation peak depends upon the column diameter, the diameter of the central conductor, plasma density and applied magnetic field. The direction of radiation peak is independent of inner diameter of the outer conductor of the coaxial line at the open end. For uniaxial plasma column, the radiation peak is obtained at 90°.

3.2.2 ANALYSIS:

An infinitely long axially magnetised plasma column of radius 'b' having a central conductor of radius 'a_I' along its axis is oriented with its axis along the z-axis of the cylindrical coordinate (ρ, ϕ , z) system (fig. 3.10). The medium surrounding the plasma column and extending to infinity is free space, with permittivity and permeability ϵ_0 and μ_0. The source of electromagnetic radiation is an open ended coaxial line, with open end at the z = 0 plane.

The expression for the radiation field of a magnetic ring source in an axially magnetised plasma column

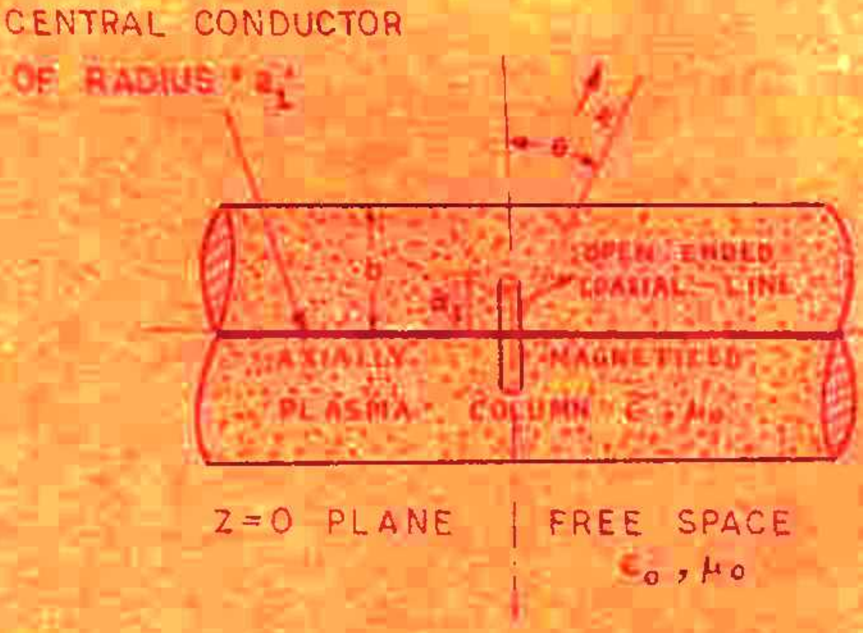
CENTRAL CONDUCTOR
OF RADIUS 'a_1'
R
θ
b
a_1
OPEN ENDED
COAXIAL LINE
AXIALLY MAGNETIZED
PLASMA COLUMN $\tilde{\epsilon}$, μ_0
Z=0 PLANE
FREE SPACE
ϵ_0, μ_0

FIG.

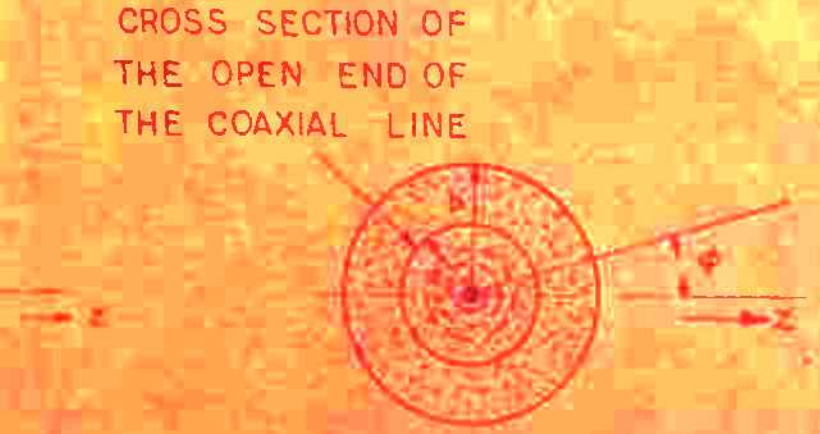
CROSS SECTION OF
THE OPEN END OF
THE COAXIAL LINE
b
a
φ
z
z

SECTION AT Z=0

3.10

having central conductor along its axis as derived in section 3.I.2 (equation 3.I.3) is

$$H_\phi (r, \theta) = \frac{-j\omega\epsilon_3}{\pi} \quad F(\theta) \frac{e^{jk_0\bar{r}}}{\bar{r}}$$

$$F(\theta) = F_I(\theta) \quad F_2(\theta)$$

$$F_I(\theta) = a \left\{ J_0(k_0 a_I v) Y_I(k_0 av) - Y_0(k_0 a_I v) J_I(k_0 av) \right\}$$

$$F_2(\theta) = \frac{I}{(k_0 bv) H_I(k_0 b \cos\theta) * \left\{ J_0(k_0 a_I v) Y_0(k_0 bv) - Y_0(k_0 a_I v) J_0(k_0 bv) \right\} - \epsilon_3 (k_0 b \cos\theta) H_0(k_0 b \cos\theta) * \left\{ J_0(k_0 a_I v) Y_I(k_0 bv) - Y_0(k_0 a_I v) J_I(k_0 bv) \right\}}$$

$F(\theta)$ is the factor which determines the variation of field with θ. $F_2(\theta)$ is independent of the source radius. The field distribution at the open end of the coaxial line (at the $z = 0$ plane) is assumed to be equivalent to the vector sum of magnetic current rings with various radii ranging from the outer radius of the inner conductor 'a_I' to the inner radius of the outer conductor 'a_3' of the coaxial line at the $z = 0$ plane. The magnitude of the magnetic current in each ring is assumed to be proportional to the value of H_ϕ at that particular location in the coaxial line. For a coaxial line excited in TEM mode, H_ϕ is proportional to $I_0/2\pi a$, where I_0 is the current. The total radial field of open ended coaxial line with its open end at the $z = 0$ plane can be obtained as a vector sum of the field components due to individual rings of magnetic current. So in the case of coaxial line excitation, $F(\theta)$ is modified to

$$F(\theta) = \int_{a_1}^{a_3} \frac{I_0}{2\pi a} \quad F_1(\theta)\, F_2(\theta)\, da$$

$$= F_2(\theta) \int_{a_1}^{a_3} a \left\{ J_0(k_0 a_1 v) Y_1(k_0 a v) - Y_0(k_0 a_1 v) J_1(k_0 a v) \right\} \cdot \frac{I_0}{2\pi a} \, da$$

$$= \frac{F_2(\theta)\, I_0}{2\pi\, (k_0 v)} \left\{ J_0(k_0 a_3 v) Y_0(k_0 a_1 v) - J_0(k_0 a_1 v) Y_0(k_0 a_3 v) \right\}$$

3.2.3 CHARACTERISTICS OF THE RADIATION FIELD:

The radiation patterns (variation of $F(\theta)$ with θ) have been computed with the help of an IBM-1130 computer for parametric values $k_0 b = 20.0$, $k_0 a_3 = 0.9$, $k_0 a_1 = 0.09$, $\epsilon_3 = .1100$ and $\epsilon_3 = .9061$. When plasma frequency is much lower than the source frequency, ϵ_3 is only slightly less than unity and we shall call it low plasma density case. On the other hand when w_p is only slightly lower than the source frequency, ϵ_3 is near zero and we shall call it a high plasma density case. Since $F(\theta)$ is an expression involving both the Bessel and Hankel functions in a complicated way, it is difficult to express analytically the behaviour of $F(\theta)$ with various parameters. Therefore computational results are presented first and then these results are analysed to give a qualitative relationship between the location of the peak and other parameters of the configuration. For given values of w/w_p, the valuesof ϵ_I change with w_c/w_p and may be divided into three sets as (i) $\epsilon_I \leq \epsilon_3$ (ii) ϵ_I is negative (iii) $\epsilon_I \geq 1$. The effects of various parameters on the shape of the radiation pattern are discussed below:

Effect of magnetic field in high density plasma (ϵ_3= .II00):

When $\epsilon_I \leq \epsilon_3$ one of the radiation peaks obtained, is a major radiation peak. The value of v becomes negative for $\epsilon_3 < \left(\frac{\epsilon_3}{\epsilon_I} \sin^2\theta\right)$ and ordinary Bessel function changes to modified form. For negative values the pattern becomes oscillatory so it has been plotted only for those values of θ for which v is positive. The radiation patterns for ϵ_I= .I020 and ϵ_I= .0325 are plotted in fig. 3.II. For ϵ_I= .I020, the radiation peaks at 5.2° and I8.63° are obtained with half power beam width equal to 2.2° and .0II° respectively. For ϵ_I= .0325, the radiation peaks at 4.5I° and I0.40° are obtained with half power beam width equal to 1.8° and .015° respectively. The detailed structure of the radiation peak

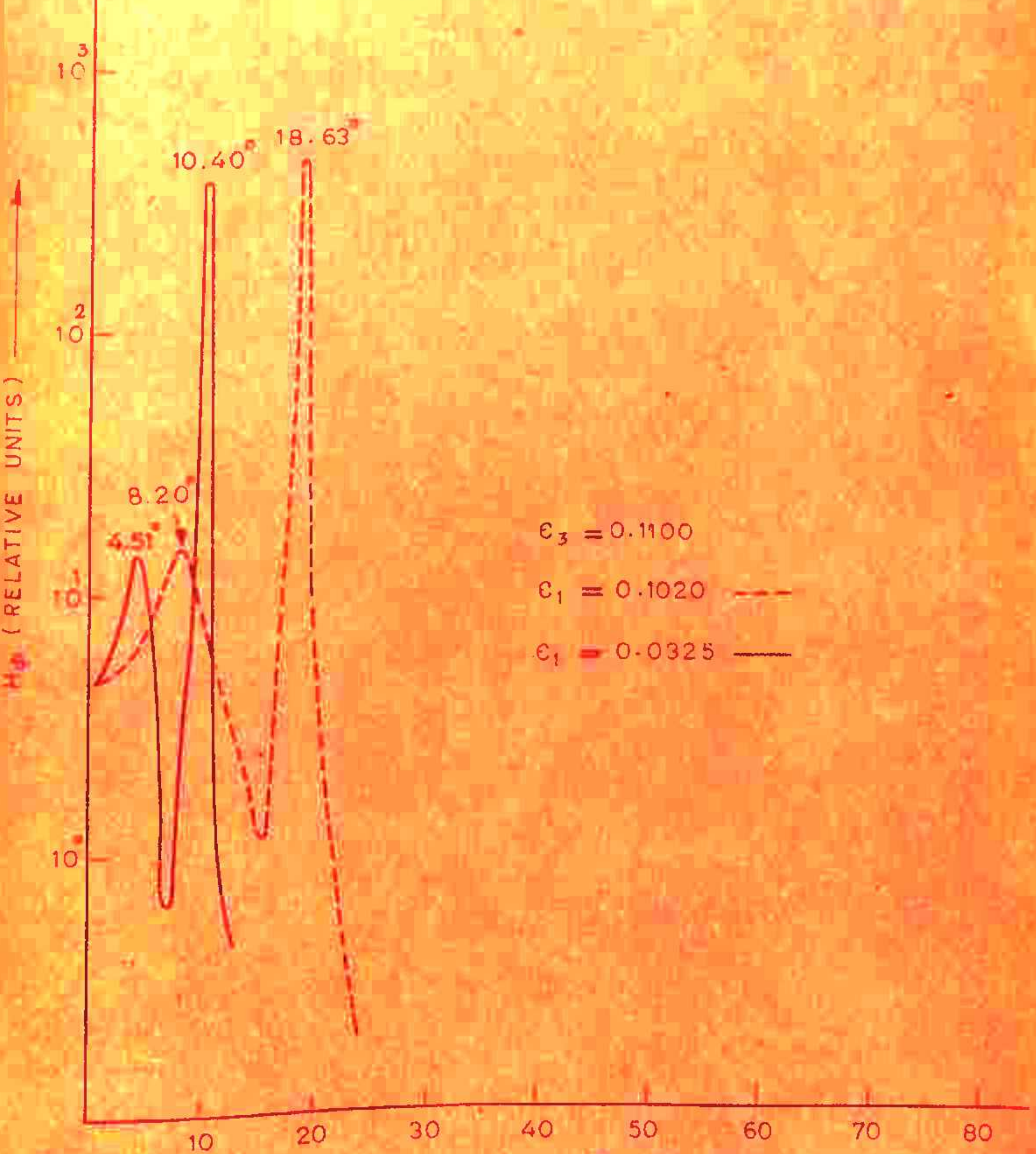
10³
10²
10¹
10⁰
H_θ (RELATIVE UNITS)
18.63°
10.40°
8.20°
4.51°
ε₃ = 0.1100
ε₁ = 0.1020
ε₁ = 0.0325
10
20
30
40
50
60
70
80
θ

FIG. 3.11

for ϵ_I = 0.0325 is shown in fig. 3.I3. The major radiation peak is obtained for minimum value of v or minimum value of $k_o bv$, $k_o a_I v$ and $k_o av$ as shown in Table 3.4. It may be noted that the major peak corresponds to the maxima of the numerator and the other peak is obtained for the minima of the denominator.

When ϵ_I is negative, the value of v increases as the value of θ increases. So, the values of $k_o bv$, $k_o a_I v$ and $k_o av$ also increase. For higher values of arguments, the Bessel functions are approximately equal to cosine and sine functions. Therefore, as θ varies from 0 to 90°, an oscillatory pattern is obtained. For ϵ_I = − 0.I446, the radiation pattern is shown in fig. 3.I4. For $\epsilon_I > I$, the value of v decreases as θ increases. No sharp radiation peaks are obtained in this case. For ϵ_I = I.04I8, the radiation pattern is shown in fig. 3.I4. When ϵ_I = I (i.e. infinite magnetic field), the numerator has maximum value at 90°, so a sharp radiation peak is obtained at 90° as shown in fig. 3.I5.

Effect of magnetic field in low density plasma (ϵ_o = .903I):

Qualitative results for the case of low density plasma are similar to that for high density plasma. The radiation patterns for ϵ_I = .9007 and ϵ_I = .7844 are plotted in fig. 3.I2.

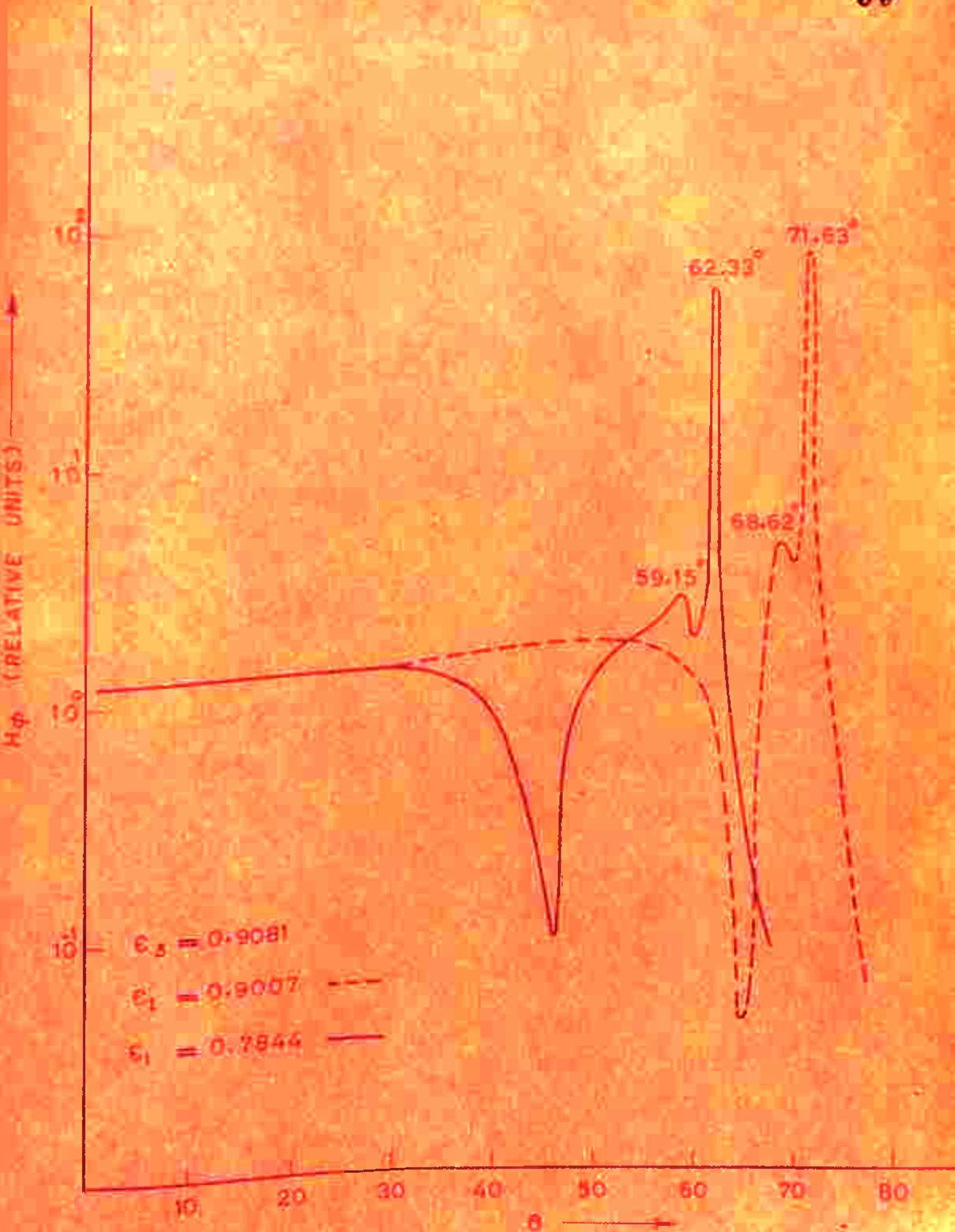
H_ϕ (RELATIVE UNITS) →
10^2
10^1
10^0
10^{-1}
71.63°
62.33°
68.62°
59.15°
ϵ_3 = 0.9081
ϵ_2 = 0.9007 ----
ϵ_1 = 0.7844 ——
10
20
30
40
50
60
70
80
θ →

FIG. 3.12

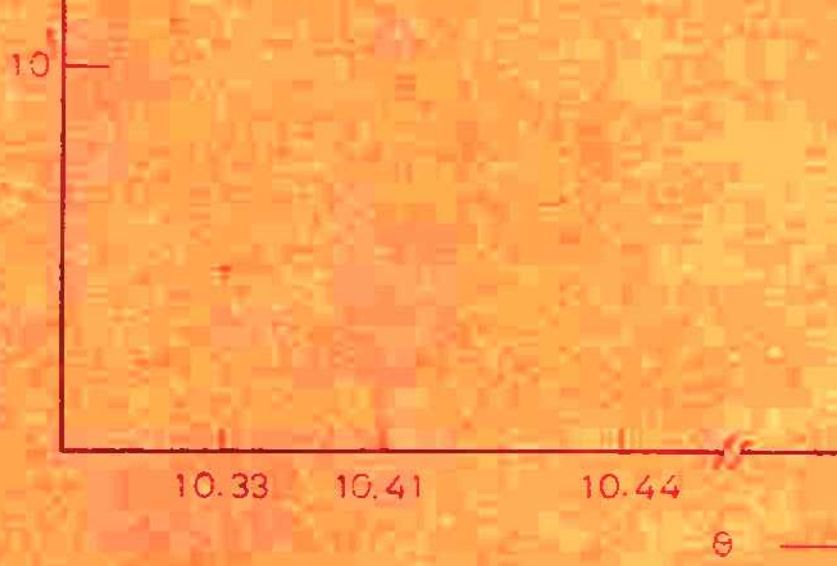

FIG. 3.1

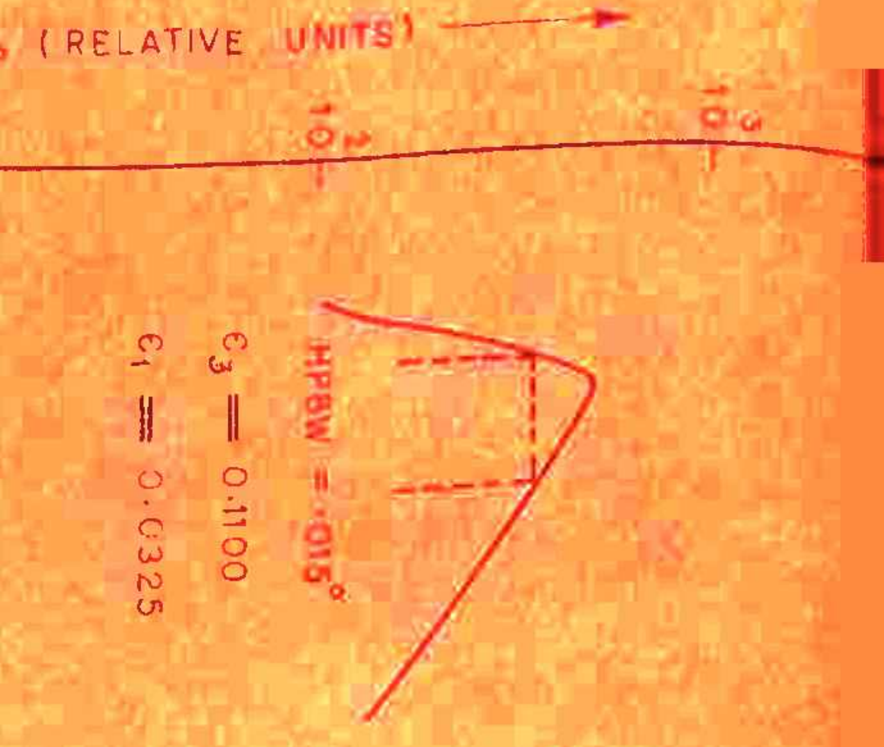
(RELATIVE UNITS)
10^2
10^3
HPBW = .015°
$\epsilon_3 = 0.1100$
$\epsilon_1 = 0.0325$

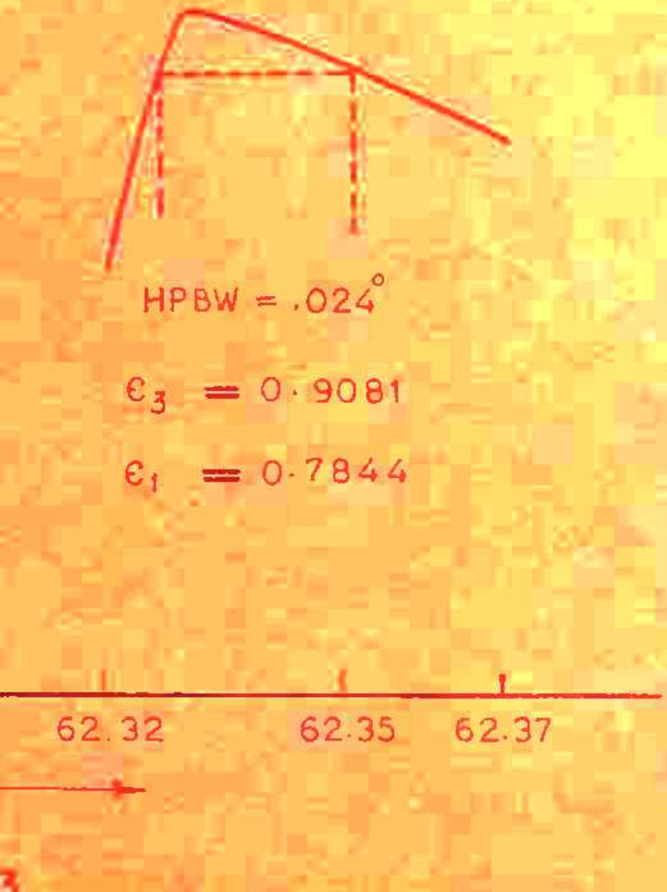
HPBW = .024°
ε3 = 0·9081
ε1 = 0·7844
62.32
62.35
62.37
3

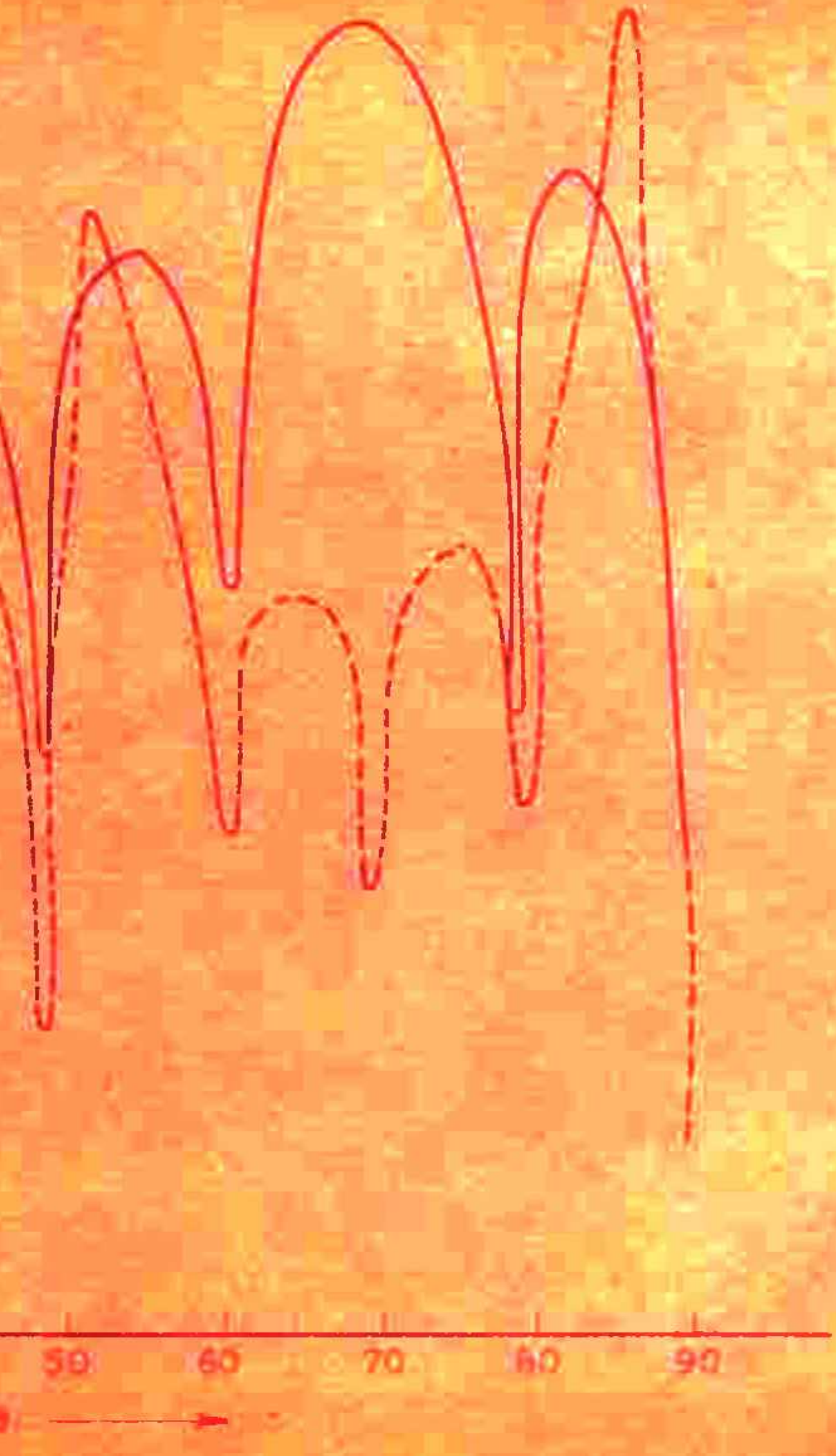

3.14

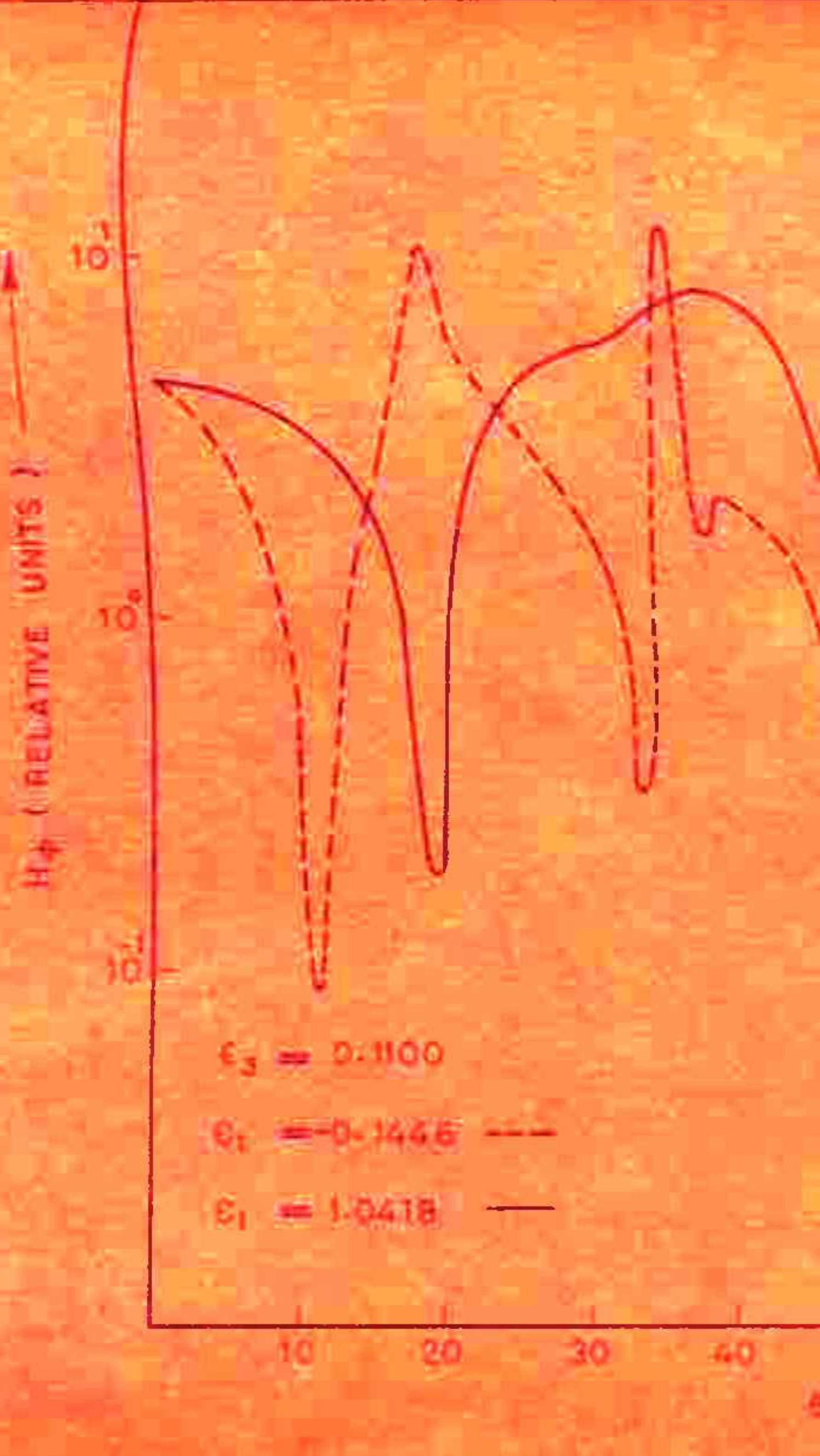10^{1}
10^{0}
10^{-1}
H_4 (RELATIVE UNITS)
ϵ_3 = 0·1100
ϵ_1 = −0·1446 ---
ϵ_1 = 1·0418 —
10
20
30
40

FIG.

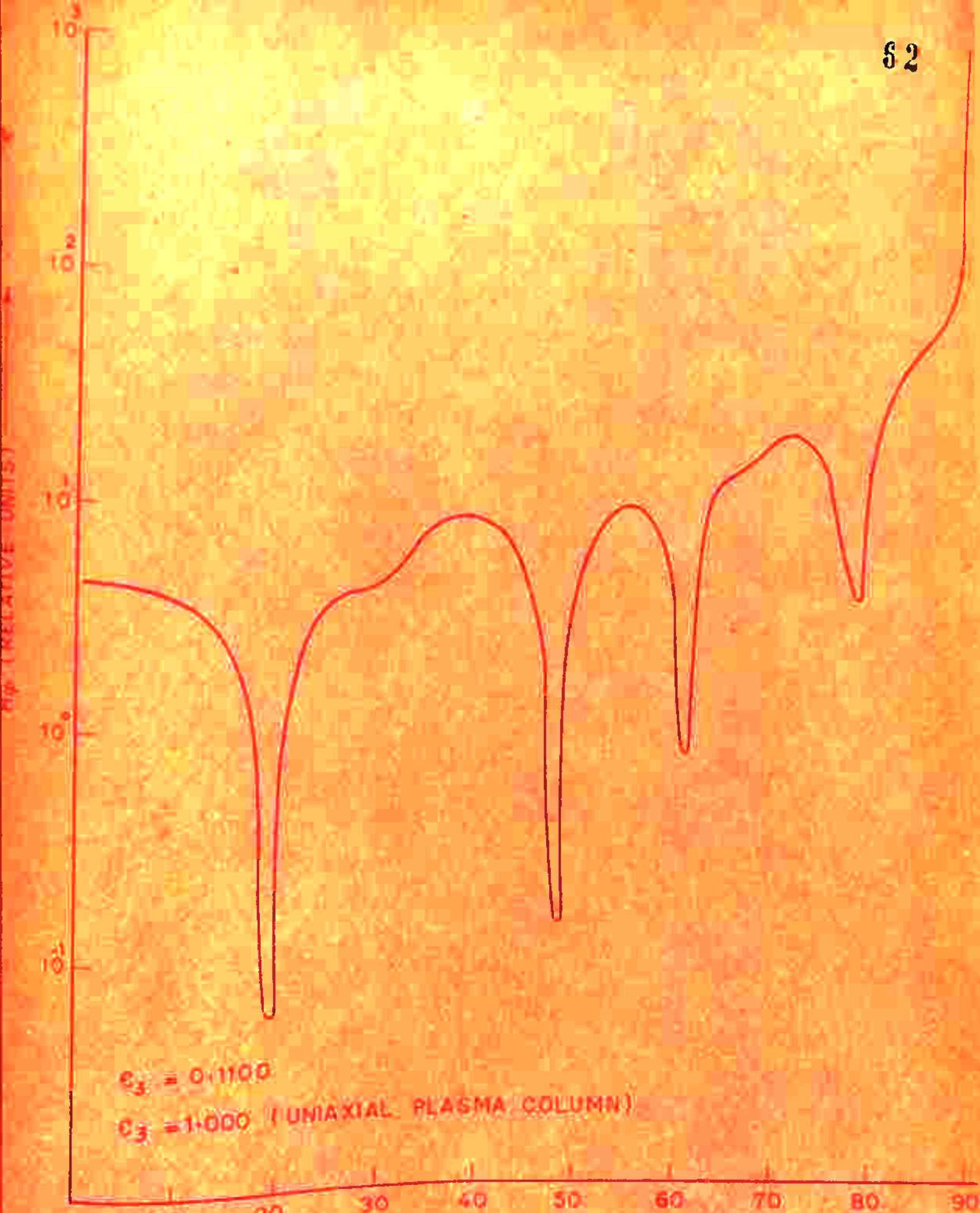
10^3
10^2
10^1
10^0
10^{-1}
Rp (RELATIVE UNITS)
$c_3 = 0{\cdot}1100$
$c_3 = 1{\cdot}000$ (UNIAXIAL PLASMA COLUMN)
10
20
30
40
50
60
70
80
90
θ

FIG. 3.15

For ϵ_I = .9007, the radiation peaks at 68.62° and 71.63° are obtained with half power beam width equal to 2.5° and .030° respectively. For ϵ_I = 0.7844, the radiation peaks at 59.15° and 62.33° are obtained with half power beam width equal to 1.7° and .024° respectively. The detailed structure of the major radiation peak for ϵ_I = 0.7844 is shown in fig. 3.13. The major radiation peak is obtained when the value of v is minimum or the value of $k_o bv$, $k_o c_I v$ and $k_o av$ is minimum as shown in Table 3.4. It may be noted that for this case also, the major peak corresponds to the maxima of the numerator and the other peak corresponds to the minima of the denominator.

When ϵ_I is negative, the F(θ) is governed by sine and cosine functions. So, as θ varies from 0 to 90°, an oscillatory pattern is obtained. For ϵ_I = −0.5384, the radiation pattern is shown in fig. 3.15. For ϵ_I = 1.1956, the pattern is plotted in fig. 3.16 and it can be seen that only shallow peaks are obtained. When ϵ_I = 1 (i.e. uniaxial case), the numerator has maximum value at 90°, so a sharp radiation peak is obtained at 90° as shown in fig. 3.17.

Effect of $k_o b$:

$k_o b$ affects the direction, number and the amplitude of the radiation peaks formed. For a fixed value of k_o, the

TABLE - 3.4

Parameters for the radiation peak.

High density plasma (ϵ_3 = 0.II00).

ϵ_I	Direction of the radiation peaks(in degrees)	K_0bv	k_0a_Iv	k_0a_3v	Denominator of F(0)	Numerator of F(0)	Amplitude of H_y (in relative unit
0.I020	8.2°	5.9346	0.0267	0.2670	$0.I094xI0^0$	$0.4889xI0^I$	$0.I409xI0^2$
	18.63°	0.2236	0.00I0	0.0I00	$0.3708xI0^I$	$0.I045xI0^4$	$0.4574xI0^3$
0.0325	4.5I°	5.9637	0.0268	0.2655	$0.II08xI0^0$	$0.4860xI0^I$	$0.I44IxI0^2$
	I0.40°	0.3755	0.00I6	0.0I68	$0.2074xI0^I$	$0.5696xI0^3$	$0.3705xI0^3$

Low density plasma (ϵ_3= 0.906I).

ϵ_I	Direction of the radiation peaks(in degrees)	K_0bv	k_0a_Iv	k_0a_3v	Denominator of F(0)	Numerator of F(0)	Amplitude of H_y (in relative unit
0.9007	68.62°	3.6689	0.0I65	0.I65I	$0.2593xI0^I$	$0.7959xI0^I$	$0.4369xI0^I$
	7I.63°	0.2638	0.00II	0.0II8	$0.6462xI0^2$	$0.864IxI0^3$	$0.7960xI0^2$
0.7874	59.I5°	4.6696	0.02I0	0.2I0I	$0.2I30xI0^I$	$0.6235xI0^I$	$0.I764xI0^I$
	62.33°	0.3I45	0.00I4	0.0I4I	$0.760IxI0^2$	$0.7025xI0^3$	$0.2064xI0^2$

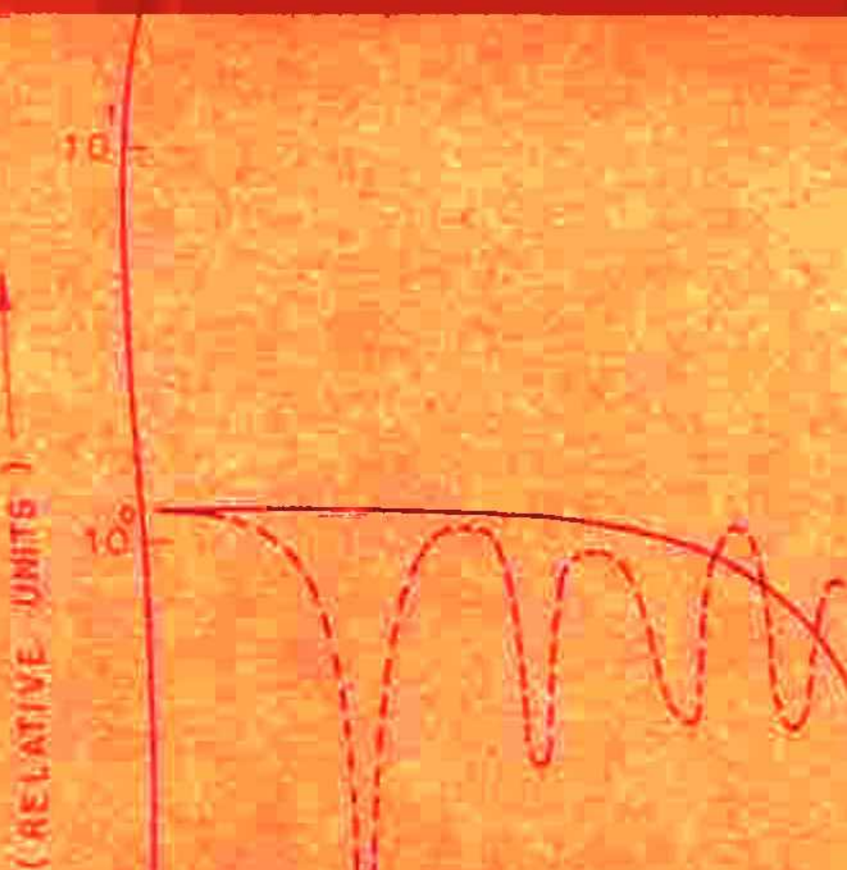
10^{1}
10^{0}
10^{-1}
Hp (RELATIVE UNITS)
$c_3 = 0.9061$
$c_1 = 1.1956$ ——
$c_1 = -0.5384$ - - - -
10
20
30
40

FI

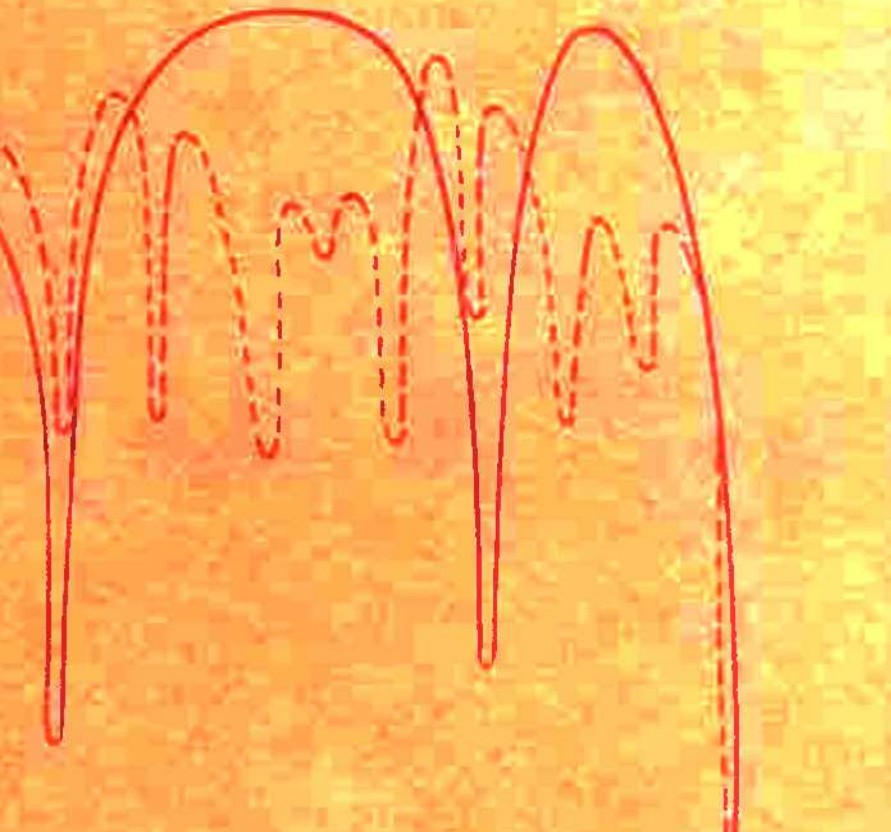

G. 3.16

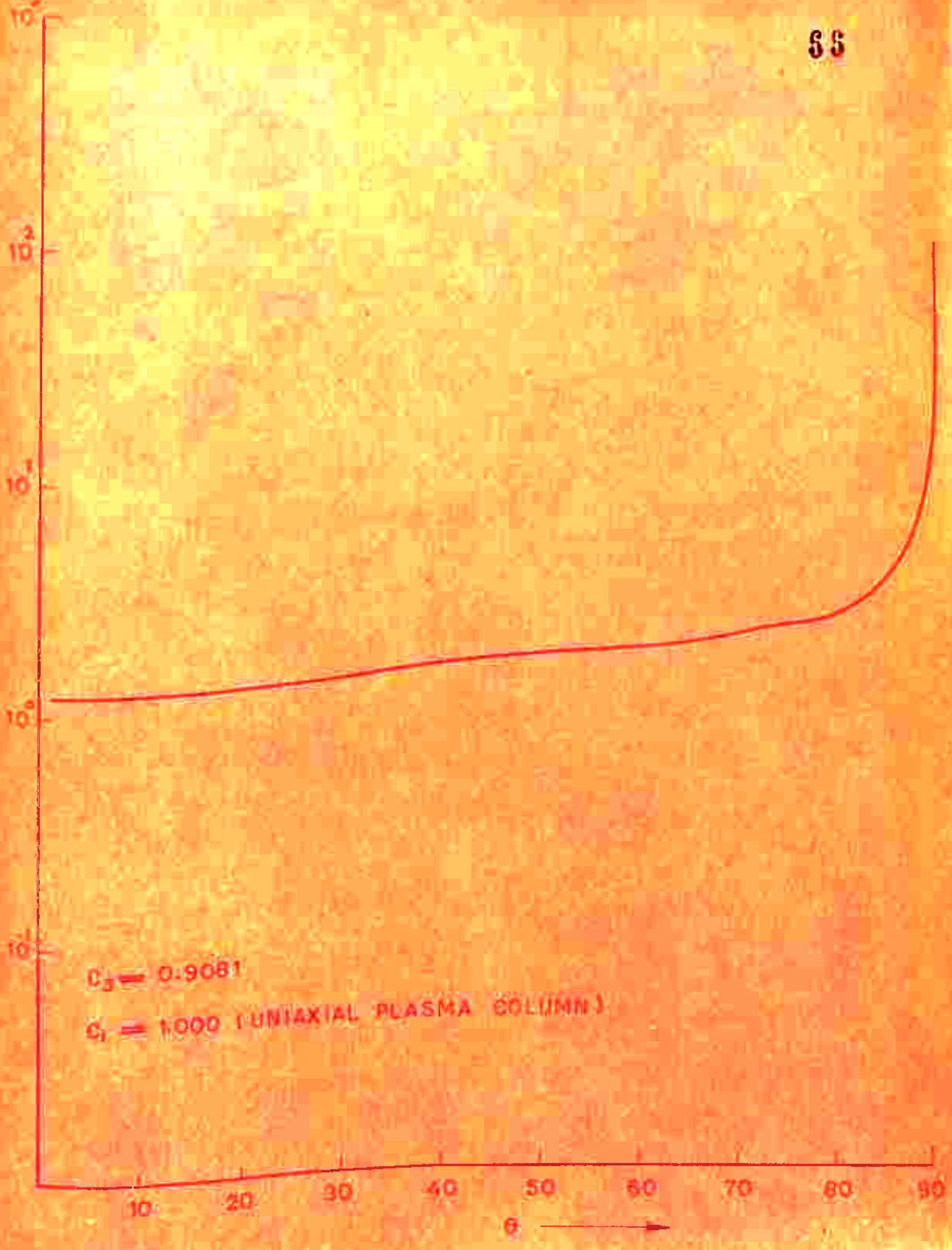
10^3
10^2
10^1
10^0
10^{-1}
C_3 = 0.9081
C_1 = 1.000 (UNIAXIAL PLASMA COLUMN)
10
20
30
40
50
60
70
80
90
θ →

FIG. 3.17

higher values of $k_o b$ mean increasing the diameter of the plasma column. Three different values of $k_o b$ = 2I.5, 23.0 and 24.0 have been taken. The directions and amplitudes of the radiation peaks for $\epsilon_3 = .II00$, $\epsilon_I = .0325$ and $\epsilon_3 = .908I$, $\epsilon_I = .7844$ are given in Table 3.5 for these three different values of $k_o b$.

Effect of $k_o a_I$:

$k_o a_I$ affects the amplitude of the radiation peaks and also their direction to a small extent. For fixed value of k_o, higher values of the diameter of central conductor give rise to weaker radiation peaks. The direction of major peak is not affected much but direction of the first peak is changed as given in Table 3.6. The directions and amplitudes of the radiation peaks for $\epsilon_3 = II00$, $\epsilon_I = .0325$ and $\epsilon_3 = .908I$, $\epsilon_I = .7844$ are given in Table 3.6 for three different values of $k_o a_I$.

Effect of plasma density:

The directions of the peaks are governed by the values of v (equ. 3.I.4). The ϵ_3 is given by $\epsilon_3 = (I - w_p^2/w^2)$ which in turn depends upon the plasma density . The radiation patterns for $\epsilon_3 = .II00$ and $\epsilon_3 = .008I$ are shown in fig. (3.II), (3.I2), (3.I3), (3.I4), (3.I5), (3.I6) and (3.I7). It may be

TABLE-3.0

Effect of varying $k_0 b$

(i.e. for a fixed value of k_0, varying the value of column diameter)

$\varepsilon_3 = 0.1100$, $\varepsilon_1 = 0.0325$, $k_0 a = 0.9$, $k_0 a_1 = 0.09$

$k_0 b$	Direction of the radiation peaks (in degrees)	Amplitude of H_z (in relative units)
21.5	4.59°	0.6405×10^1
	6.64°	0.9413×10^1
	9.10°	0.1208×10^2
23.0	6.54°	0.1537×10^2
	10.4°	0.3816×10^3
24.5	6.4°	0.8599×10^1
	9.39°	0.1500×10^2

$\varepsilon_3 = 0.9061$, $\varepsilon_1 = 0.7844$, $k_0 a = 0.9$, $k_0 a_1 = 0.09$

$k_0 b$	Direction of the radiation peaks (in degrees)	Amplitude of H_z (in relative units)
21.5	55.46°	0.3172×10^1
	6[illegible].80°	0.5276×10^1
	62.05°	0.7926×10^2
23.0	55.35°	0.2625×10^1
	62.93°	0.7039×10^2
24.5	55.90°	0.1624×10^1
	60.58°	0.7619×10^1
	62.29°	0.3829×10^2

TABLE -3.6

Effect of varying $k_o a_I$

(i.e. for a fixed value of k_o, varying the diameter of the central conductor)

$\varepsilon_3 = 0.1100$, $\varepsilon_I = 0.0325$, $k_o b = 20.0$, $k_o a = 0.9$

$k_o a_I$	Direction of the radiation peaks (in degrees)	Amplitude of H_ϕ (in relative units)
0.06	4.63°	0.1553×10^2
	10.38°	0.3817×10^3
0.07	4.60°	0.1512×10^2
	10.40°	0.3805×10^3
0.08	4.55°	0.1476×10^2
	10.40°	0.3794×10^3

$\varepsilon_3 = 0.9081$, $\varepsilon_I = 0.7644$, $k_o b = 20$, $k_o a = 0.9$

$k_o a_I$	Direction of the radiation peaks (in degrees)	Amplitude of H_ϕ (in (relative units)
0.06	59.21°	0.3051×10^1
	62.29°	0.5668×10^2
0.07	59.19°	0.2946×10^1
	62.32°	0.5139×10^2
0.08	59.17°	0.2857×10^1
	62.33°	0.5099×10^2

noted that the amplitude and half power beam width is also affected by the plasma density.

Effect of $k_0 a_3$:

$k_0 a_3$ does not affect the direction of radiation peaks of the radiation pattern but affects their amplitudes only. For excitation of the TEM-mode in a coaxial line, $k_0 a_3$ should be less than one ($k_0 a_3 < 1$). The variation of peak amplitude with $k_0 a_3$ is shown in fig. 3.18.

3.2.4 DISCUSSION:

The radiation patterns of an open ended coaxial line in an axially magnetised plasma column having a central conductor along its axis are studied in this section. The direction of the peak can be changed by varying plasma density, applied magnetic field, column diameter and diameter of the central conductor. This geometry gives rise to stronger radiation peak with a smaller value of half power width in comparison to the geometry analysed in section 3.1.

In case of magnetic ring source excitation (section 3.1), the field distribution of source is given by Kronecker's delta function. The physical realisation of such an ideal

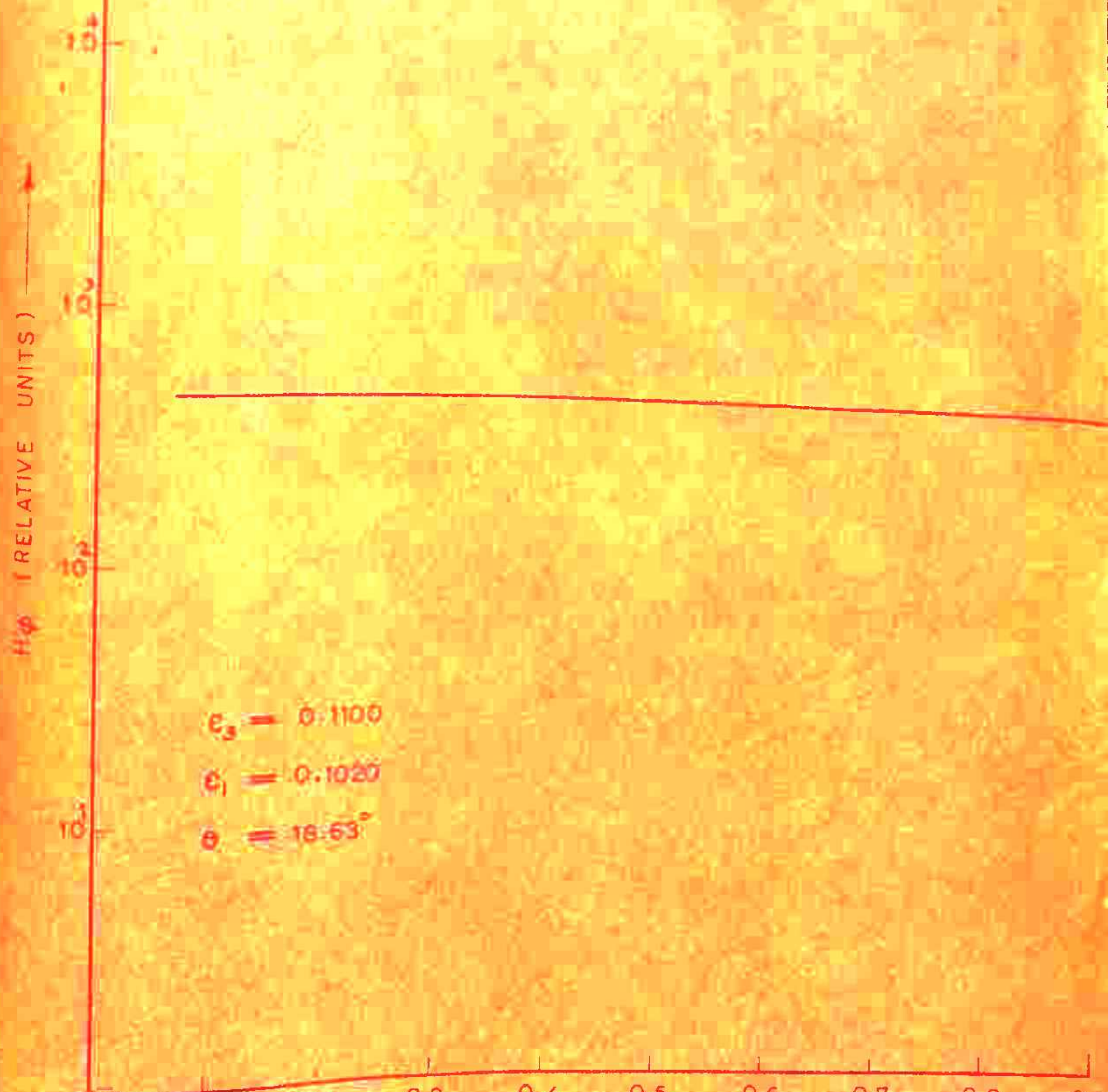
10^4
10^3
10^2
10^1
H_ϕ (RELATIVE UNITS)
ϵ_3 = 0.1100
ϵ_1 = 0.1020
θ = 18.53°
0.1
0.2
0.3
0.4
0.5
0.6
0.7
0.8
0.9
$K_0 a_3$

FIG. 3.18

source is not very convenient. It is also found in ring source excitation that the direction of peak is not affected by the diameter of ring source but its amplitude decreases with the increase in the diameter of ring source. This fact inspired the author to study the radiation patterns for the case of an open ended coaxial line excitation which provides the smaller value of $k_o a_3$ (for TEM mode excitation in coaxial line $k_o a_3 < I$) where k_o is free space propagation constant and 'a_3' is the inner radius of the outer conductor of the coaxial line. The study of coaxial line excitation is also an attempt in the direction of studying a more practically feasible source of excitation.

CHAPTER 4.

EXCITATION OF ANNULAR AXIALLY MAGNETIZED PLASMA COLUMN SURROUNDING AN AIR CORE HAVING CENTRAL CONDUCTOR

4.I Excitation by magnetic ring source

4.I.I Introduction 74
4.I.2 Analysis 75
4.I.3 Characteristics of the radiation field 80
4.I.4 Discussion IOI

4.2 Excitation by open ended coaxial line

4.2.I Introduction I04
4.2.2 Analysis I05
4.2.3 Characteristics of the radiation field I09
4.2.4 Discussion I26

CHAPTER 4.

EXCITATION OF ANNULAR AXIALLY MAGNETIZED PLASMA COLUMN SURROUNDING AN AIR CORE HAVING CENTRAL CONDUCTOR:

4.I EXCITATIONS BY MAGNETIC RING SOURCE:

4.I.I INTRODUCTION:

Harrison[22] studied the radiation patterns of an infinite magnetic line source in air gap between grounded plane and plasma slab. He predicted the presence of sharp narrow beam radiation peaks beyond the critical angle. The corresponding cylindrical plasma geometry (annular isotropic plasma column surrounding an air core having central conduc-tor along its axis) excited by the magnetic ring source in air core has been studied by Dhani Ram and Verma[I2]. They have also predicted the presence of well enhanced radiation peak beyond the critical angle and suggested to develop an electronically scannable narrow beam plasma antenna system.

In this chapter, the radiation patterns of a magnetic ring source of electromagnetic waves, in an air column having a central conductor along its axis and surrounded by an annular axially magnetized plasma column are studied. The radiation peaks or a peak is obtained in the patterns depending upon the parametric values of the configuration. The direction of radiation peak depends upon the inner and outer diameters of the annular plasma column, diameter of the central conductor, plasma density and applied magnetic field. The direction of the radiation peak is independent of the diameter of ring source. For uniaxial plasma column, a sharp radiation peak at 90° is obtained.

In the analysis carried out, the plasma is considered to be a lossless and anisotropic dielectric medium with the permittivity given by the commonly used permittivity tensor. Thermal effects are neglected and plasma density is considered to be uniform over the cross- section of the column. The existence of a pure E-mode is considered. The inhomogeneous wave equations are solved by the method of Fourier-Transform . This yields the solution for the field in form of a definite integral. The radiation field is obtained from the asymptotic evaluation of the integral by saddle point integration. The method of saddle point integration is given in Appendix D.

4.I.2 ANALYSIS:

The geometry of configuration analysed is illustrated in fig. 4.I. An infinitely long air column of radius 'a_2' having infinitely long conductor of radius 'a_1' along the longitudinal axis and surrounded by axially magnetised annular plasma column of inner radius 'a_2' and outer radius 'b' is oriented with its axis along the z-axis of the (ρ, ϕ , z)

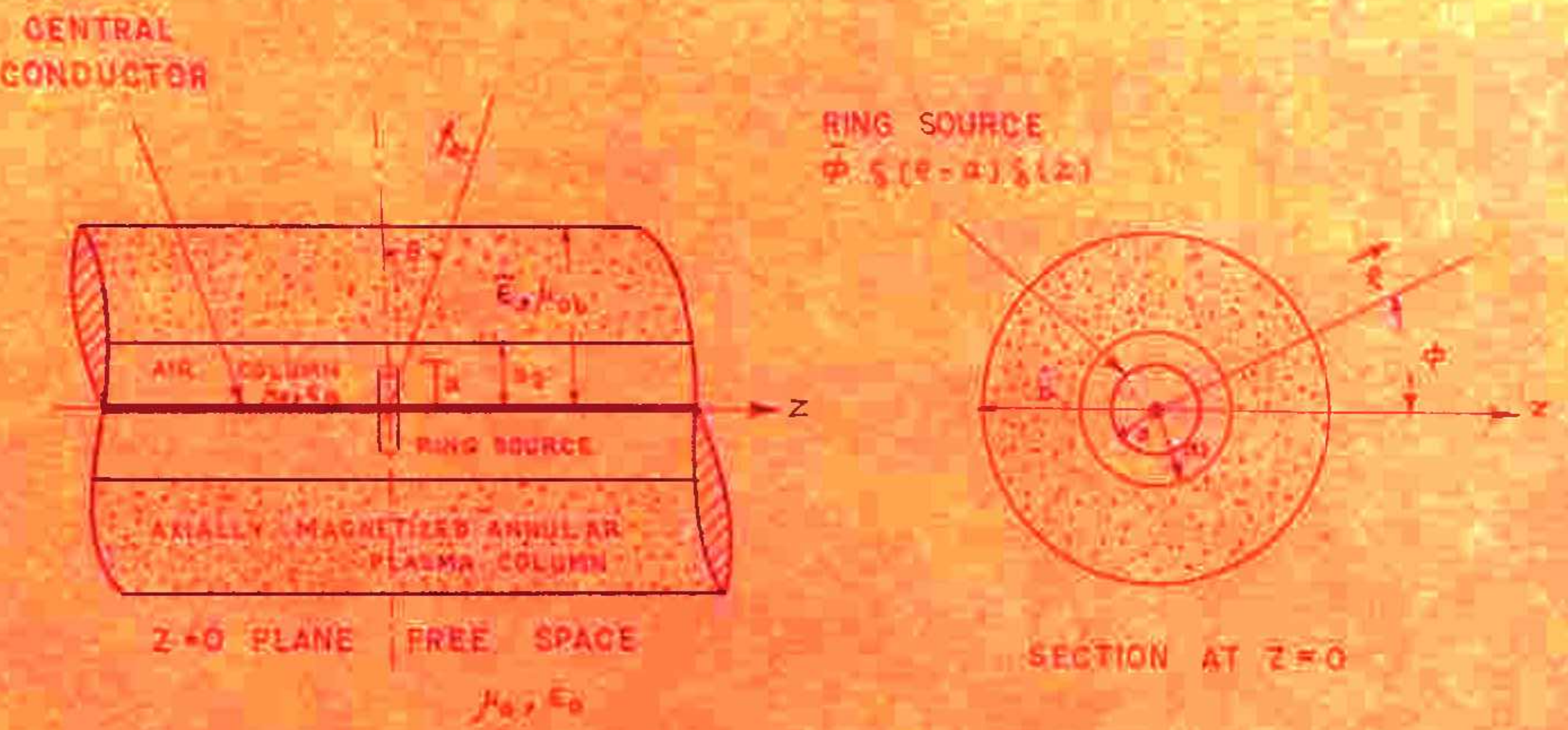
CENTRAL CONDUCTOR
ρ_o
b
$\bar{\epsilon}_p, \mu_{0b}$
AIR COLUMN μ_0, ϵ_0
a
b_2
Z
RING SOURCE
AXIALLY MAGNETIZED ANNULAR PLASMA COLUMN
Z=0 PLANE
FREE SPACE
μ_0, ϵ_0
RING SOURCE
$\bar{\Phi}\,\delta(\rho-a)\,\delta(z)$
ρ
ϕ
b
a
b_2
z
SECTION AT Z=0

FIG. 4.1

cylindrical coordinate system. The medium surrounding the plasma column and extending to infinity is free space, with permittivity and permeability ϵ_o and μ_o . The source of electromagnetic wave is a filamentary ring of magnetic current of radius 'a' ($a < a_2$) concentric with air column and situated at $z=0$ plane. The field distribution of such a ring source can mathematically be represented as

$$\bar{K} = \bar{\phi}\,\delta(\,\rho - a\,)\,\delta(\,z\,) \qquad (4.I.I)$$

where δ represents Kronecker's delta function and $\bar{\phi}$ is a unit vector in ϕ - direction.

Due to the choice of the source of excitation, the electromagnetic fields will be independent of the angular coordinate (i.e. $\partial/\partial\phi = 0$). For the circular symmetric TM_{0I} mode, the inhomogeneous wave equation for H_ϕ (the ϕ - component of the magnetic field) may be written as

$$\frac{\partial^2 H_\phi}{\partial\rho^2} + \frac{I}{\rho^2}\,\frac{\partial H_\phi}{\partial\rho} - \frac{I}{\rho^2}H_\phi + \frac{\epsilon_3}{\epsilon_I}\,\frac{\partial^2 H_\phi}{\partial z^2}$$

$$+ k_o^2\epsilon_3 H_\phi = -\,jw\epsilon_o\epsilon_3\,\delta(\rho - a)\,\delta(\,z\,) \qquad (4.I.2)$$

where $k_o^2 = w^2\mu_o\epsilon_o$, and ϵ_I and ϵ_3 are the components of the dielectric tensor given in Appendix A.

In order to slove equation (4.I.2) for H_ϕ it is first reduced to a homogeneous ordinary differential equation by the method of Fourier-Transform. Then it can be solved in terms of Bessel function, with particular reference to the radiation field, by essentially the procedure outlined by Duncan[3I] and Gupta and Singh[27], with appropriate boundary conditions at the junctions of different radial zones. The details of analysis are given in Appendix C. The solution of the radiation field in spherical coordinate system (r, θ, ϕ) can be put in the form,

$$H_\phi (r, \theta) = \frac{j\omega\epsilon_0\epsilon_a\ a}{\pi} F(\theta) \frac{e^{jk_0\bar{r}}}{\bar{r}} \qquad (4.I.3)$$

where

$$F(\theta) = \frac{J_0(k_0 a_I v_I)Y_I(k_0 a v_I) - Y_0(k_0 a_I v_I)\, J_I(k_0 a v_I)}{J_0(k_0 a_I v_I)G_I(\theta) - Y_0(k_0 a_I v_I)\, G_2(\theta)} \qquad (4.I.4)$$

$G_I(\theta) = AC + BD$

$G_2(\theta) = AF + BE$

$A = \epsilon_3(k_0 b \cos\theta)\ Y_I(k_0 bv)\ H_0(k_0 b \cos\theta)$

$\quad - (k_0 bv)\ Y_0(k_0 bv)\ H_I(k_0 b \cos\theta)$

$B = \epsilon_3 (k_0 b \cos\theta)\ H_0(k_0 b \cos\theta)\ J_I(k_0 bv)$

$\quad - (k_0 bv)\ J_0(k_0 bv)\ H_I(k_0 b \cos\theta)$

$$C = (k_o a_2 v_I)\, J_I(k_o a_2 v)\, Y_o(k_o a_2 v_I) - \frac{\epsilon_a}{\epsilon_3} (k_o a_2 v)\, Y_I(k_o a_2 v_I)\, J_o(k_o a_2 v)$$

$$D = \frac{\epsilon_a}{\epsilon_3} (k_o a_2 v)\, Y_o(k_o a_2 v)\, Y_I(k_o a_2 v_I) -(k_o a_2 v_I)\, Y_I(k_o a_2 v)\, Y_o(k_o a_2 v_I)$$

$$E = \frac{\epsilon_a}{\epsilon_3} (k_o a_2 v)\, J_I(k_o a_2 v_I)\, Y_o(k_o a_2 v) - (k_o a_2 v_I)\, Y_I (k_o a_2 v)\, J_o(k_o a_2 v_I)$$

$$F = (k_o a_2 v_I)\, J_I(k_o a_2 v_I)\, J_o(k_o a_2 v_I) - \frac{\epsilon_a}{\epsilon_3} (k_o a_2 v)\, J_o(k_o a_2 v)\, J_I(k_o a_2 v_I)$$

$$v_I = \sqrt{(\epsilon_a - \sin^2\theta)} \qquad (4.I.5)$$

$$v = \sqrt{\left(\epsilon_3 - \frac{\epsilon_3}{\epsilon_I} \sin^2 \theta \right)} \qquad (4.I.6)$$

ϵ_o, μ_o are free space permittivity and permeability respectively. k_o is free space propagation constant, ϵ_a is the permittivity of air and ϵ_I and ϵ_3 are components of the permittivity tensor. J_n, Y_n, H_n are Bessel functions of first kind, second kind, Hankel function of first kind and of nth order respectively, and $F(\theta)$ is the factor which determines the variation of field with θ.

4.1.3 CHARACTERISTICS OF THE RADIATION FIELD:

The radiation patterns (variation of $F(\theta)$ with θ) have been computed with the help of of an IBM-1130 computer for parametric values $k_o a_1 = 0.2$, $k_o a = 2.0$, $k_o a_2 = 5.0$, $k_o b = 1.0$, $\epsilon_3 = .1100$ and $\epsilon_3 = .9081$. When plasma frequency is much lower than the source frequency, ϵ_3 is only slightly less than unity and we shall call it low plasma density case. On the other hand when w_p is only slightly lower than the source frequency, ϵ_3 is near zero and we shall call it a high plasma density case. Since $F(\theta)$ is an expression involving both the Bessel and Hankel functions in a very complicated way, it is difficult to express analytically the behaviour of $F(\theta)$ with various parameters. Therefore, the computational results are presented first and then these results are analysed to give a qualitative relationship between the location of peak and other parameters of the configuration. For given values of w/w_p , the value of ϵ_1 changes with w_o/w_p and may be divided into three sets as (i) $\epsilon_1 \leq \epsilon_3$ (ii) ϵ_1 is negative (iii) $\epsilon_1 \geq 1$. The effects of various parameters on the shape of the radiation pattern are discussed below:

Effect of magnetic field in high density plasma ($\epsilon_3 = 0.1100$):

When $\epsilon_1 < \epsilon_3$, the radiation pattern has peaks as shown in fig. 4.2a. The detailed structure of the radiation peaks

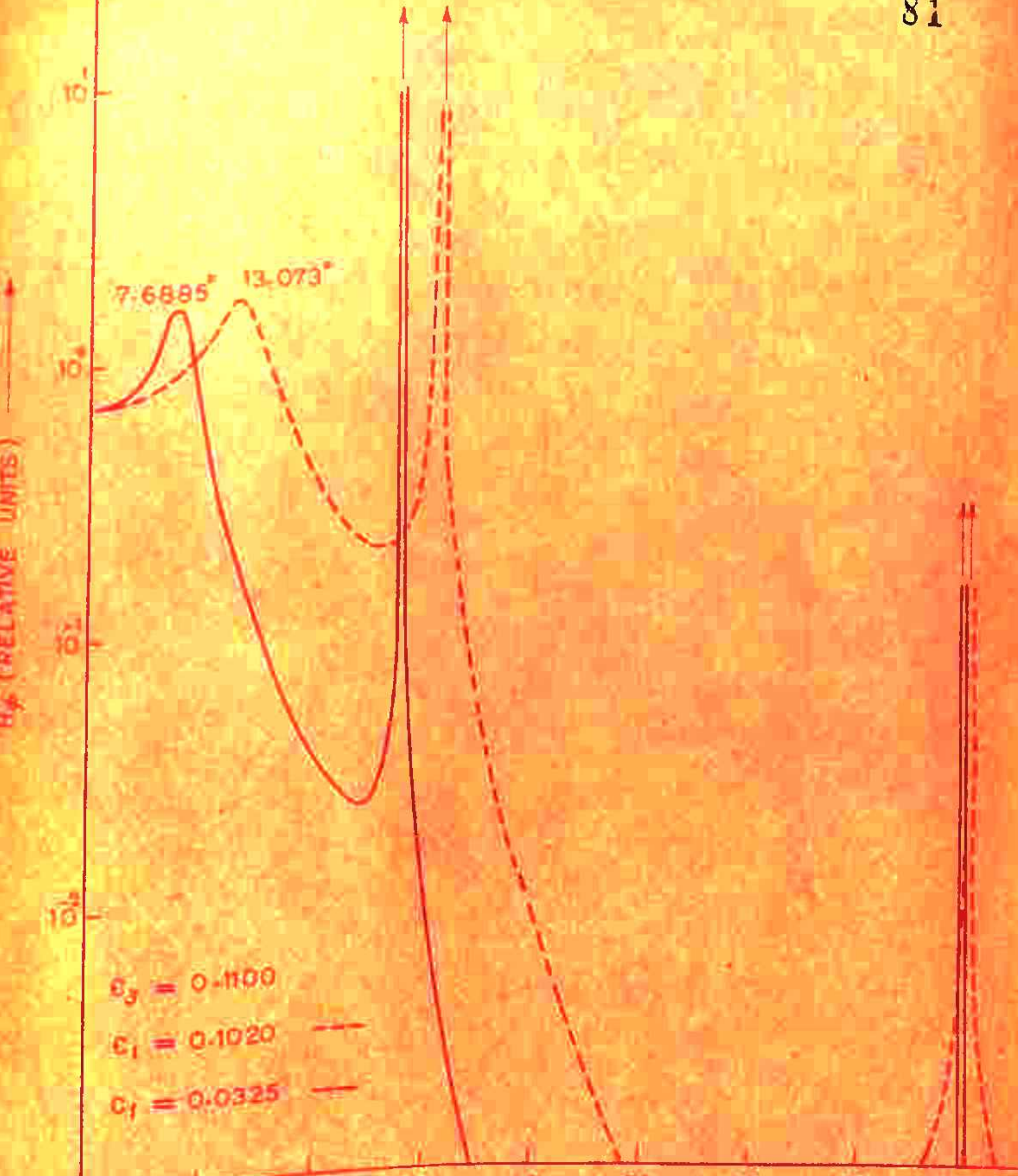
10^{1}
10^{0}
10^{-1}
10^{-2}
H_ϕ (RELATIVE UNITS)
7.6885°
13.073°
c_3 = 0.1100
c_1 = 0.1020
c_1 = 0.0325
10
20
30
40
50
60
70
80
θ

FIG. 4.2 a

is shown in fig. 4.2b and fig. 4.2c. For this case, the value of v becomes negative for values $\epsilon_3 < \left(\frac{\epsilon_3}{\epsilon_1} \sin^2\theta \right)$ and ordinary Bessel functions change to modified form. The values of $k_o bv$, $k_o a_2 v$ and $k_o a_1 v$ first decrease as θ increases and then increase as θ increases, while values of $k_o a_1 v_1$, $k_o a v_1$ and $k_o a_2 v_1$ always decrease with increasing θ. The denominator of $F(\theta)$ for $\epsilon_3 = 0.1020$ varies with θ as shown in fig. 4.3(a,b). The peaks in the radiation patterns correspond to the minima of the denominator of $F(\theta)$. For $\epsilon_1 = 0.1020$, the peak occurs at 13.073°, 31.0517° and 80.002° with half power beam width equal to 4.4°, .00039° and .00032° respectively. For $\epsilon_1 = 0.0325$, the peaks occur at 7.6885°, 27.8987° and 79.882° with half power beam widths equal to 2.8°, 0.00026° and 0.00052° respectively. The parameters for which peaks occur are given in Table 4.1. It may be pointed that at $v = 0$, (that is near $\theta = 18^\circ$ for $\epsilon_1 = 0.1020$ and near $\theta = 10^\circ$ for $\epsilon_1 = 0.0325$) the radiation pattern does not have a peak although the denominator tends to zero. This is because of the fact that for $v = 0$, numerator also tends to zero and their ratio is finite.

When ϵ_1 is negative, the value of v increases as θ increases. The values of $k_o bv$, $k_o a_2 v$ and $k_o a_1 v$ increase as θ increases but $k_o a_1 v_1$, $k_o a v_1$ and $k_o a_2 v_1$ decrease with

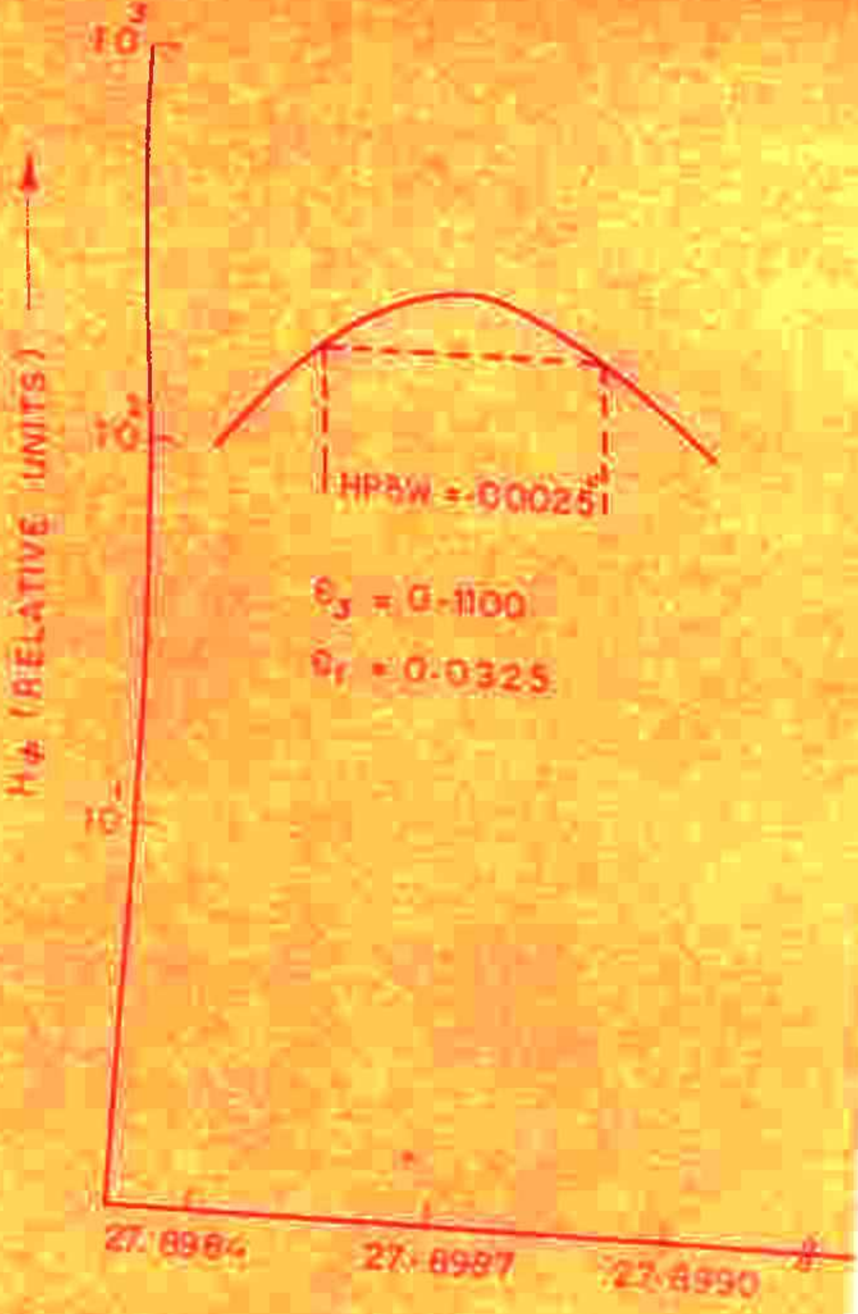
10^3
10^2
10^1
Hφ (RELATIVE UNITS)
HPBW = 0.0025
$\varepsilon_3 = 0.1100$
$a_r = 0.0325$
27.8984
27.8987
27.8990
θ

FIG.

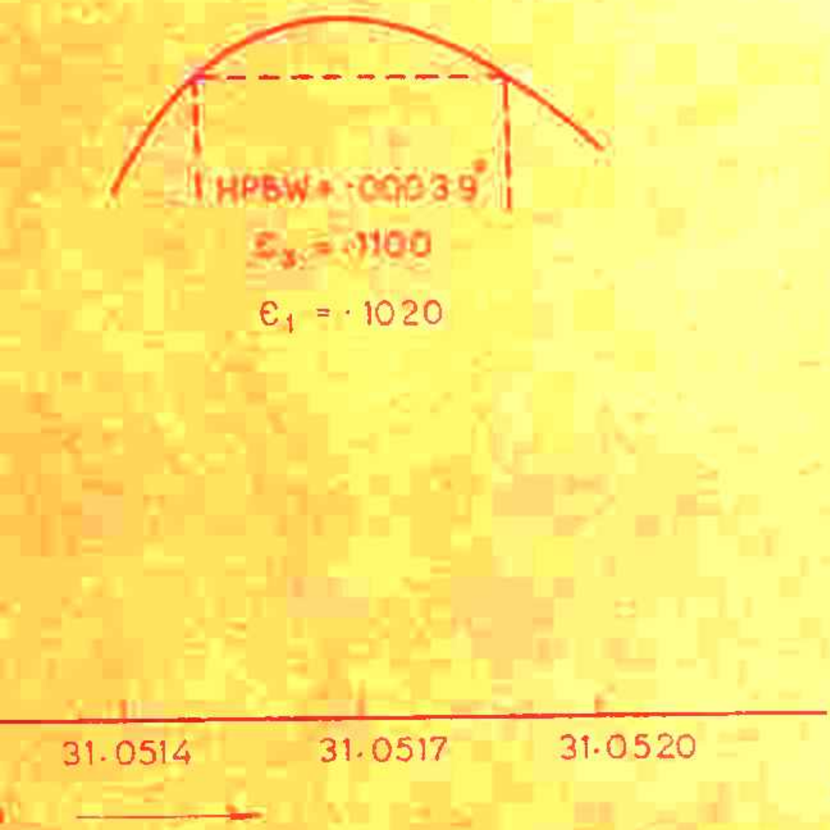
HPBW = ·00039°
ε_3 = ·1100
ε_1 = ·1020
31·0514
31·0517
31·0520

4. 2b

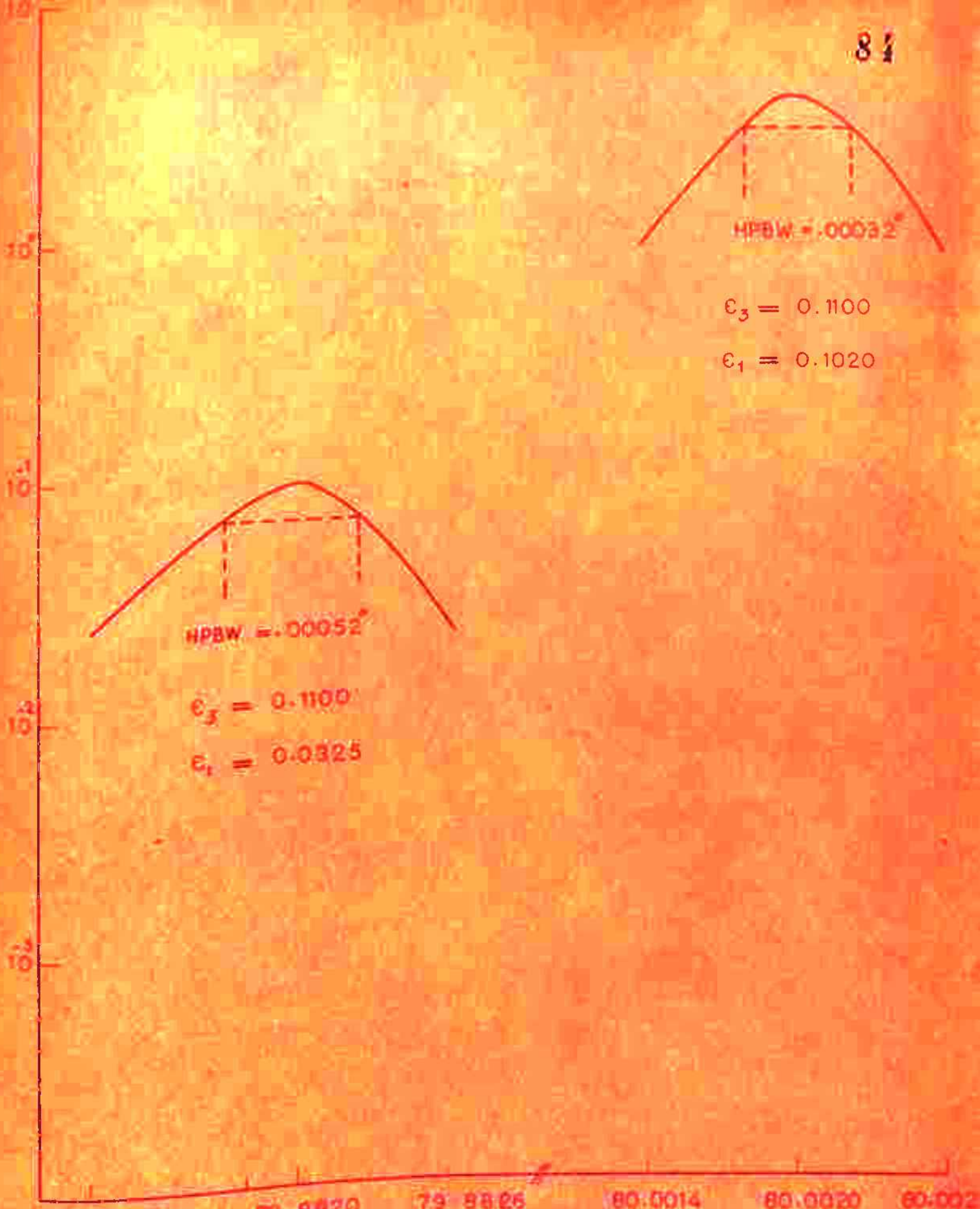
10
10^{0}
10^{-1}
10^{-2}
10^{-3}
HPBW = .00032°
$\epsilon_3 = 0.1100$
$\epsilon_1 = 0.1020$
HPBW = .00052°
$\epsilon_3 = 0.1100$
$\epsilon_1 = 0.0325$
79.8812
79.8820
79.8826
80.0014
80.0020
80.002
θ ⟶

FIG. 4.2C

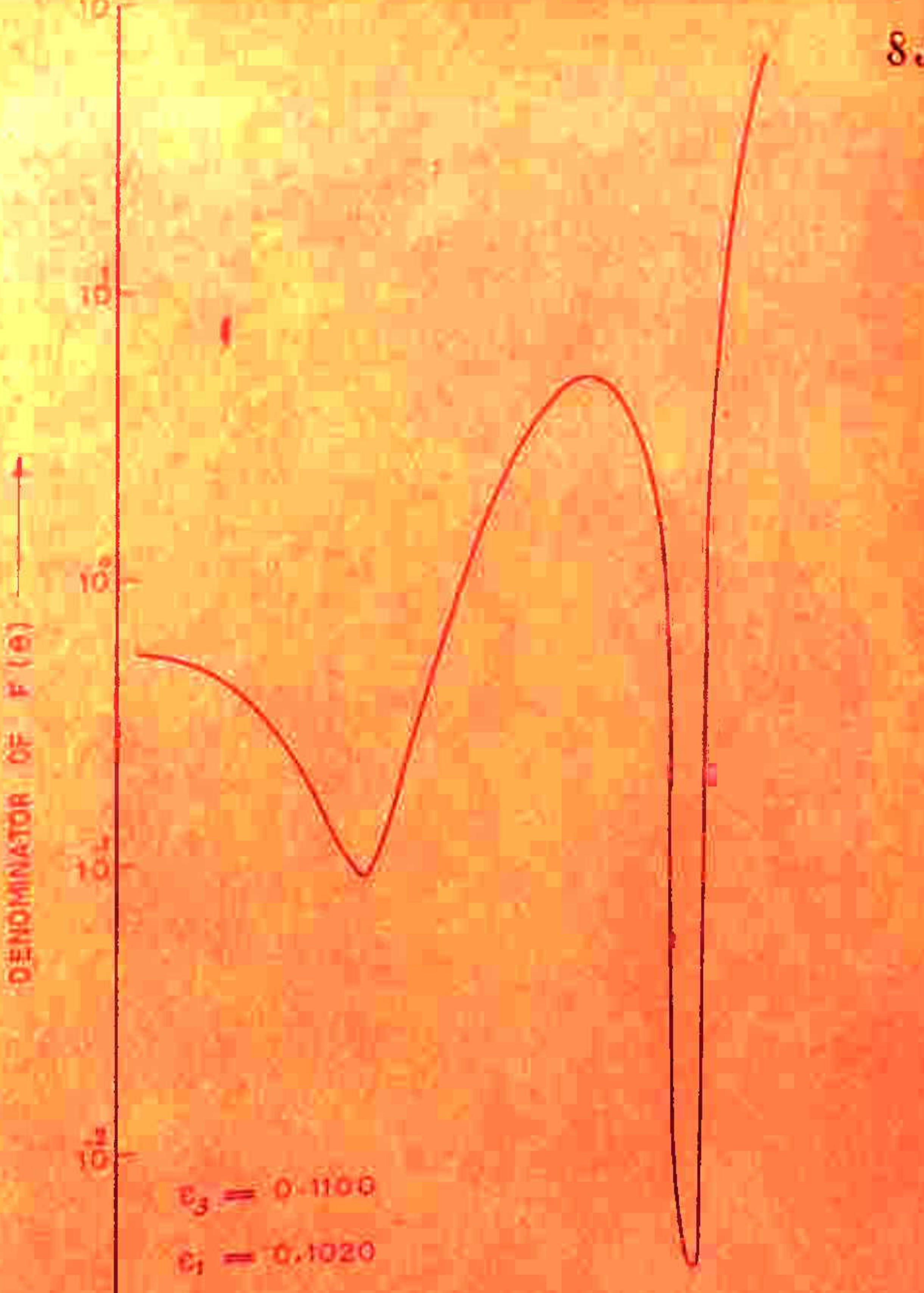
10^{2}
10^{1}
10^{0}
10^{-1}
10^{-2}
DENOMINATOR OF F (θ) ⟶
$\varepsilon_3 = 0.1100$
$\varepsilon_1 = 0.1020$
10
20
30
40
θ ⟶

FIG. 4.3 *a*

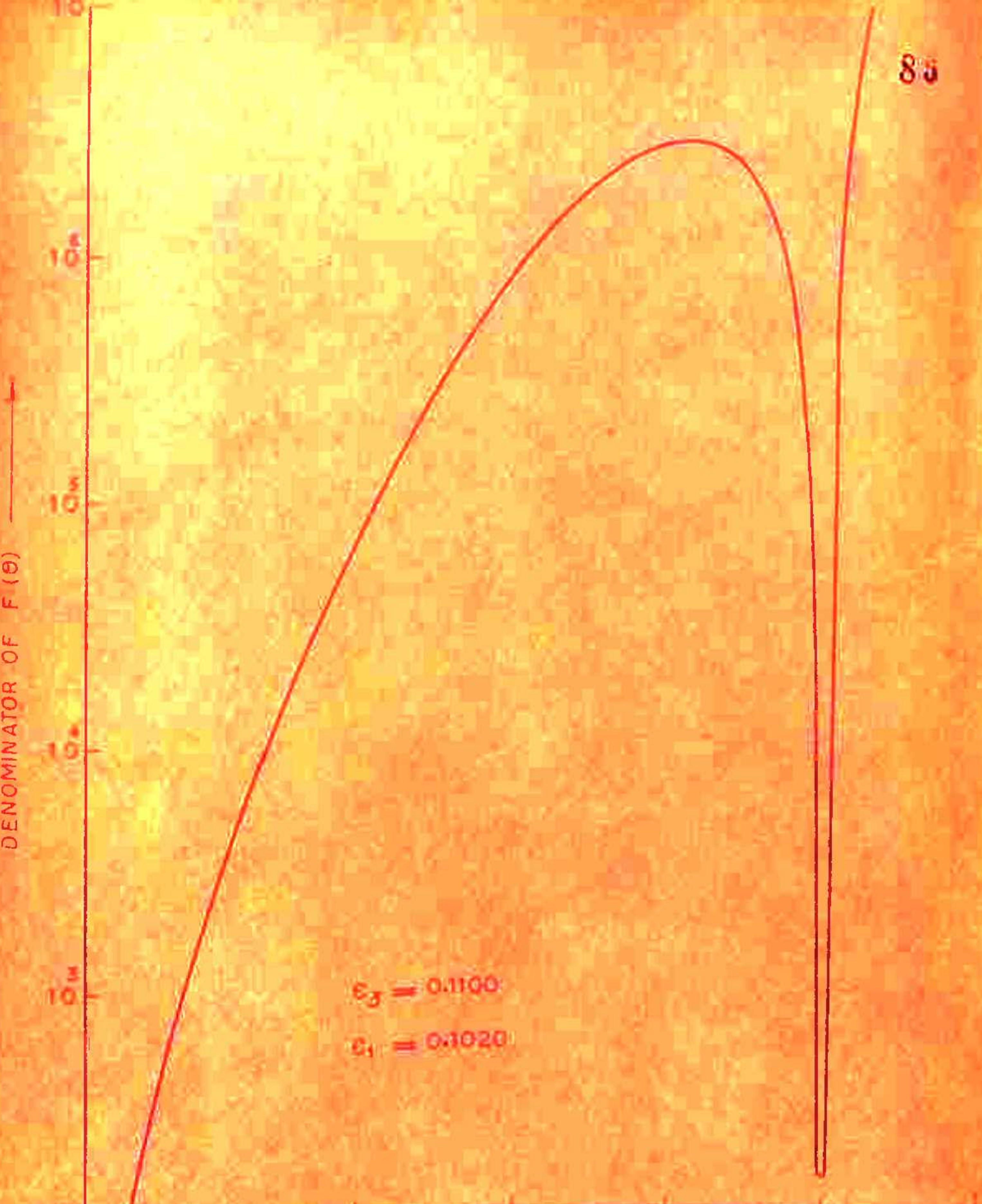
10
10^6
10^5
10^4
10^3
DENOMINATOR OF F(θ)
ϵ_3 = 0.1100
ϵ_1 = 0.1020
40
50
60
70
80
90
θ

FIG. 4.3b

increasing θ. Since the parametric values chosen are small, the argument of Bessel function is not very large as v increases. The radiation pattern for $\epsilon_1 = -0.1446$ is shown in fig. 4.4. The peaks correspond to the minima of the denominator. For $\epsilon_1 > 1$, the values of all parameters (i.e. $k_o bv$ etc) decrease as θ increases. The radiation peaks for $\epsilon_1 = 1.0418$ are obtained as shown in fig. 4.4. For $\epsilon_1 = 1.000$, a sharp peak corresponding to the maxima of numerator at 90° is obtained as shown in fig. 4.5. The other peak corresponds to the minima of the denominator.

Effect of magnetic field in low density plasma ($\epsilon_3 = 0.9081$):

For $\epsilon_1 < \epsilon_3$, the radiation patterns are shown in fig. 4.6. For $\epsilon_1 = 0.9007$, the radiation peaks occur at 65.4725° and 84.1348° with half power beam widths equal to 6.5° and $.0083^\circ$ respectively. For $\epsilon_1 = 0.7844$, the radiation peaks occur at 59.551° and 82.9456° with half power beam widths equal to 4.5° and $.0076^\circ$ respectively. The peaks correspond to the minima of the denominator of F(θ). The first peak is shallow since the minima of denominator at that value of θ is not sharp. The parameters for which peaks occur are given in Table 4.1. It may be pointed out that at v = 0, (that is near θ = 71° for $\epsilon_1 = .9007$ and near θ = 63° for $\epsilon_1 = .7844$)

TABLE [illegible]

Parameters for the radiation peaks.

High density plasma (C_3= 0.IIC0)

C_I	Direction of peaks(in degrees)	$k_o bv$	$k_o av_I$	$k_o a_I v_I$	$k_o a_I v$	$k_o a_2 v_I$	$k_o a_2 v$	Denominator of F(θ)	Amplitude of E_y (relative units
0.1020	13.0730	2.5748	I.9451	0.1948	0.0468	4.8703	I.1703	0.8327x10^{-I}	0.1737x10^{1}
	31.0517	4.6292	I.7131	0.1731	0.0841	4.2020	2.1041	0.4430x10^{-3}	0.6939x10^{2}
	60.0020	10.6430	0.3455	0.0345	0.1935	0.0638	4.6377	0.1469x10^{0}	0.4291x10^{I}
0.0325	7.6855	2.4445	I.9820	0.1982	0.0444	4.9550	I.IIII	0.9670x10^{-I}	0.1646x10^{I}
	27.6957	8.7406	I.7673	0.1767	0.1504	4.4104	3.0730	0.2637x10^{-5}	0.2671x10^{3}
	79.6820	19.5852	0.3502	0.0350	0.3560	0.8757	8.9033	0.2718x10^{3}	0.9810x10^{-I}

Low density plasma (C_3= 0.9061)

0.9007	65.4725	2.9799	0.8294	0.0829	0.054I	2.0136	I.3545	0.7006x10^{0}	0.3762x10^{0}
	84.1349	3.2927	0.2032	0.0203	0.0508	0.508I	I.4967	0.5309x10^{-2}	0.4177x10^{2}
0.7844	59.5510	2 .3550	I.0128	0.I012	0.0435	2.532I	I.0858	0.5554x10^{0}	0 I210x10^{0}
	82.9456	8.3005	0.2445	0.0244	0.0363	0.6II2	2.4093	0.372Ix10^{-3}	0.1277x10^{3}

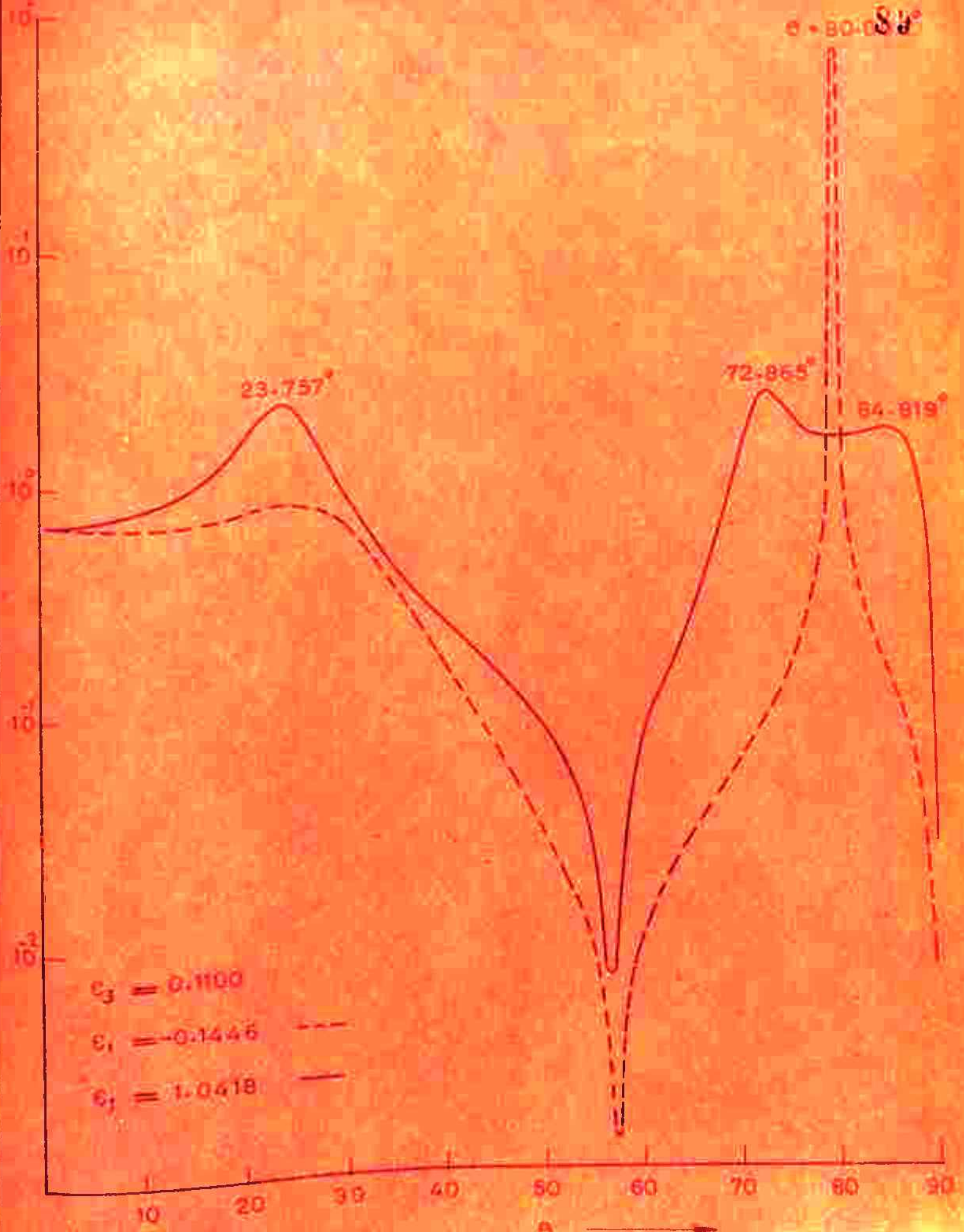
10^{2}
10^{1}
10^{0}
10^{-1}
10^{-2}
θ = 80.0°
23.757°
72.865°
84.819°
ϵ_3 = 0.1100
ϵ_1 = −0.1446
ϵ_1 = 1.0418
10
20
30
40
50
60
70
80
90
θ →

FIG. 4.4

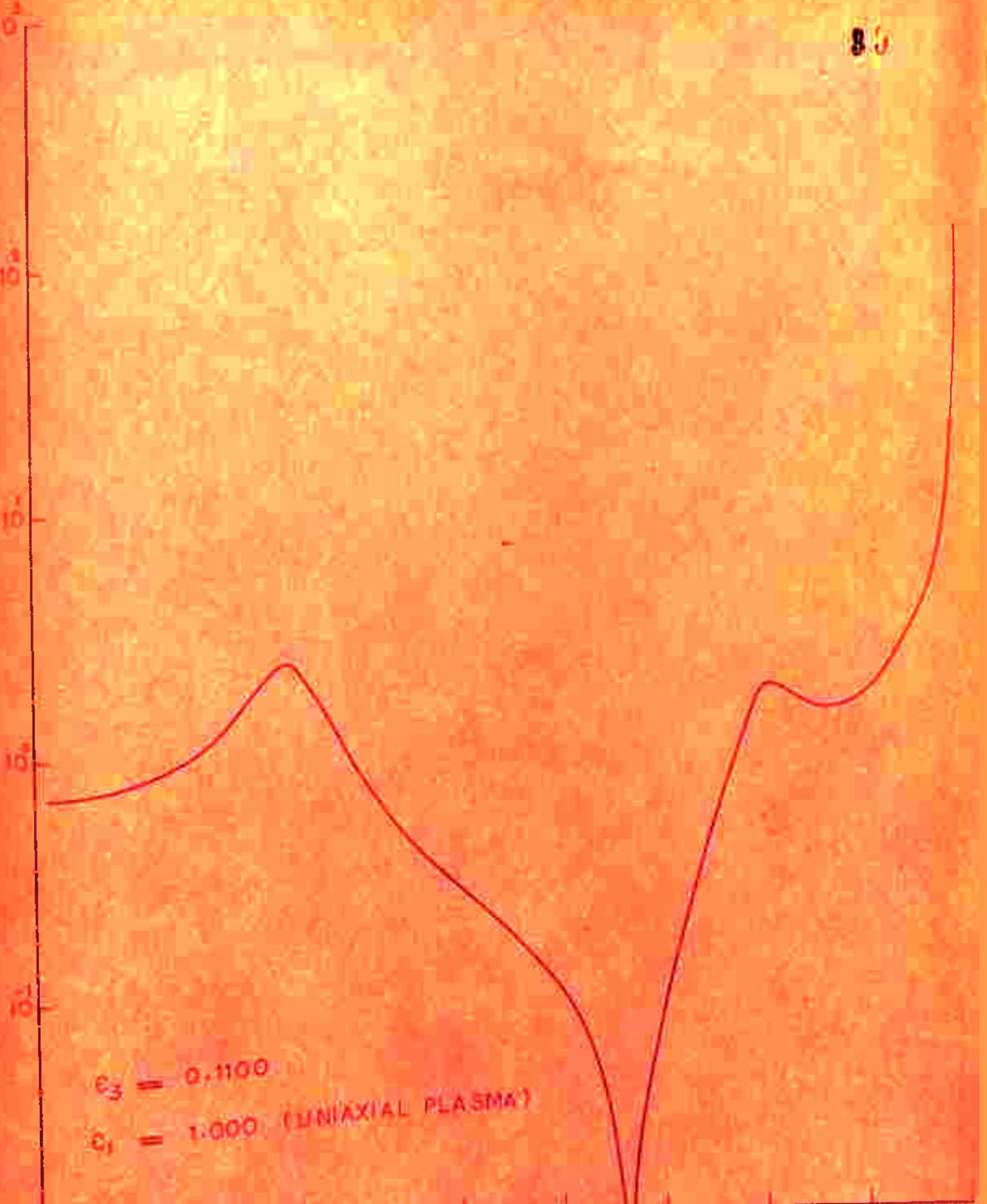
10^3
10^2
10^1
10^0
10^{-1}
$\epsilon_3 = 0.1100$
$\epsilon_1 = 1.000$ (UNIAXIAL PLASMA)
10
20
30
40
50
60
70
80
90
θ

FIG. 4.5

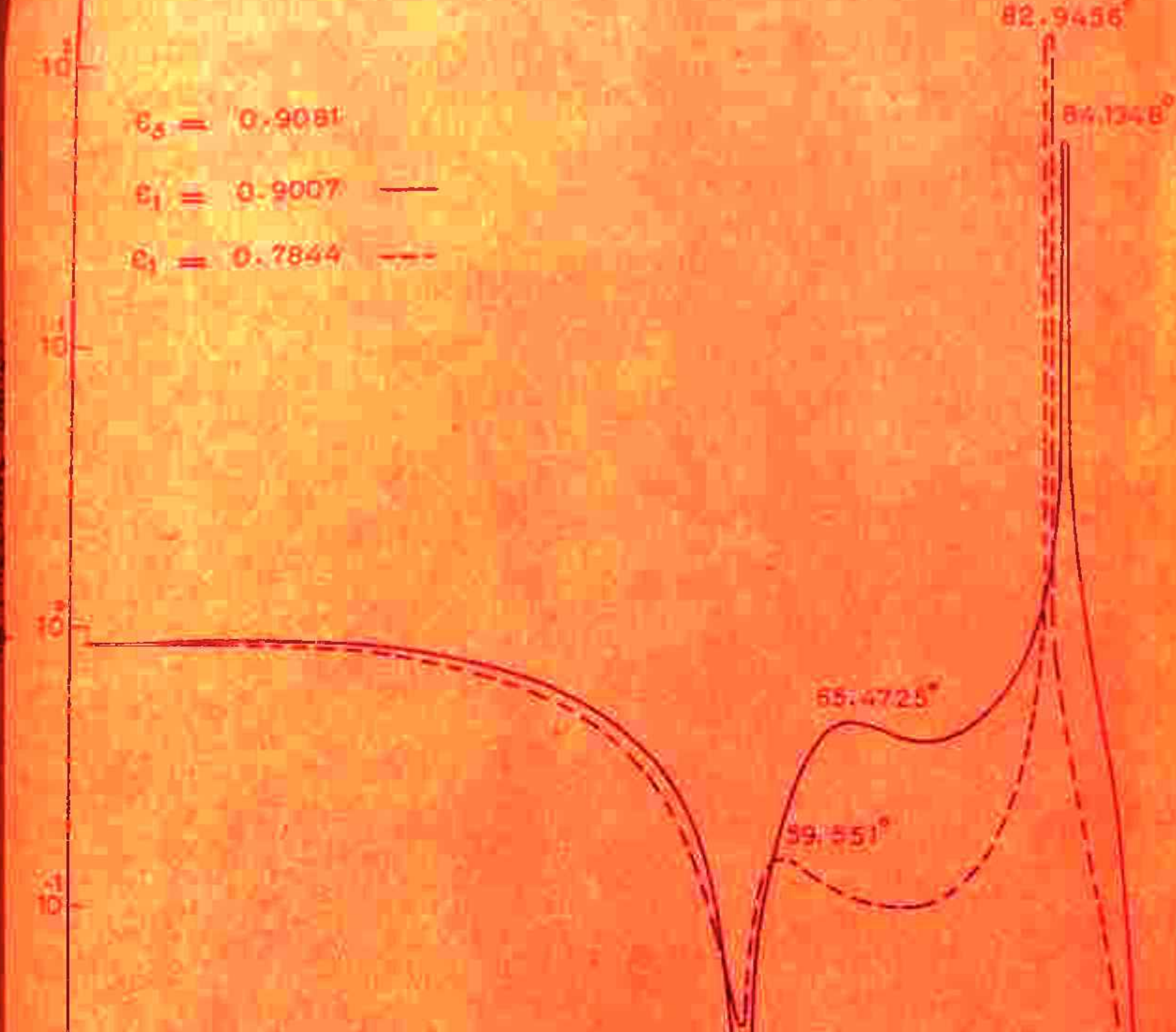
10^{2}
10^{1}
10^{0}
10^{-1}
RELATIVE UNITS
$\varepsilon_s = 0.9081$
$\varepsilon_1 = 0.9007$ ——
$\varepsilon_1 = 0.7844$ - - -
82.9456°
84.1348°
65.4725°
59.551°
10
20
30
40
50
60
70
80
90
θ

FIG. 4.6

the radiation pattern does not have a peak although the denominator tends to zero. This is because of the fact that for $y = 0$, the numerator also tends to zero and their ratio is finite. It may also be noted that for low density plasma, sharp radiation peak is obtained only in an end fire direction.

For $\epsilon_I = -0.5384$, the radiation peak occurs at 80.0090 as shown in fig. 4.7. The peak corresponds to the minima of the denominator. For $\epsilon_I = I.1956$, the radiation peak occurs at 83.3094° as shown in fig. 4.7. For $\epsilon_I = I$ (uniaxial plasma column), a sharp peak corresponding to the maxima of numerator is obtained at 90° as shown in fig. 4.8.

Effect of $k_o b$:

$k_o b$ affects the amplitude of radiation peak and to a very small extent its direction too. Higher values of $k_o b$ give rise to weaker radiation peak. That means for a fixed value of k_o, the higher values of the outer diameter of annular plasma column give rise to weaker radiation peak. The amplitude variation of peak with $k_o b$ is shown in fig. 4.9.

Effect of $k_o a_2$:

$k_o a_2$ affects the direction as well as the amplitude of the radiation peaks formed. For some parametric values,

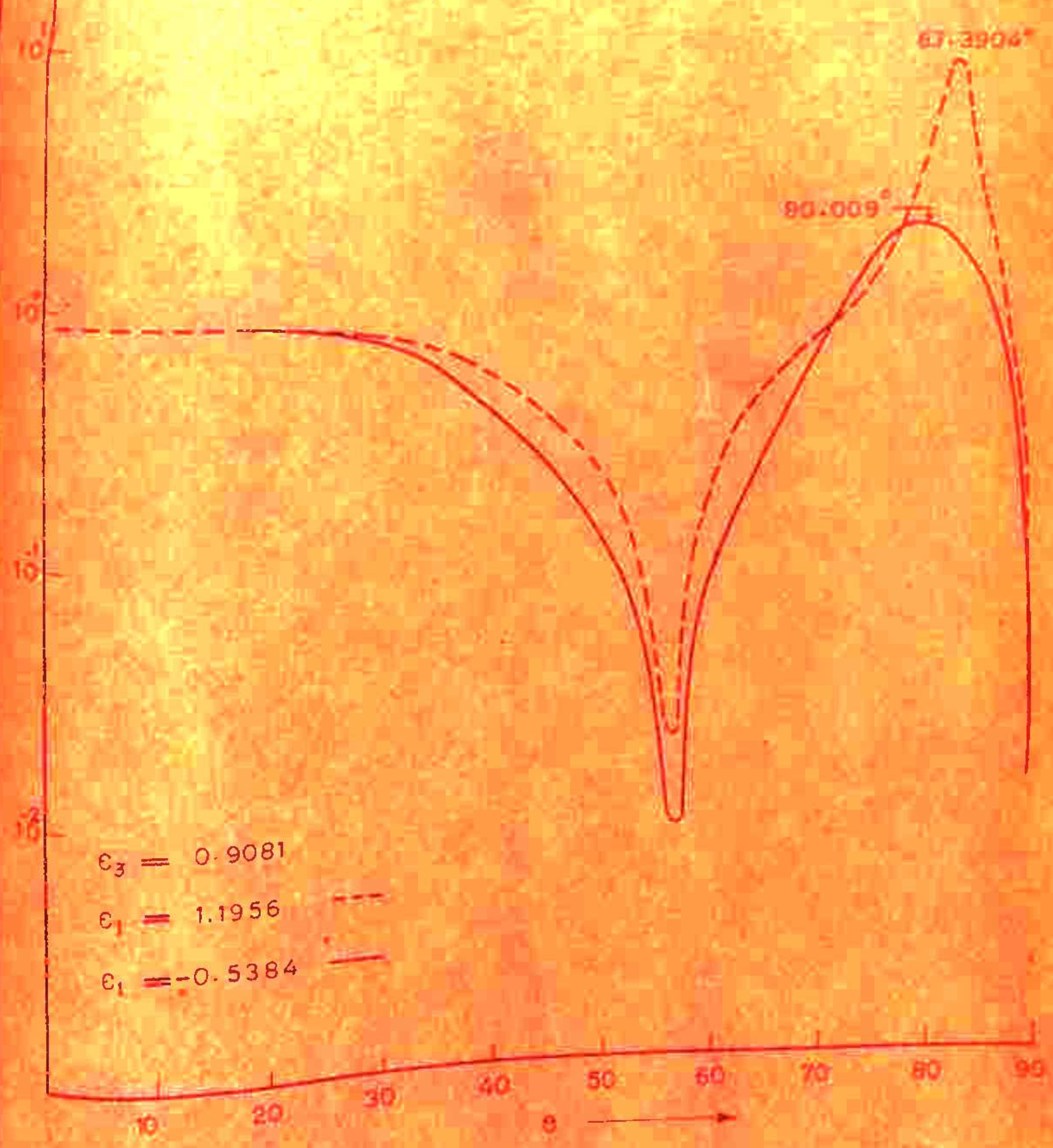
83.3904°
80.009°
10^{1}
10^{0}
10^{-1}
10^{-2}
$\epsilon_3 = 0.9081$
$\epsilon_1 = 1.1956$
$\epsilon_1 = -0.5384$
10
20
30
40
50
60
70
80
90
θ

FIG. 4.7

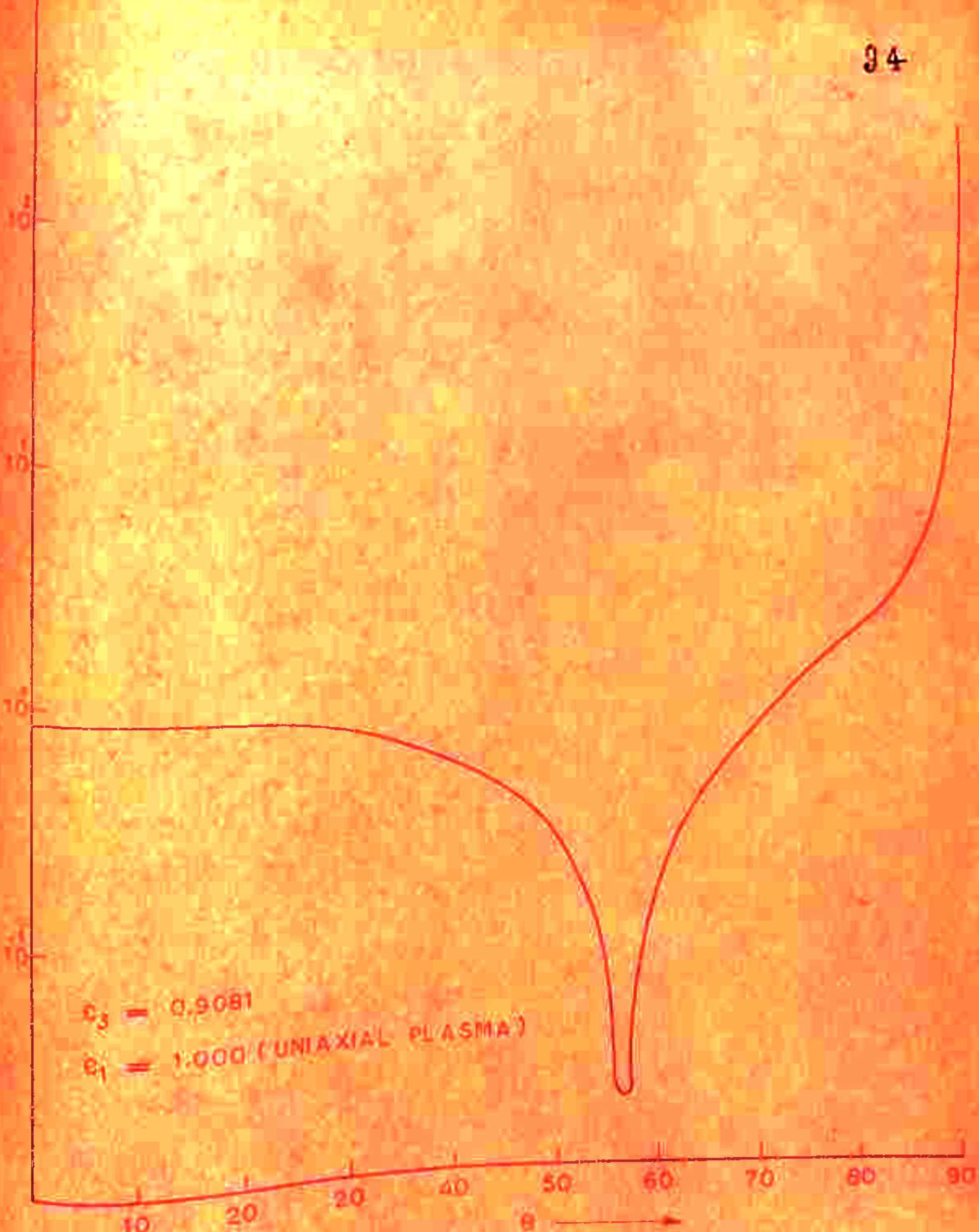

10^2
10^1
10^0
10^{-1}
e_3 = 0.9081
e_1 = 1.000 (UNIAXIAL PLASMA)
10
20
30
40
50
60
70
80
90
θ →

FIG. 4.8

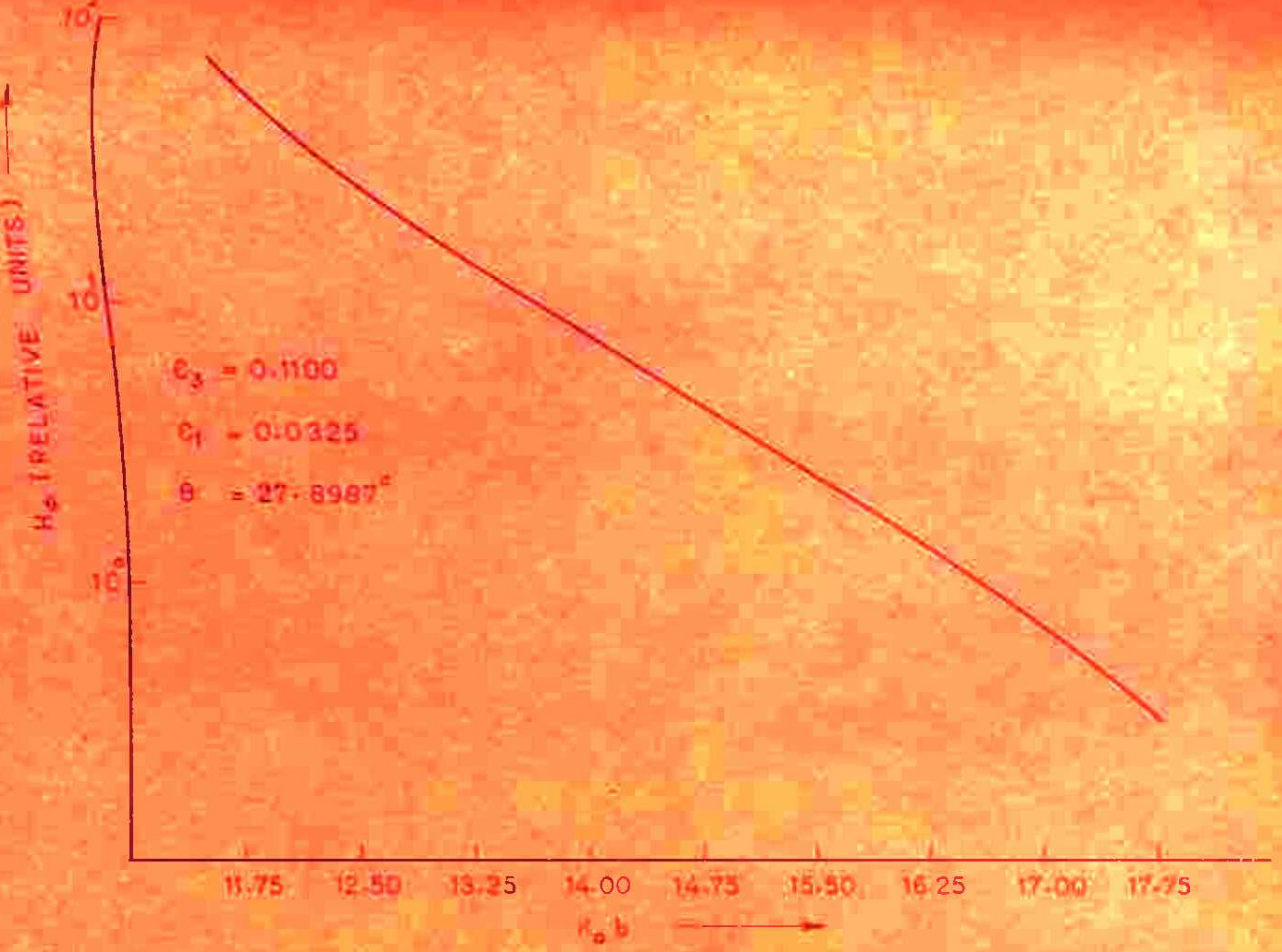
H_ϕ (RELATIVE UNITS)
10^2
10^1
10^0
$\epsilon_3 = 0.1100$
$\epsilon_1 = 0.0325$
$\theta = 27.8987^\circ$
11.75
12.50
13.25
14.00
14.75
15.50
16.25
17.00
17.75
$K_o b$

FIG. 4.9

the numberof peaks also varies as $k_o a_2$ changes. For fixed k_o, the higher values of $k_o a_2$ mean increasing the inner diameter of plasma column. Four different values of $k_o a_2$ = 6.0, 7.0, 8.0 and 9.0 have been taken. The direction and amplitude of radiation peaks for ε_3 = .1100 , ε_I = .0325 and ε_3 = .9081, ε_I = .7844 are given in Table 4.2 for these different values of $k_o a_2$.

Effect of $k_o a_I$:

$k_o a_I$ affects the direction as well as the amplitude of the radiation peaks. For fixed k_o, the higher values of $k_o a_I$ mean increasing the diameter of central conductor. Four different values of $k_o a_I$ = 0.04, 0.08, 0.12 and 0.16 have been taken. The direction and amplitude of radiation peaks for ε_3 = .1100 , ε_I = .0325 and ε_3 = .9081, ε_I = .7844 are given in Table 4.3 for these different values of $k_o a_I$.

Effect of plasma density:

The direction of the peak depends upon the plasma density. The location of the radiation peaks for two different values of ε_3 which for a constant source frequency corresponds to different plasma densities is shown in fig. (4.2), (4.4), (4.5), (4.6), (4.7) and (4.8). For low density plasma the sharp radiation peak is obtained only in an end fire

TABLE -4.2

Effect of varying $k_o a_2$ (i.e. for a fixed k_o, changing the inner diameter of the annular plasma column)

$\epsilon_3 = 0.II00$, $\epsilon_I = 0.0325$, $k_o a = 2.0$, $k_o b = II.0$, $k_o a_I = 0.2$

$k_o a_2$	Direction of peaks (in degrees)	Amplitude of H_ϕ (relative units)
6.0	9.7275	0.I094 x I0^{0}
	42.3402	0.I653 x I0^{2}
	8I.8355	0.6099 x I0^{0}
7.0	II.4923	0.I647 x I0^{0}
	50.86I2	0.9476 x I0^{I}
	83.I773	0.2623 x I0^{I}
8.0	I9.9457	0.I0I3 x I0^{2}
	56.6326	0.2866 x I0^{0}
	84.I53	0.I439 x I0^{2}
9.0	8.68I	0.9864 x I0^{0}
	32.3202	0.200I x I0^{2}
	80.855	0.4944 x I0^{2}
	84.8926	0.I298 x I0^{3}

Contd. Table 4.[illegible]

$\epsilon_3 = 0.908I$, $\epsilon_I = 0.7844$, $k_o a = 2.0$, $k_o b = II.0$, $k_o a_I = 0.2$

$k_o a_2$	Direction of peaks (in degrees)	Amplitude of H_z (relative units)
6.0	60.3636	$0.2057 \times IO^{0}$
	83.9878	$0.1096 \times IO^{3}$
7.0	62.6535	$0.5631 \times IO^{0}$
	84.7894	$0.8349 \times IO^{2}$
8.0	65.I2I8	$0.7888 \times IO^{0}$
	85.4470	$0.7024 \times IO^{2}$
9.0	67.5876	$0.9043 \times IO^{0}$
	86.0550	$0.5302 \times IO^{2}$

TABLE -4.3

Effect of varying k_oa_I (i.e. for a fixed k_o, changing the diameter of the central conductor).

e_3= 0.1100, e_I= 0.0325, k_oa = 2.0, k_ob = II.0, k_oa_2= 6.0

k_oa_I	Direction of radiation peaks (in degrees)	Amplitude of H_{ϕ} (relative units)
0.04	8.6680	0.I828 x IO^{I}
	33.4173	0.8470 x IO^{2}
	82.6780	0.2865 x IO^{0}
0.08	8.4205	0.I734 x IO^{I}
	3I.9396	0.I7I2 x IO^{3}
	8I.3II7	0.I390 x IO^{0}
0.I2	8. I887	0.I74I x IO^{I}
	30.4782	0.3302 x IO^{3}
	80.7566	0.8656 x IO^{-I}
0.I6	7.9492	0.I605 x IO^{I}
	29.I527	0.I632 x IO^{3}
	80.2927	0.I3I6 x IO^{0}

Contd. Table 4.3:

$\varepsilon_3 = 0.9081$, $\varepsilon_1 = 0.7844$, $k_o a = 2.0$, $k_o b = 11.0$, $k_o a_2 = 5.0$

$k_o a_1$	Direction of radiation peaks (in degrees)	Amplitude of H_ϕ (in relative units)
0.04	61.1564	0.7264×10^{0}
	84.3367	0.1550×10^{3}
0.08	60.4445	0.4505×10^{0}
	83.8462	0.1440×10^{3}
0.12	60.1248	0.2606×10^{0}
	83.4917	0.1374×10^{3}
0.16	59.8958	0.7068×10^{-1}
	83.2000	0.1319×10^{3}

direction. It may also be noted that the amplitude and the value of half power beam width are affected by the plasma density.

Effect of $k_o a$:

$k_o a$ does not affect the direction of radiation peak of radiation pattern but it affects the amplitude. It means that the direction of radiation peak is independent of the diameter of ring source. The variation of peak amplitude with $k_o a$ shown in fig. 4.10.

4.1.4 DISCUSSION:

The study of the radiation patterns of a magnetic ring source in an air core having central conductor and surrounded by an annular axially magnetized plasma column has shown the presence of well enhanced radiation peak. when $\epsilon_I < \epsilon_3$, ϵ_I is negative or ϵ_I is greater than one, the peak corresponds to the minimas of the denominator of $F(0)$. For uniaxial plasma column, a sharp radiation peak at 90° is obtained corresponding to the maxima of numerator. For low density plasma, sharp peak is obtained in an end fire direction. The direction of the beam can be varied by changing the plasma density, applied magnetic field, diameter

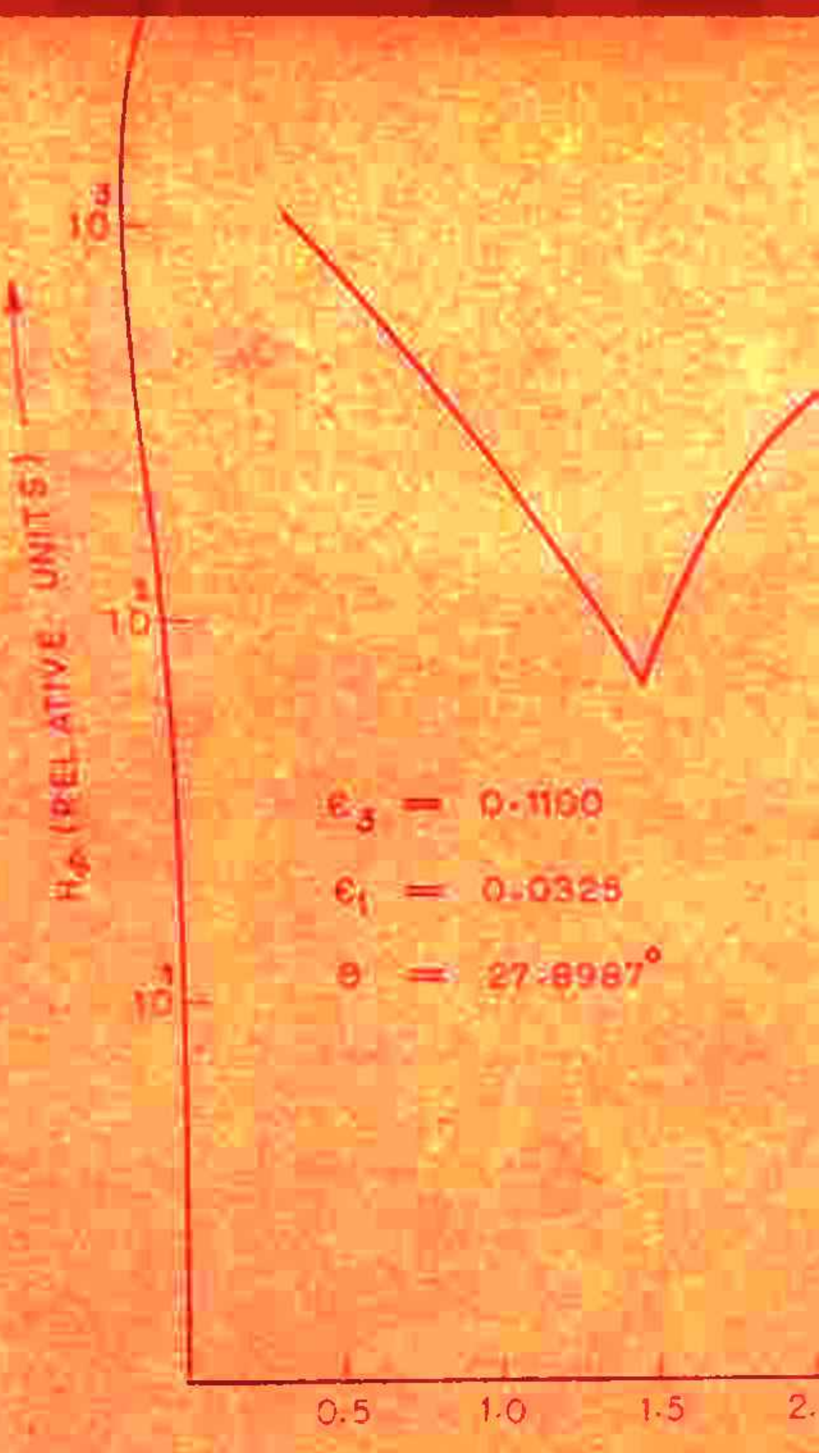
10^3
10^2
10^1
H_A (RELATIVE UNITS)
$\epsilon_3 = 0{\cdot}1100$
$\epsilon_1 = 0{\cdot}0325$
$\theta = 27{\cdot}8987^\circ$
0.5
1.0
1.5
2.

FI

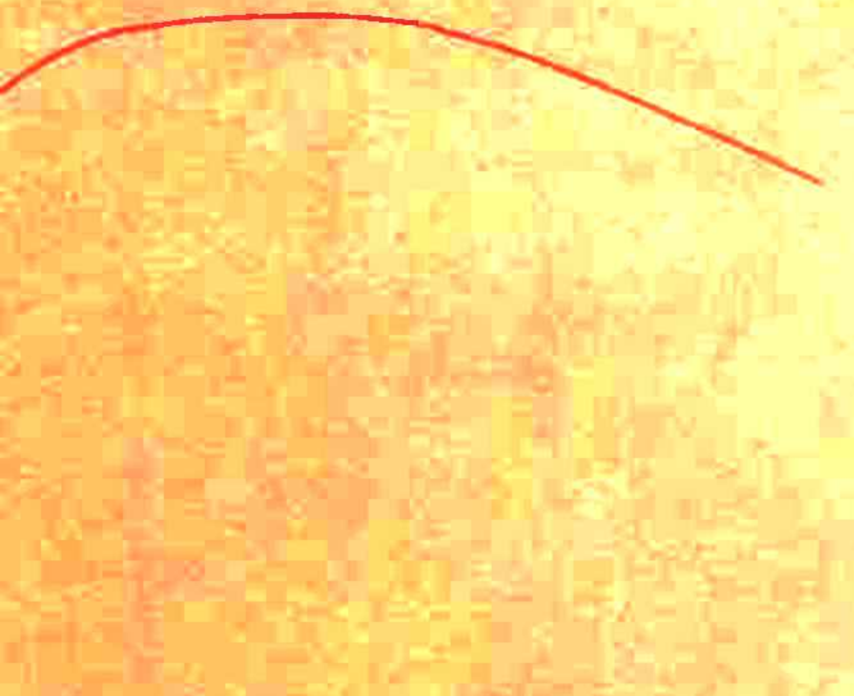

G. 4. 10

of annular plasma column and diameter of central conductor. The direction of the radiation peak is independent of the diameter of ring source.

This geometry gives rise to most sharp peaks with the smallest value of half power beam width as compared to the previously analysed geometries (in chapter 2 and chapter 3). The change in the radiation pattern may be attributed to the presence of air gap. Moreover, the parametric values of the configuration are also small compared to the previously analysed geometries (in chapter 2 and chapter 3).

4.2 EXCITATION BY OPEN ENDED COAXIAL LINE:

4.2.1 INTRODUCTION:

In this section, it is shown that a system consisting of an open ended coaxial line excited in the TEM mode in an air column having a central conductor and surrounded by annular axially magnetized plasma column may give rise to a well enhanced narrow beam radiation peak with a very small value of half power beam width. The field distribution at the open end cross-section of the coaxial line is assumed to be equivalent to the vector sum of magnetic current rings of various radii ranging from the outer radius of the inner conductor to the inner radius of the outer conductor of the coaxial line. The radiation field is obtained as a vector sum of the field components due to individual rings of magnetic current.

The direction of radiation peak depends upon the dimensions of annular plasma column, the diameter of the central conductor, plasma density and applied magnetic field. The direction of radiation peak is independent of inner diameter of the outer conductor of the coaxial line at the open end. The pattern for the case of uniaxially magnetized plasma column is also studied.

In section 4.I, the same geometry excited by a magnetic ring source has been studied. In this case it is found that the diameter of magnetic ring source does not affect the direction of radiation peaks but affects only their amplitude. The field distribution of a magnetic ring source is given by Kronecker's delta function. The physical realisation of such an ideal magnetic ring source is not very convenient . This study of the radiation pattern of an open ended coaxial line excited in TEM mode in an air core having central conductor and surrounded by an annular axially magnetised plasma column is an attempt in the direction of studying the case of more practically feasible source of electromagnetic waves.

4.2.2 ANALYSIS:

An infinitely long air core of radius 'a_2' having infinitely long conductor of radius 'a_1' along the longitudinal axis and surrounded by an axially magnetised annular plasma column of inner radius 'a_2' and outer radius 'b' is oriented with its axis along the z-axis of the cylindrical coordinate system (ρ, ϕ , z) (fig. 4.II). The medium surrounding the plasma column and extending to infinity is free space, with permittivity and permeability ϵ_0 and μ_0.

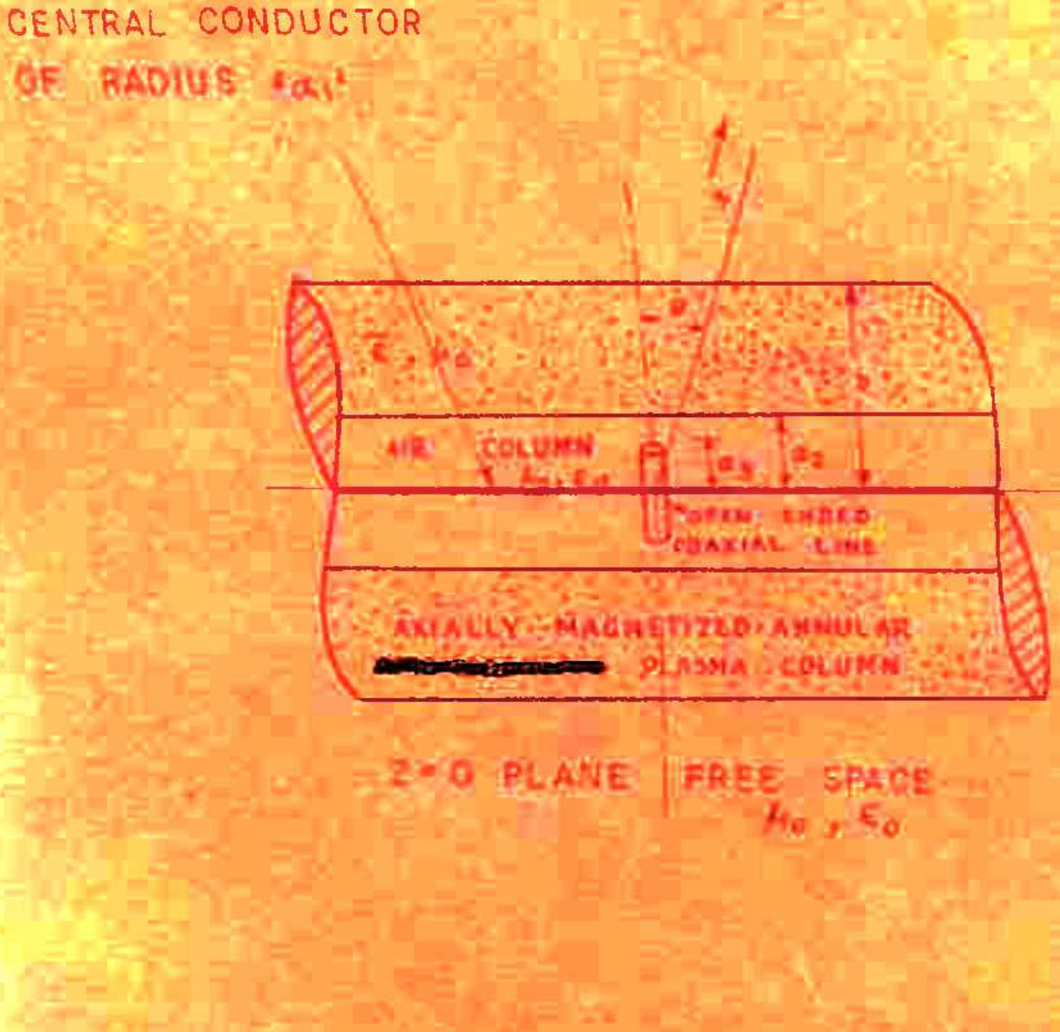
CENTRAL CONDUCTOR
OF RADIUS a_1
ϵ, μ_0
D
b
AIR COLUMN
μ_0, ϵ_0
a_1
a_2
OPEN ENDED
COAXIAL LINE
AXIALLY MAGNETIZED ANNULAR
[redacted] PLASMA COLUMN
Z=0 PLANE
FREE SPACE
μ_0, ϵ_0

FIG.

CROSS SECTION OF
THE OPEN ENDED
COAXIAL LINE

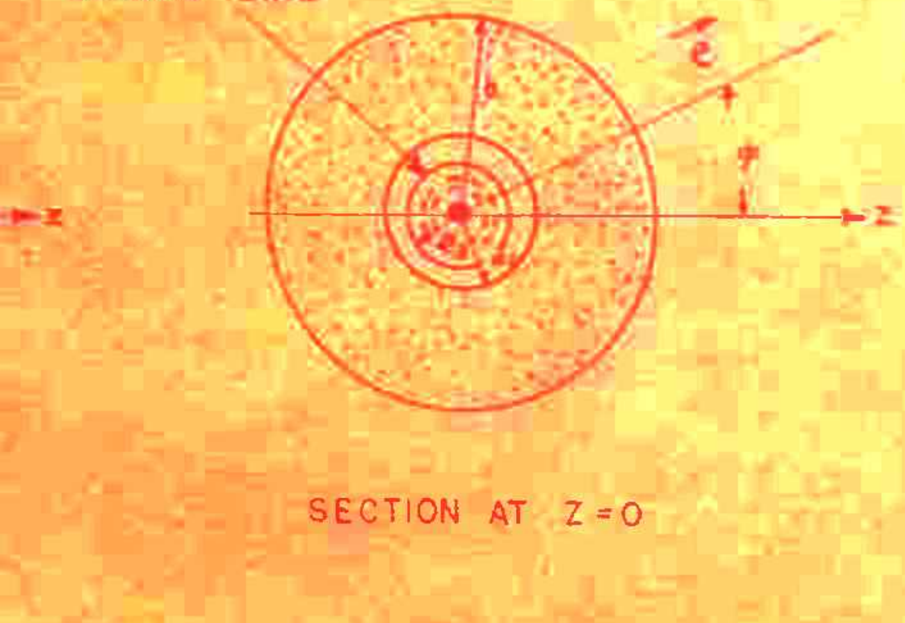

SECTION AT Z = 0

4.11

The source of electromagnetic radiation is an open ended coaxial line, with open end at the $z = 0$ plane.

The expression for the radiation field of a magnetic ring source of radius 'a' in an infinitely long air core having central conductor and surrounded by axially magnetised annular plasma column as derived in section (4.I.2) (equ. 4.I.3) after some simplification can be written as

$$H_\phi = - \frac{j\omega\epsilon_0\epsilon_a\, a}{\pi} F(\theta) \frac{e^{jk_0\bar{r}}}{\bar{r}}$$

where

$$F(\theta) = F_I(\theta) \quad F_2(\theta)$$

$$F_I(\theta) = a\left\{J_0(k_0 a_I v_I)\, Y_I(k_0 a v_I) - Y_0(k_0 a_I v_I) J_I(k_0 a v_I)\right\}$$

$$F_2(\theta) = \frac{I}{J_0(k_0 a_I v_I) G_I(\theta) - Y_0(k_0 a_I v_I) G_2(\theta)}$$

$$G_I(\theta) = AC + BD$$

$$G_2(\theta) = AF + BE$$

$$A = \epsilon_3(k_0 b \cos\theta) Y_I(k_0 bv) H_0(k_0 b \cos\theta)$$
$$- (k_0 bv)\, Y_0(k_0 bv)\, H_I(k_0 b \cos\theta)$$

$$B = \epsilon_3\, (k_0 b \cos\theta)\, H_0(k_0 b \cos\theta)\, J_I(k_0 bv)$$
$$- (k_0 bv)\, J_0(k_0 bv)\, H_I(k_0 b \cos\theta)$$

$$C = (k_0 a_2 v_I)\, J_I(k_0 a_2 v)\, Y_0(k_0 a_2 v_I)$$
$$- \frac{\epsilon_a}{\epsilon_3} (k_0 a_2 v)\, Y_I(k_0 a_2 v_I)\, J_0(k_0 a_2 v)$$

$$D = \frac{\epsilon_a}{\epsilon_3} (k_0 a_2 v)\, Y_0(k_0 a_2 v)\, Y_I(k_0 a_2 v_I)$$
$$- (k_0 a_2 v_I)\, Y_I(k_0 a_2 v)\, Y_0(k_0 a_2 v_I)$$

$$E = \frac{\epsilon_a}{\epsilon_3} (k_0 a_2 v)\, J_I(k_0 a_2 v_I)\, Y_0(k_0 a_2 v)$$
$$- (k_0 a_2 v_I)\, Y_I(k_0 a_2 v)\, J_0(k_0 a_2 v_I)$$

$$F = (k_0 a_2 v_I)\, J_I(k_0 a_2 v_I)\, J_0(k_0 a_2 v_I)$$
$$- \frac{\epsilon_a}{\epsilon_3} (k_0 a_2 v)\, J_0(k_0 a_2 v)\, J_I(k_0 a_2 v_I)$$

$$v_I = \sqrt{(\epsilon_a - \sin^2\theta)}$$
$$v = \sqrt{(\epsilon_3 - \frac{\epsilon_3}{\epsilon_I} \sin^2\theta)}$$

$F(\theta)$ is the factor which determines the variation of field with θ. $F_2(\theta)$ is the term which does not depend upon the diameter of ring source. The field distribution at the open end of the coaxial line is assumed to be equivalent to the vector sum of magnetic current ring with various radii ranging from the outer radius of the inner conductor 'a_I' to the inner radius of the outer conductor 'a_3' of the coaxial line at the $z = 0$ plane. The magnitude of the magnetic current in each ring is assumed to be proportional to the value H_ϕ at that particular location in the coaxial line. For a coaxial line excited in TEM mode, H_ϕ is proportional to $I_o/2\pi a$, where I_o is the current. The total radiation field of open ended coaxial line with its open end at the $z = 0$ plane can be obtained as a vector sum of the field components due to individual rings of magnetic current. So in the case of coaxial line excitation $F(\theta)$ is modified to

$$F(\theta) = \int_{a_I}^{a_3} \frac{I_o}{2\pi a} \quad F_I(\theta)\, F_2(\theta)\, da.$$

$$F = F_2(\theta) \int_{a_I}^{a_3} a \left\{ J_o(k_o a_I v_I)\, Y_I(k_o a v_I) - Y_o(k_o a_I v_I)\, J_I(k_o a v_I) \right\}^* \frac{I_o}{2\pi a}\, da$$

$$= \frac{F_2(\theta) I_o}{2\pi (k_o v_I})^* \left\{ J_o(k_o a_3 v_I)\, Y_o(k_o a_I v_I) - J_o(k_o a_I v_I)\, Y_o(k_o a_3 v_I) \right\}$$

4.2.3 CHARACTERISTICS OF THE RADIATION FIELD

The radiation patterns (variation of $F(\theta)$ with θ) have been computed with the help of an IBM-II30 computer for parametric values $k_o a_I = 0.08$, $k_o a_3 = 0.8$, $k_o a_2 = 3.0$, $k_o b = 6.0$,

ϵ_a= I.0, ϵ_3= .II00 and ϵ_3= .9081. When plasma frequency is much lower than the source frequency, ϵ_3 is only slightly less than unity and we shall call it low plasma density case. On the other hand when w_p is only slightly lower than the source frequency, ϵ_3 is near zero and we shall call it a high plasma density case. Since F(θ) is an expression involving both the Bessel and Hankel function in a very complicated way, it is difficult to express analytically the behaviour of F(θ) with various parameters. Therefore, the computational results are presented first and then these results are analysed to give a qualitative relationship between the location of peak and other parameters of the configuration. For given values of w/w_p, the value of ϵ_I changes with w_o/w_p and may be divided into three sets as (i) $\epsilon_I \leq \epsilon_3$ (ii) ϵ_I is negative (iii) $\epsilon_I \geq$ I. The effects of various parameters on the shape of the radiation pattern are discussed below:

Effect of magnetic field on high density plasma(ϵ_3=.II00):

When $\epsilon_I \ll \epsilon_3$ the radiation pattern has radiation peaks shown in fig. 4.I2a. The detailed structure of the radiation peak is shown in fig. 4.I2b. The value of v becomes negative for $\epsilon_3 < \frac{\epsilon_3}{\epsilon_I}$ sin$^2\theta$ and ordinary Bessel functions

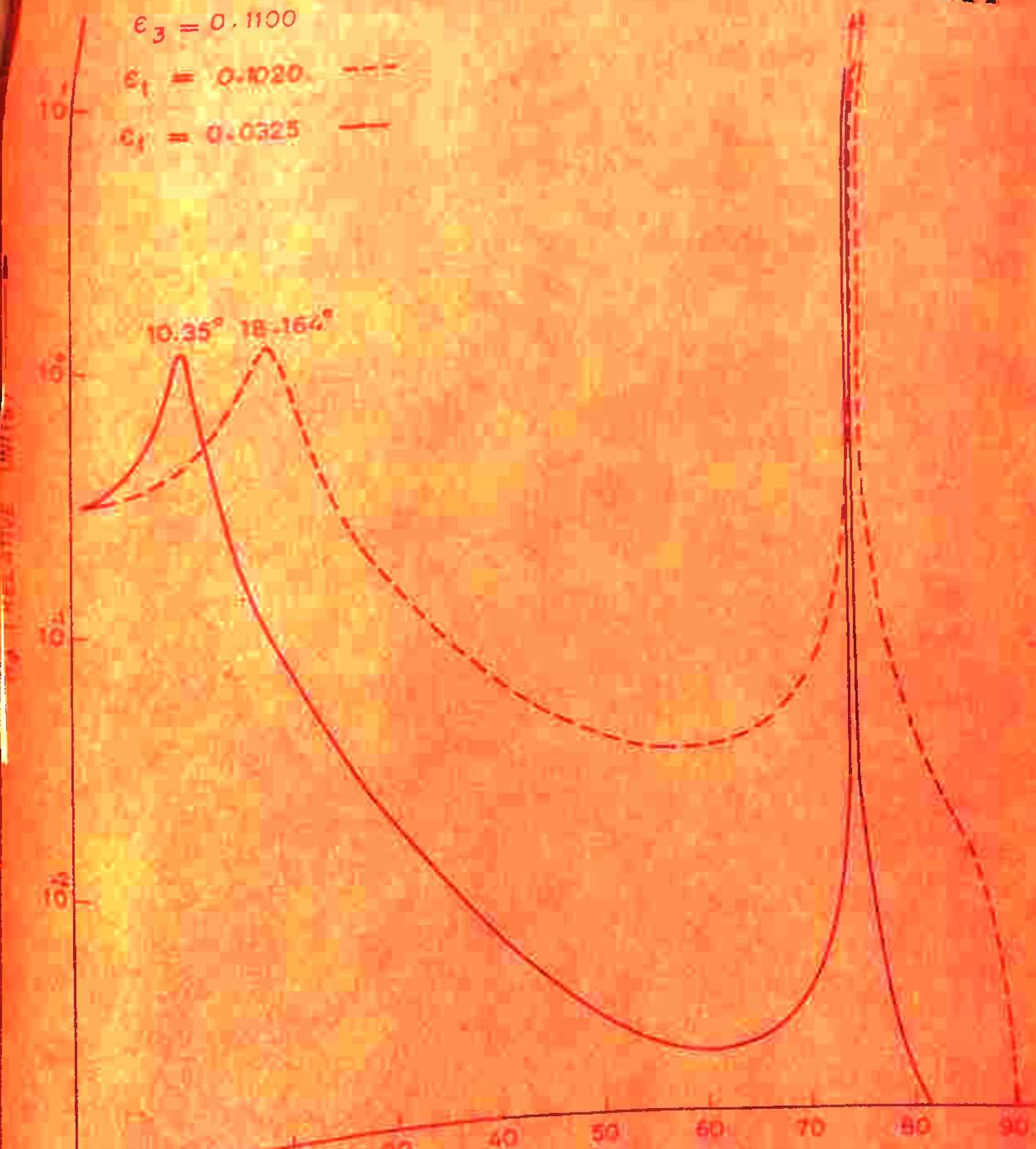
$\epsilon_3 = 0.1100$
$\epsilon_1 = 0.1020$ ----
$\epsilon_1 = 0.0325$ ——
10.35°
18.164°
10^1
10^0
10^{-1}
10^{-2}
10
20
30
40
50
60
70
80
90
θ →

FIG. 4.12 a

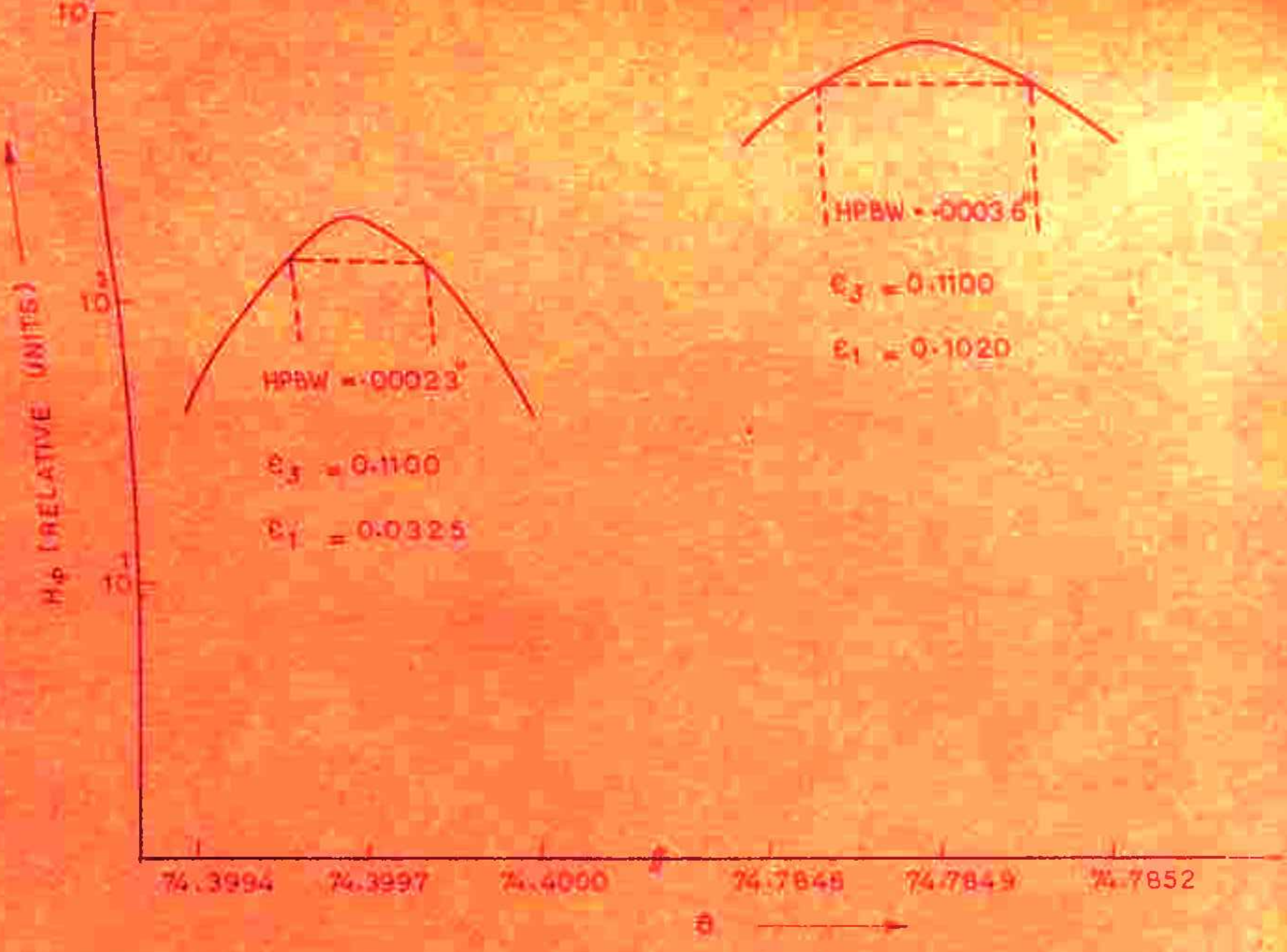
10^3
10^2
10^1
H_ϕ (RELATIVE UNITS)
HPBW = ·00023°
ϵ_3 = 0·1100
ϵ_1 = 0·0325
HPBW = ·0003.6°
ϵ_3 = 0·1100
ϵ_1 = 0·1020
74.3994
74.3997
74.4000
74.7846
74.7849
74.7852
θ

FIG. 4.12 b

change to modified form. The values of k_0bv, k_0a_2v and k_0a_Iv first decrease as θ increases and then increases as θ increases, while values of $k_0a_Iv_I$, $k_0a_3v_I$ and $k_0a_2v_I$ always decrease with increasing θ. The denominator of $F(\theta)$ for $\epsilon_I = 0.I020$ varies with θ as shown in fig. 4.I3(a,b). The peaks in the radiation patterns correspond to the minimas of the denominator of $F(\theta)$. For $\epsilon_I = 0.I020$, the peaks occur at I8.I64° and 74.785° with half power beam width equal to 3.86° and 0.00036° respectively. For $\epsilon_I = 0.0325$, the peaks occur at I0.35° and 74.3997° with half power beam width equal to 2.43° and 0.00023° respectively. The parameters for which peaks occur are given in Table 4.4. It may be pointed out that at $v = 0$, the ratio of the denominator and the numerator remains finite, so no radiation peak for $v = 0$ is obtained.

When ϵ_I is negative the value of v increase as θ increases. Since the parametric values choosen for this configuration is small, the argument of Bessel function is not very large as v. increases. The radiation pattern for $\epsilon_I = -0.I446$ is shown in fig. 4.I4. A single radiation peak at 75.803° is obtained corresponding to the denominator of $F(\theta)$. The radiation peaks for $\epsilon_I = I.04I8$ are also shown in fig. 4.I4. The radiation peaks for $\epsilon_I > I$ are not so sharp.

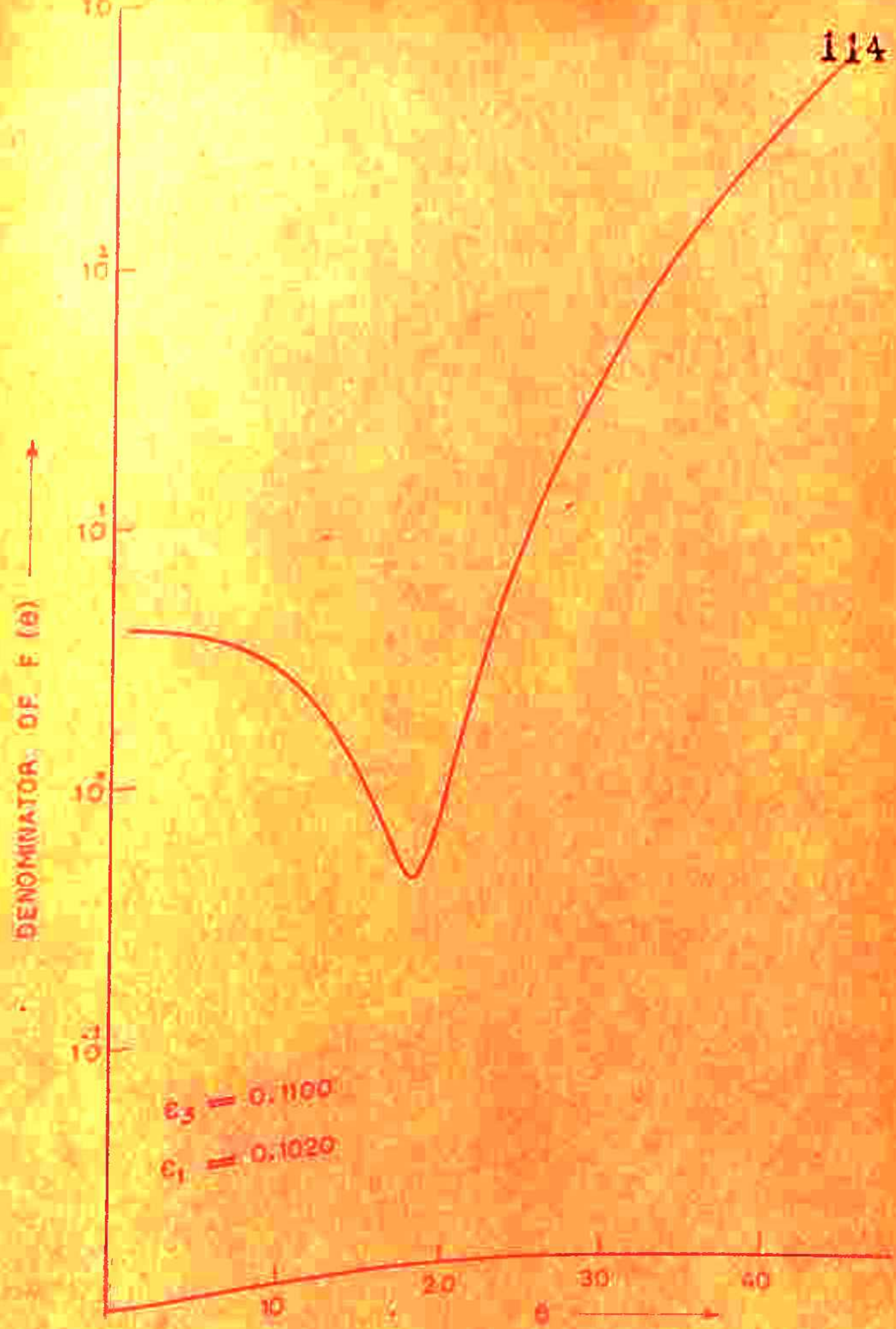

10^3
10^2
10^1
10^0
10^{-1}
DENOMINATOR OF F (θ) →
$\varepsilon_3 = 0.1100$
$\varepsilon_1 = 0.1020$
10
20
30
40
θ →

FIG. 4.13 a

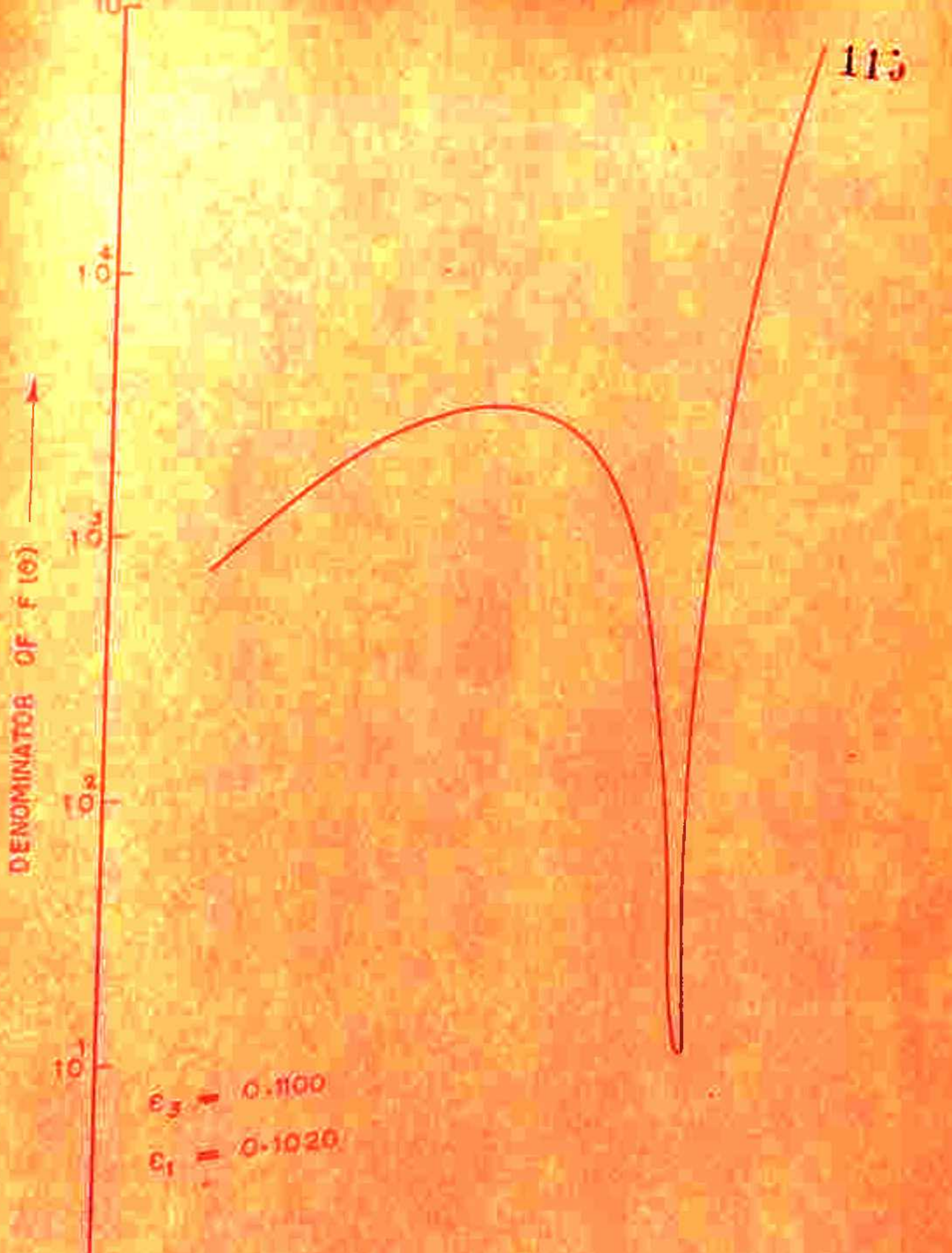
DENOMINATOR OF F(θ)
10^4
10^3
10^2
10^1
ε_3 = 0.1100
ε_1 = 0.1020
50
60
70
80
90
θ

FIG. 4-13b

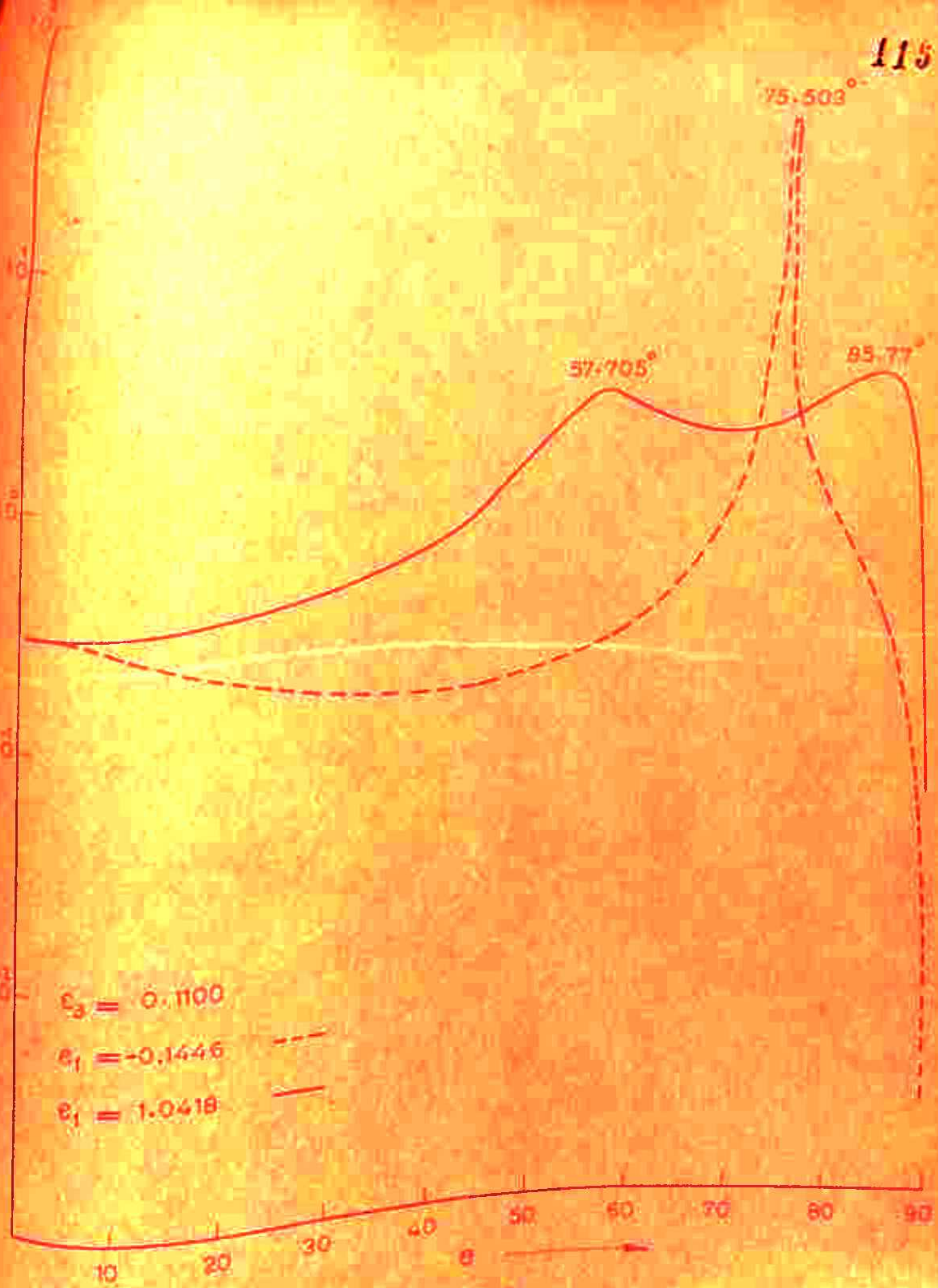
75.503°
57.705°
85.77°
10^{1}
10^{0}
10^{-1}
10^{-2}
$\epsilon_3 = 0.1100$
$\epsilon_1 = -0.1446$
$\epsilon_1 = 1.0418$
10
20
30
40
50
60
70
80
90
θ

FIG. 4.14

For $\epsilon_I = 1.000$, a sharp radiation peak corresponding to the maxima of numerator at 90° is obtained as shown in fig. 4.15. The other peak corresponds to the minima of the denominator.

Effect of magnetic field in low density plasma ($\epsilon_3 = 0.9061$):

For $\epsilon_I < \epsilon_3$ the radiation patterns are as shown in fig. 4.16. For $\epsilon_I = 0.9007$, the radiation peak occurs at 83.5648° with half power beam width equal to $.0094^\circ$. For $\epsilon_I = 0.7844$, the radiation peak occurs at 81.222° with half power beam width equal to $.0062^\circ$. The peak corresponds to the minima of the denominator of $F(\theta)$. The parameters for which peaks occur are given in Table 4.4. It may be pointed out that at $v = 0$, the ratio of the denominator and the numerator is finite, so no radiation peak is obtained at $v = 0$. For low density plasma, a single radiation peak in an end fire direction is obtained.

For $\epsilon_I = -0.5384$, the radiation peak occurs at 73.0092° as shown in fig. 4.17. For $\epsilon_I = 1.1956$, the radiation peak occurs at 74.856° as shown in fig. 4.17. In both the cases, the peak corresponds to the minima of the denominator. For $\epsilon_I = 1.000$, a sharp peak corresponding to the maxima of numerator is obtained at 90° as shown in fig. 4.18.

TABLE-4.4

Parameters for the radiation peaks

High density plasma (C_3= .1100)

C_I	Direction of peaks(in degrees)	k_0bv	$k_0a_3v_I$	$k_0a_Iv_I$	k_0a_Iv	$k_0a_2v_I$	k_0a_2v	Denominator of $F(\theta)$	Amplitude of H_ϕ (relative units)
0.1020	18.1640	0.4298	0.7601	0.0770	0.0017	2.0503	0.1149	0.3398×10^{0}	0.1100×10^{1}
	74.7850	5.8741	0.1006	0.0219	0.0756	0.7858	1.8370	0.1074×10^{-3}	0.0007×10^{3}
0.0325	10.3500	0.1581	0.7860	0.0786	0.0021	2.9511	0.0790	0.3200×10^{0}	0.1160×10^{1}
	74.3997	10.4442	0.2147	0.0214	0.1392	0.8053	5.0210	0.1724×10^{-3}	0.1971×10^{3}

Low density plasma (C_3= .9081)

0.9007	83.5648	1.7748	0.0892	0.0029	0.0236	0.3345	0.6073	0.4561×10^{-1}	0.2927×10^{2}
0.7844	81.2220	2.8316	0.1216	0.0121	0.0377	0.4162	1.4150	0.1219×10^{-1}	0.4156×10^{2}

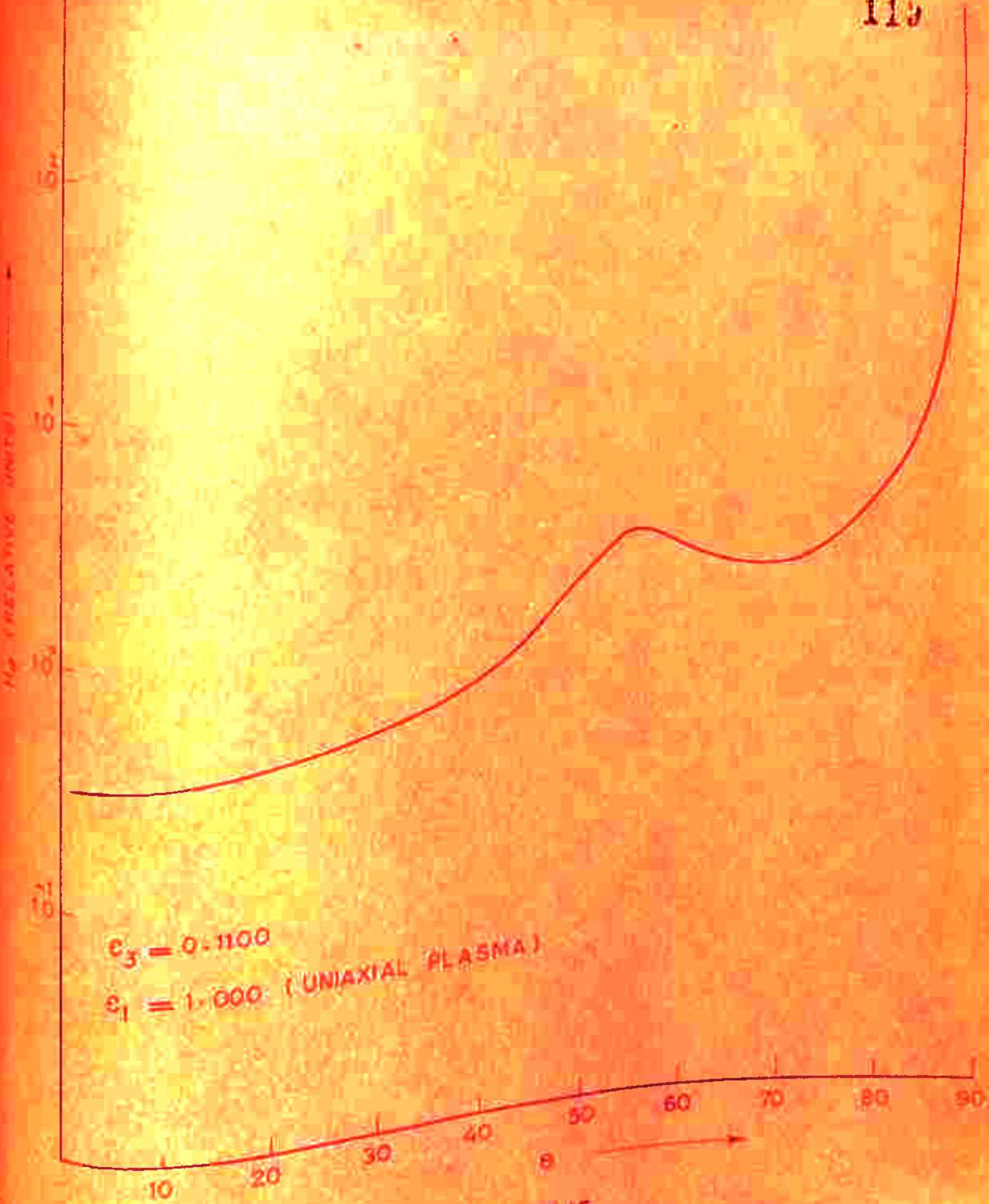
10^{2}
10^{1}
10^{0}
10^{-1}
(RELATIVE UNITS)
$\varepsilon_3 = 0.1100$
$\varepsilon_1 = 1.000$ (UNIAXIAL PLASMA)
10
20
30
40
50
60
70
80
90
θ

FIG. 4.15

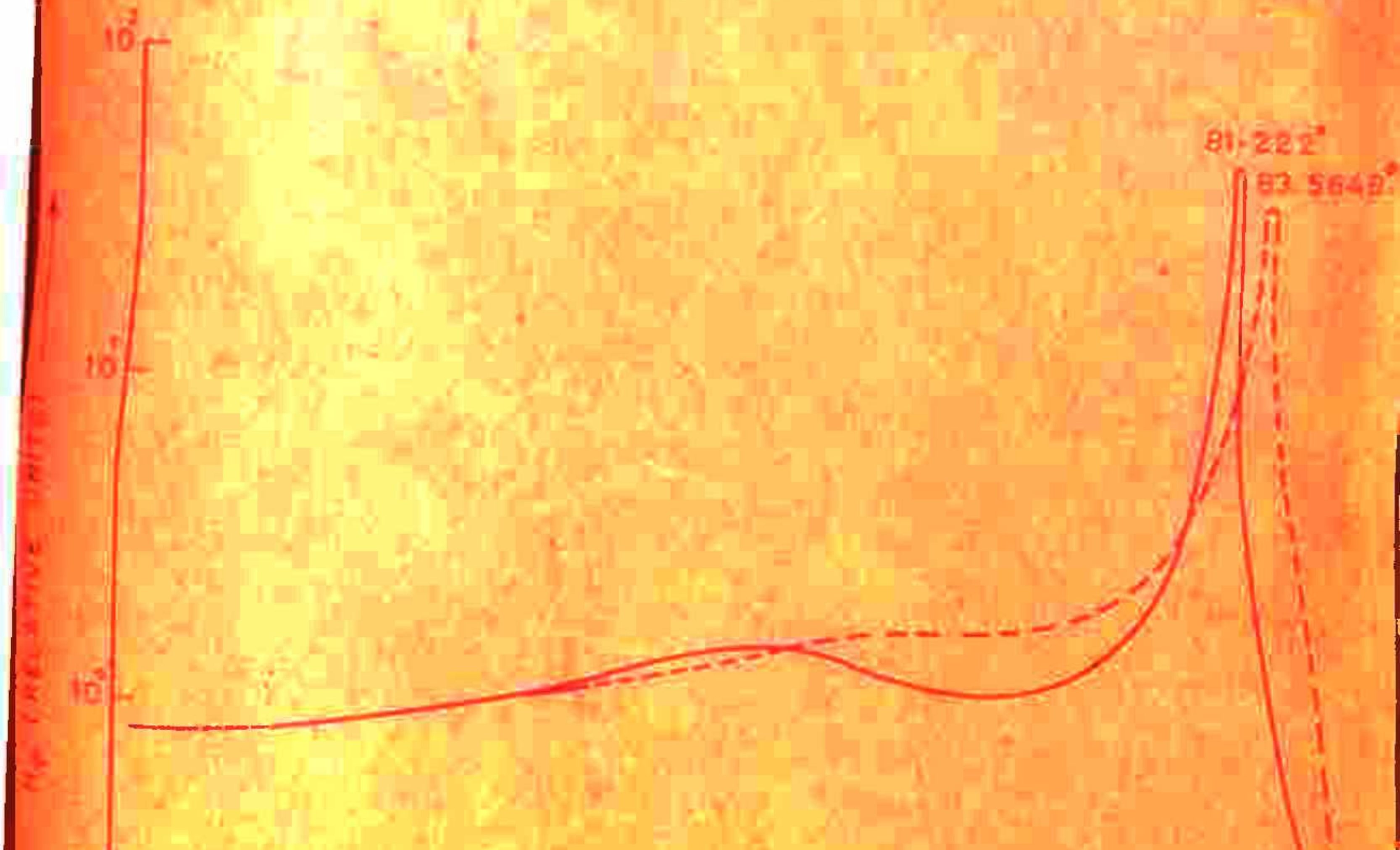
10^2
10^1
10^0
10^{-1}
81·222°
83·5649°
ε_3 = 0·9081
ε_1 = 0·9007
ε_1 = 0·7844
10
20
30
40
50
60
70
80
90
θ

FIG. 4.16

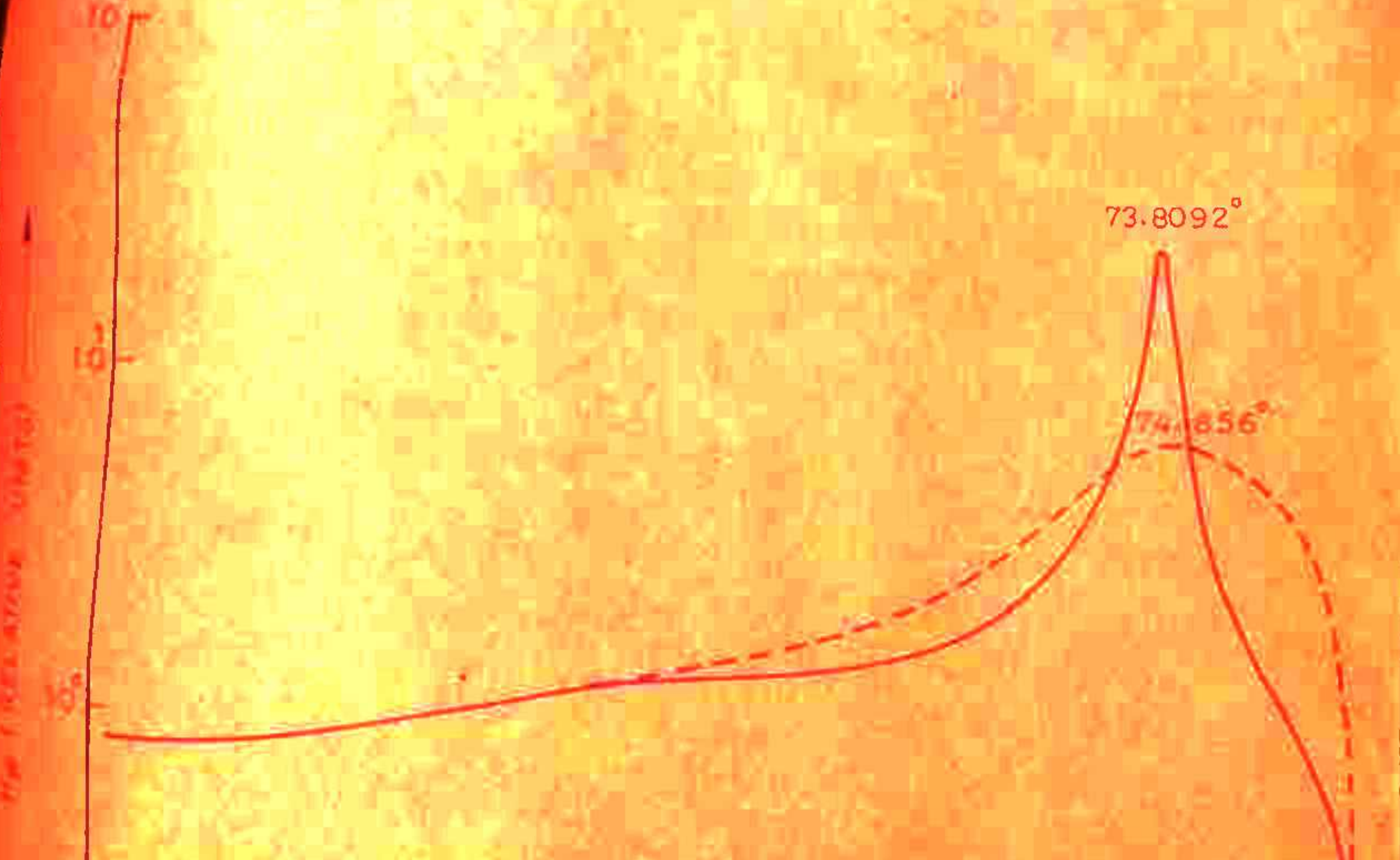
10^2
10^1
10^0
10^{-1}
73.8092°
74.856°
$\epsilon_3 = 0.9081$
$\epsilon_1 = -0.5384$
$\epsilon_1 = 1.1956$
10
20
30
40
50
60
70
80
90
θ

FIG. 4.17

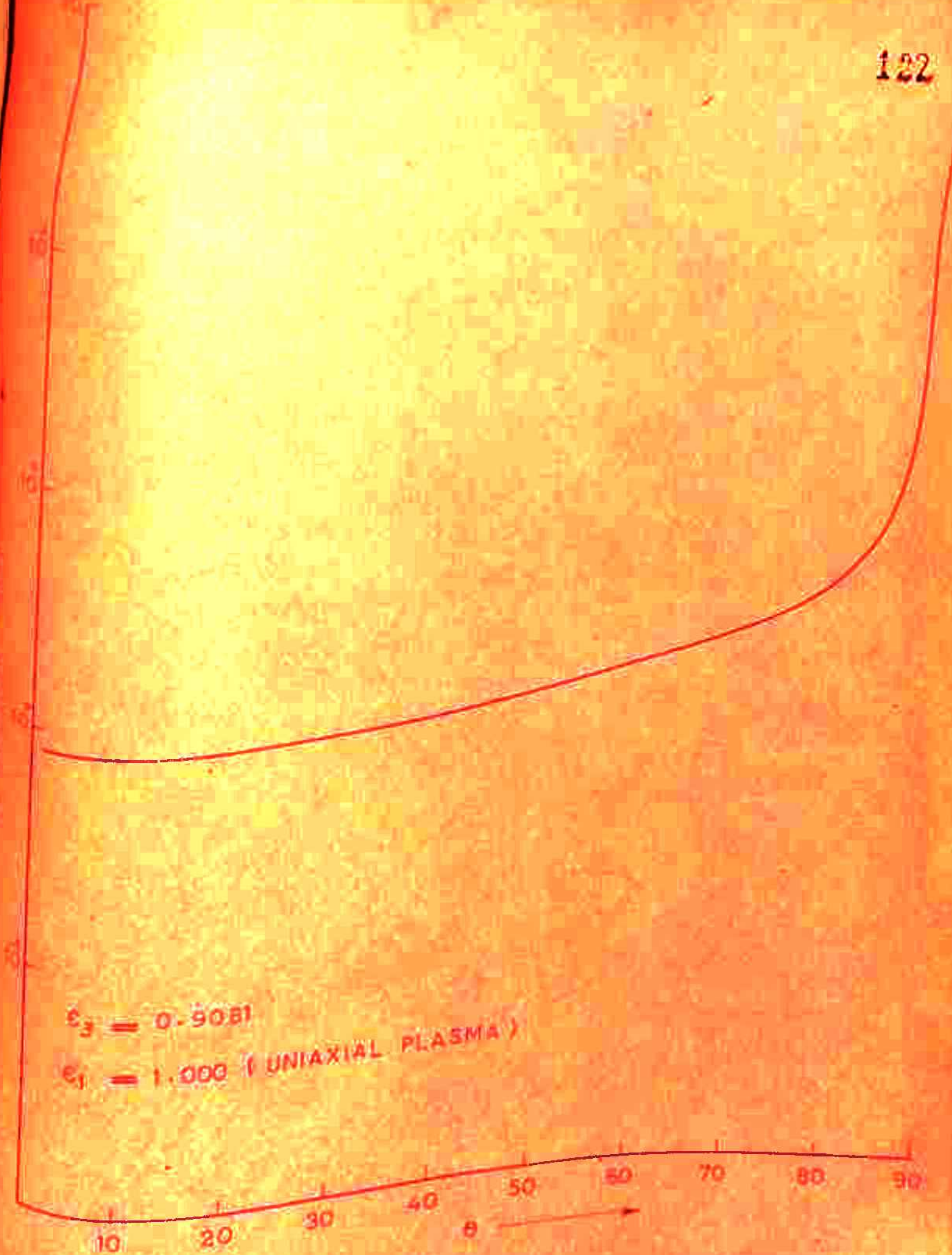
10
10
10
10
$\epsilon_3 = 0.9081$
$\epsilon_1 = 1.000$ (UNIAXIAL PLASMA)
10
20
30
40
50
60
70
80
90
θ

FIG. 4.18

Effect of $k_o b$:

$k_o b$ affects the amplitude of the radiation peak and to a very small extent its direction too. Higher values of $k_o b$ give rise to weaker radiation peak. The amplitude variation of peak with $k_o b$ is shown in fig. 4.19.

Effect of $k_o a_2$:

$k_o a_2$ affects both direction and amplitude of the radiation peak formed. For fixed k_o, the higher values of $k_o a_2$ means increasing the inner diameter of the annular plasma column. Four different values of $k_o a_2$ = 3.5, 4.0, 4.5 and 5.0 have been taken. The directions and amplitudes of the radiation peaks for ε_3 = .1100, ε_1 = .0325 and ε_3 = .9081, ε_1 = .7844 are given in Table 4.5 for these different values of $k_o a_2$.

Effect of $k_o a_1$:

$k_o a_1$ affects the direction as well as the amplitude of the radiation peaks. For fixed k_o, the higher values of $k_o a_1$ means increasing the diameter of central conductor. Four different values of $k_o a_1$ = 0.04, 0.05, 0.06 and 0.07 have been taken. The directions and amplitudes of radiation peaks

TABLE -4.5

Effect of varying $k_o a_2$ (i.e. for a fixed k_o, changing the inner diameter of the annular plasma column).

$\epsilon_3 = 0.1100$, $\epsilon_1 = 0.0325$, $k_o a_3 = 0.8$, $k_o b = 6.0$, $k_o a_1 = 0.08$

$k_o a_2$	Direction of peaks (in degrees)	Amplitude of H_z (relative units)
3.5	11.8914	0.1450×10^1
	76.9478	0.1342×10^3
4.0	15.1231	0.2559×10^1
	78.8020	0.2698×10^3
4.5	23.0902	0.6543×10^1
	80.2101	0.1052×10^4
5.0	32.6320	0.1057×10^2
	81.5187	0.1009×10^4

$\epsilon_3 = 0.9081$, $\epsilon_1 = 0.7844$, $k_o a_3 = 0.8$, $k_o b = 6.0$, $k_o a_1 = 0.08$

$k_o a_2$	Direction of peaks (in degrees)	Amplitude of H_z (relative units)
3.5	82.2911	0.4133×10^2
4.0	83.2450	0.4040×10^2
4.5	84.1623	0.3195×10^2
5.0	85.1601	0.3827×10^2

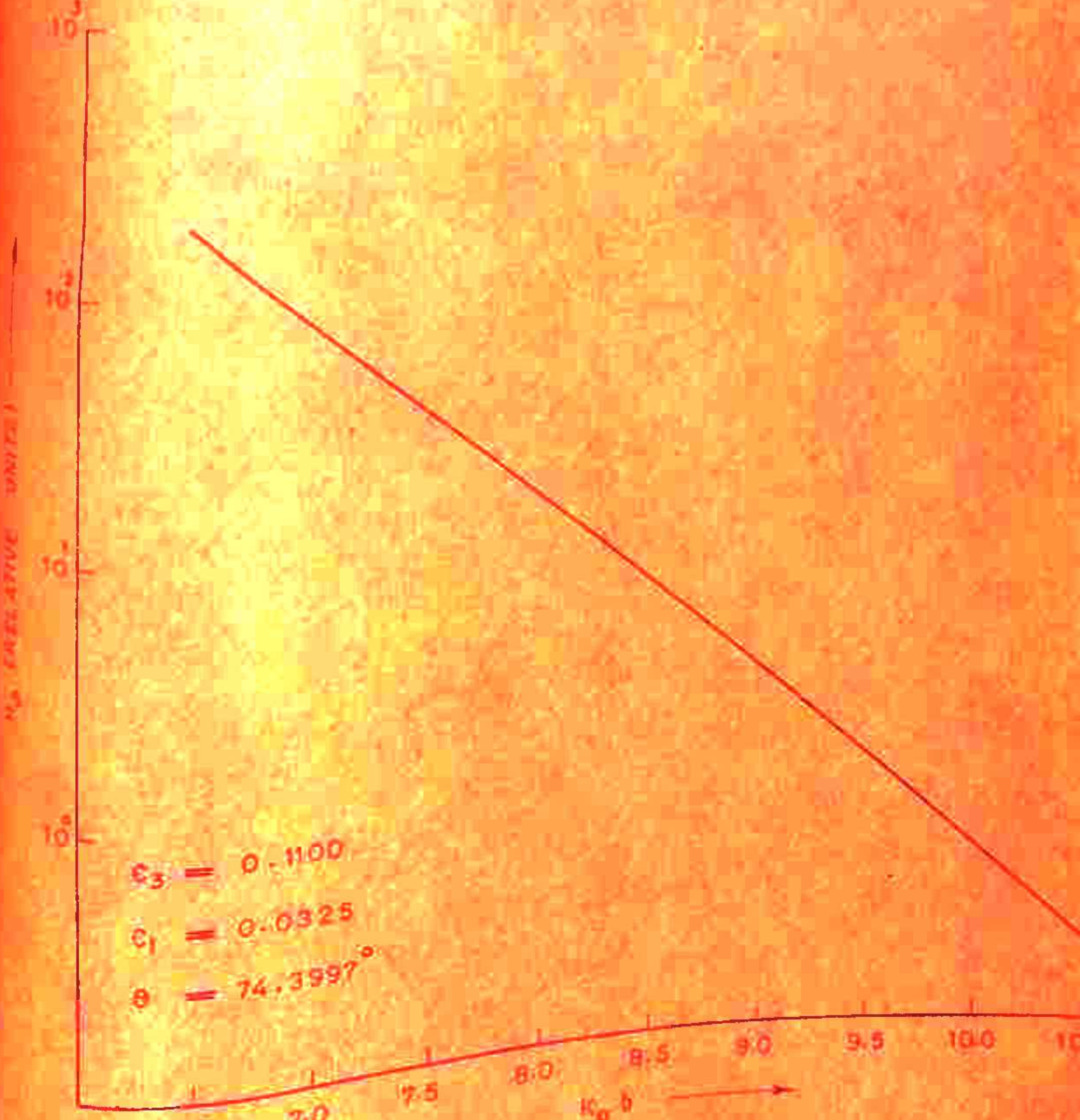
10^3
10^2
10^1
10^0
Q (RELATIVE UNITS)
ϵ_3 = 0.1100
c_1 = 0.0325
θ = 74.3997°
6.5
7.0
7.5
8.0
8.5
9.0
9.5
10.0
$k_0 b$

FIG. 4.19

for ϵ_3= 0.1100, ϵ_I= 0.0325 and ϵ_3 = 0.0081, ϵ_I= 0.7844 are given in Table 4.6 for these different values of $k_o a_I$.

Effect of plasma density:

The direction of radiation peak is affected by ϵ_3, which in turn depends upon plasma density. The radiation patterns for two different values of ϵ_3 are shown in fig. (4.12), (4.14), (4.15), (4.16), (4.17) and (4.18). The amplitude and value of half power beam width is also affected by the plasma density. For low density plasma a single radiation peak is obtained in an end fire direc-tion.

Effect of $k_o a_3$:

$k_o a_3$ does not affect the direction of radiation peak of the radiation pattern but affects its amplitude. For excitation of the TEM mode in a coaxial line, $k_o a_3$ should be < I. The variation of peak amplitude with $k_o a_3$ is shown in fig. 4.20.

4.2.4 DISCUSSION:

In the previous section 4.I, it has been noted that the direction of radiation peak is independent of the

TABLE -4.6

Effect of varying k_oa_1 (i.e. for a fixed k_o, changing the diameter of the central conductor).

$\epsilon_3 = 0.1100$, $\epsilon_1 = 0.0325$, $k_oa_3 = 0.8$, $k_ob = 6.0$, $k_oa_2 = 3.0$

k_oa_1	Direction of peaks (in degrees)	Amplitude of H_ϕ (relative units)
0.04	10.5905	0.1291×10^1
	75.9707	0.1066×10^3
0.05	10.5222	0.1253×10^1
	75.5170	0.8017×10^3
0.06	10.4604	0.1219×10^1
	75.1122	0.9912×10^2
0.07	10.4110	0.1180×10^1
	74.7427	0.7319×10^2

$\epsilon_3 = 0.9081$, $\epsilon_1 = 0.7844$, $k_oa_3 = 0.8$, $k_ob = 6.0$, $k_oa_2 = 3.0$

k_oa_1	Direction of peaks (in degrees)	Amplitude of H_ϕ (relative units)
0.04	81.9694	0.5092×10^2
0.05	81.7498	0.5315×10^2
0.06	81.5565	0.4856×10^2
0.07	81.3382	0.4478×10^2

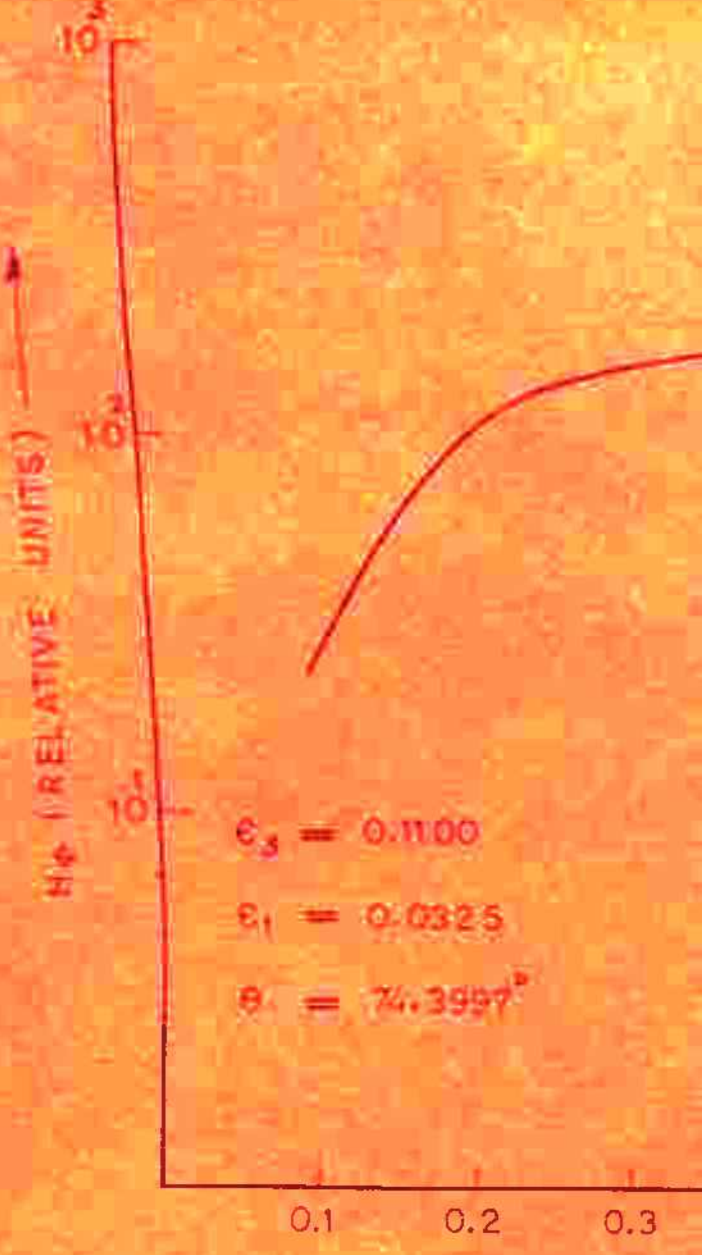

10^3
10^2
10^1
H_ϕ (RELATIVE UNITS)
$\epsilon_s = 0.1100$
$\epsilon_1 = 0.0325$
$\theta = 74.3997^\circ$
0.1
0.2
0.3

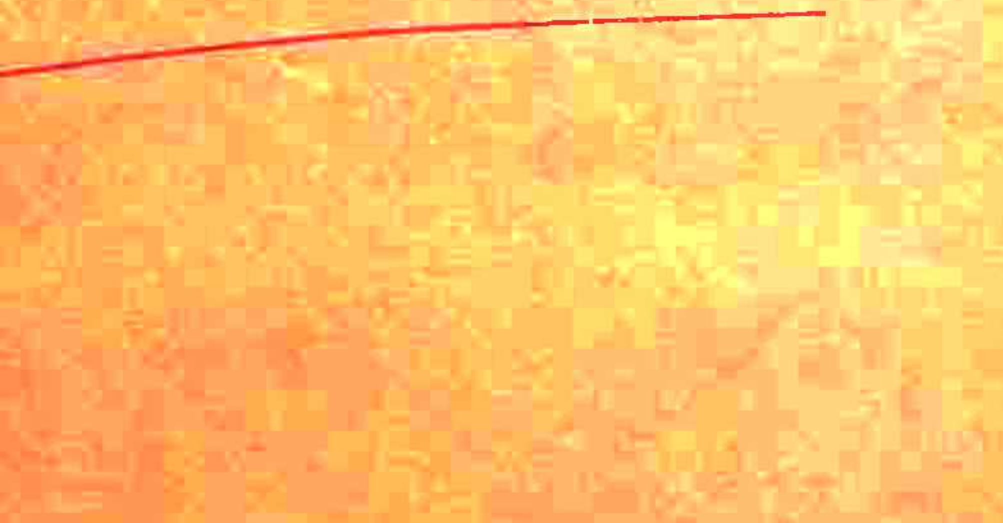

FIG. 4.20

diameter of magnetic ring source. The field distribution of magnetic ring source is given by Kronecker's delta function. The physical realisation of such an ideal magnetic ring source is not very convenient. In this section, the radiation patterns of an open ended coaxial line in an air core having central conductor and surrounded by an annular axially magnetised plasma column have been studied. Sharp radiation peak or peaks are obtained depending upon the plasma density and applied magnetic field. For low density plasma, a sharp radiation peak is obtained in an end fire direction . The peak corresponds to the minimas of the denominator of F(0). The direction of the beam is in-dependent of the inner diameter of the outer conductor of the open ended coaxial line. This geometry has smaller parametric values and gives rise to sharp radiation peaks with a very small value of half power beam width. For uniaxial plasma column, a sharp radiation peak at 90° corresponding to the maxima of numerator is obtained. This geometry is also an attempt in the direction of studying the case of more practically feasible source of electromagnetic waves.

* * *

CHAPTER 5.

RADIATION FIELD OF A MAGNETIC RING SOURCE SURROUNDED BY INHOMOGENEOUS ANISOTROPIC PLASMA COLUMN.

5.I Introduction I31

5.2 Radiation field in case of axially magnetized inhomogeneous plasma column

5.2.I Formulation of the problem I33

5.2.2 Calculation of the radiation field I37

5.3 Radiation field in case of axially magnetized inhomogeneous plasma column having central conductor along its axis

5.3.I Formulation of the problem I40

5.3.2 Calculation of the radiation field I44

5.4 Radiation field in case of an air core having central conductor and surrounded by annular axially magnetized inhomogeneous plasma column

5.4.I Formulation of the problem I48

5.4.2 Calculation of the radiation field I5I

5.5 Conclusion I55

CHAPTER-5.

RADIATION FIELD OF A MAGNETIC RING SOURCE SURROUNDED BY INHOMOGENEOUS ANISOTROPIC PLASMA COLUMN.

5.I INTRODUCTION.

In actual laboratory plasma, the plasma column does not have uniform density over the cross-section and the density varies in certain fashion. Because of the complexity of the wave coupling in inhomogeneous anisotropic regions, the analysis of radiation has been limited primarily to homogeneous media or to inhomogeneous media simulated by piece wise constant density layers. Yeh and Rusch[32] have studied the interaction of a microwave with an inhomogeneous and anisotropic plasma column. Samaddar[33] has treated the excitation of interface surface waves by a magnetic ring source concentric with an inhomogeneous plasma column having a continuous radial variation of dielectric constant. Samaddar[34] has also studied the radiation field of a magnetic ring source in a plasma clad metal cylinder in a uniform , angular, static magnetic field. The radiation patterns of a slotted cylinderical antenna in the presence of an inhomogeneous lossy plasma have been calculated[35].

In this chapter, the radiation field of a magnetic ring source in three geometries [(i) axially magnetized plasma column (ii) axially magnetized plasma column with central conductor (iii) an air core having a central conductor and surrounded by an annular axially magnetized plasma column] have been obtained assuming the plasma column to be inhomogeneous. It has been assumed that the free electron density within the plasma cylinder is inhomogeneous in the radial direction and density profile is parabolic.

The method of analysis involves the solution of inhomogeneous wave equations using Fourier-Transform. This yields the solution for the field in form of a definite integral. The radiation field is obtained from the asymptotic evaluation of integral by saddle point. The plasma is anisotropic by virtue of an impressed magneto-static field in the axial direction and its electromagnetic properties may be described in terms of local, macroscopic dielectric tensor. It has been assumed that the free electron density within the plasma cylinder is inhomogeneous in the radial direction and the density profile is parabolic. The existence of a pure E-mode is considered. It has been shown[30] that the E-mode can be considered to exist independently when the operating frequency is away from the cyclotron frequency.

5.2 RADIATION FIELD IN CASE OF AN AXIALLY MAGNETIZED INHOMOGENEOUS PLASMA COLUMN.

5.2.I FORMULATION OF THE PROBLEM:

An infinitely long column of plasma of radius 'b' is oriented with its axis along the z-axis of the (ρ, ϕ, z) cylindrical coordinate system (fig. 5.I). The source of electromagnetic radiation is a ring of magnetic current of radius 'a' (a < b) , concentric with the plasma column and situated in the z = 0 plane. The source field distribution is mathematically represented as,

$$\bar{K} = \bar{\phi}\, \delta (\rho - a)\, \delta(z) \qquad (5.2.I)$$

where δ represents Kronecker's delta function and $\bar{\phi}$ is a unit vector in ϕ -direction.

The source form of Maxwell's equations governing the electromagnetic field written in differential form for an e^{-jwt} time dependence can be written as,

$$\nabla \times \bar{E} = j\omega\mu_0\, \bar{H} - \bar{K} \qquad (5.2.2)$$

$$\nabla \times \bar{H} = - j\omega\tilde{\epsilon}\, (\rho).\, \bar{E} \qquad (5.2.3)$$

where $\tilde{\epsilon}\, (\rho)$ is the permittivity tensor of the cold inhomogeneous and anisotropic plasma with the magnetostatic field in the positive z-direction.

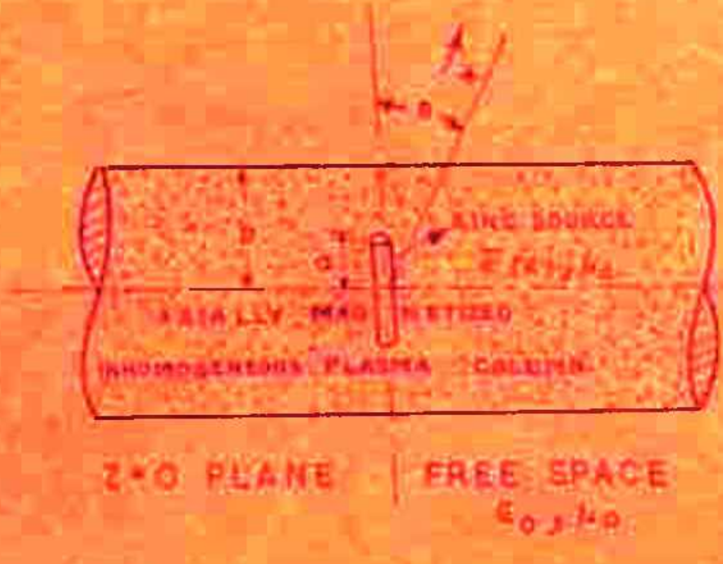
θ
b
a
LINE SOURCE
AXIALLY MAGNETIZED
INHOMOGENEOUS PLASMA COLUMN
Z=0 PLANE
FREE SPACE
ϵ_0, μ_0

FIG.

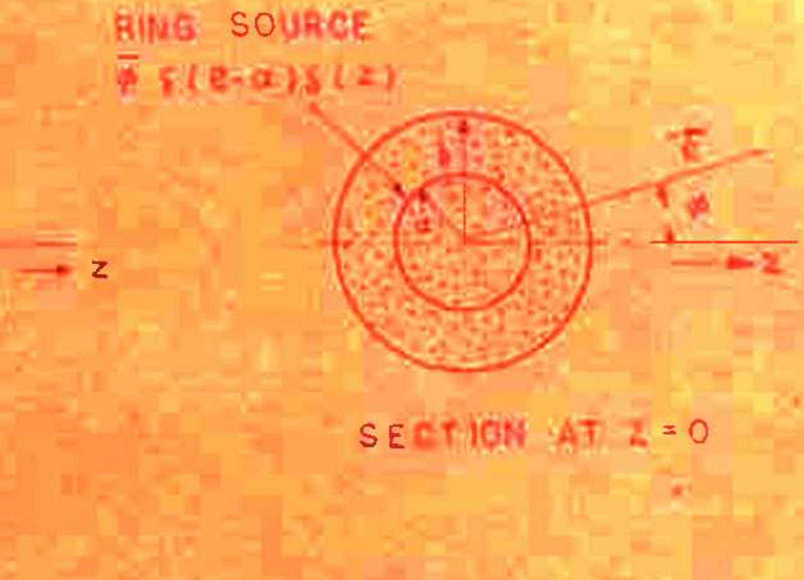
RING SOURCE
$\bar{\Phi}\,\delta(\rho-a)\,\delta(z)$
b
a
$\bar{r}$
θ
z
z

SECTION AT Z = 0

5.1

$$\tilde{\varepsilon}(\rho) = \begin{vmatrix} \varepsilon_1(\rho) & j\varepsilon_2(\rho) & 0 \\ -j\varepsilon_2(\rho) & \varepsilon_1(\rho) & 0 \\ 0 & 0 & \varepsilon_3(\rho) \end{vmatrix} \qquad (5.2.4)$$

where

$$\varepsilon_1(\rho) = \varepsilon_0 \left\{ 1 + \frac{w_p^2(\rho)}{w_c^2 - w^2} \right\} \qquad (5.2.4a)$$

$$\varepsilon_2(\rho) = \varepsilon_0 \left\{ \frac{w_c}{w} \left(\frac{w_p^2(\rho)}{w_c^2 - w^2} \right) \right\} \qquad (5.2.4b)$$

$$\varepsilon_3(\rho) = \varepsilon_0 \left\{ 1 - \frac{w_p^2(\rho)}{w^2} \right\} \qquad (5.2.4c)$$

$$w_p^2(\rho) = \left(\frac{n(\rho)\, e^2}{m\varepsilon_0} \right)$$

where $n(\rho)$ is the free electron density, e is the electron charge, m is the electron mass, ε_0 is free space permittivity, w is source frequency, w_p is the plasma frequency and w_c is the cyclotron frequency.

Due to the choice of the source of excitation, the electromagnetic fields will be independent of the angular coordinate ϕ (i.e. $\frac{\partial}{\partial \phi} = 0$). For circular symmetric TM_{01} mode, it follows that,

$$\frac{\partial^2 H_\phi}{\partial \rho^2} + \frac{1}{\rho}\,\frac{\partial H_\phi}{\partial \rho} - \frac{1}{\rho^2} H_\phi + \frac{\varepsilon_3(\rho)}{\varepsilon_1(\rho)}\,\frac{\partial^2 H_\phi}{\partial z^2} +$$

$$k_0^2\, \varepsilon_3(\rho) H_\phi + \left(\frac{H_\phi}{\rho} + \frac{\partial H_\phi}{\partial \rho} \right) \varepsilon_3(\rho)\, \frac{\partial}{\partial \rho} \left\{ \frac{1}{\varepsilon_3(\rho)} \right\} = -$$

$$- j\omega\varepsilon_0\, \varepsilon_3(\rho)\, \delta(\rho - a)\, \delta(z) \qquad (5.2.5)$$

where $k_0^2 = \omega^2 \mu_0 \varepsilon_0$. In order to solve equation (5.2.5), the method of integral transform is applied. Let the Fourier transform $H_\phi(\rho, z)$ be defined as

$$h(\rho, \xi) = \int_{-\infty}^{+\infty} H_\phi(\rho, z)\, e^{-j\xi z}\, dz$$

and inverse transform be given by

$$H_\phi(\rho, z) = \frac{1}{2\pi} \int_{-\infty}^{+\infty} h(\rho, \xi)\, e^{j\xi z}\, d\xi$$

Now multiplying each term of equation (5.2.5) by $e^{-j\xi z}$ and integrating over the infinite range with respect to z we get

$$\frac{d^2 h}{d\rho^2} + \left[\frac{1}{\rho} + \varepsilon_3(\rho)\, \frac{\partial}{\partial \rho} \left\{ \frac{1}{\varepsilon_3(\rho)} \right\} \right] \frac{dh}{d\rho} +$$

$$\left[k_0^2\, \varepsilon_3(\rho) - \frac{\varepsilon_3(\rho)}{\varepsilon_1(\rho)}\, \xi^2 + \frac{\varepsilon_3(\rho)}{\rho}\, \frac{\partial}{\partial \rho} \left\{ \frac{1}{\varepsilon_3(\rho)} \right\} - \frac{1}{\rho^2} \right] h =$$

$$= - j\omega\varepsilon_0\, \varepsilon_3(\rho)\, \delta(\rho - a) \qquad (5.2.6)$$

Equation (5.2.6) is an ordinary differential equation with ξ as a parameter constant. Boundary conditions on h follow from the boundary condition on its inverse Fourier-transform. Taking into account the appropriate boundary conditions on h and its derivative with respect to ρ, the solution for h in free space is found and then its inverse Fourier-transform gives the field in free space.

5.2.2 CALCULATION OF THE RADIATION FIELD.

The delta function is defined as follows:

$$\int_{a-\Delta}^{a+\Delta} \delta(\rho-a)\, d\rho = I \text{ , and } \delta(\rho-a) = 0 \text{ for } \rho \neq a \qquad (5.2.8)$$

consequently for all ρ other than $\rho = a$ equation (5.2.6) reduces to differential equation,

$$\frac{d^2h}{d\rho^2} + a_I(\rho)\frac{dh}{d\rho} + \left[a_2(\rho) - \frac{\varepsilon_3(\rho)}{\varepsilon_I(\rho)}\xi^2\right] h = 0 \quad (5.2.7$$

where

$$a_I(\rho) = \frac{I}{\rho} + \varepsilon_3(\rho)\frac{\partial}{\partial\rho}\left\{\frac{I}{\varepsilon_3(\rho)}\right\}$$

$$a_2(\rho) = k_o^2\,\varepsilon_3(\rho) + \frac{\varepsilon_3(\rho)}{\rho}\frac{\partial}{\partial\rho}\left\{\frac{I}{\varepsilon_3(\rho)}\right\} - \frac{I}{\rho^2}$$

The solutions of equation (5.2.7) have been obtained for a radially inhomogeneous plasma region within which the free electron density is given by

$$n(\rho) = n_o \left[I - \left(\frac{\rho}{b} \right)^2 \right], \quad 0 \leq \rho \leq b \qquad (5.2.8)$$

where n_o is the electron density on axis, and 'b' is the outer radius of the plasma column. The two independent series solutions are obtained.

$$R_n(k_o\rho) = (k_o\rho)^s \sum_{m=0}^{\infty} f(s,m)\,(k_o\rho)^m \qquad (5.2.9)$$

$$S_n(k_o\rho) = (k_o\rho)\,\text{In}(k_o\rho) + \sum_{m=0}^{\infty} g(s,m)(k_o\rho)^{m-I} \qquad (5.2.IO)$$

The series coefficients f(s,m) and g(s,m) involve the parameter constant ξ. These coefficients can be evaluated by inserting equation (5.2.9) and (5.2.IO) into equation (5.2.7).

Now solution of equation (5.2.7) in region $I(0<\rho<a)$, will be

$$h = A_I\, R_n(k_o\rho)$$

In region $II(a<\rho<b)$, it will be

$$h = A_2\, R_n(k_o\rho) + B_2 S_n(k_o\rho)$$

and the solution in free space is

$$h = A_3\, H_I(\nu_o\,\rho)$$

where

$$\nu_0^2 = k_0^2 - \xi^2$$

Applying the appropriate boundary conditions at the junctions of different radial zones, four simultaneous equations will be obtained. By these equations, the value of A_3 is found out and which in turn by inverting the Fourier transform will give the radiation field in free space. By this procedure the calculated value of A_3 is

$$A_3 = -j\omega\epsilon_0 \ \epsilon_3(a) \ F[\nu_0, f(s,m), g(s,m)]$$

where

$$F[\nu_0, f(s,m), g(s,m)] = \frac{a_{11}(a_{32}\, a_{43} - a_{33}\, a_{42})}{(a_{32}\, a_{44} - a_{34}\, a_{42})(a_{11}\, a_{23} - a_{13}\, a_{21})}$$

$a_{11} = R_n(k_0 a)$, $\quad a_{32} = R_n(k_0 b)$, $\quad a_{42} = k_0 R_n'(k_0 b)$

$a_{34} = -H_1(\nu_0 b)$, $\quad a_{44} = \epsilon_3(b)(\nu_0 b) H_0(\nu_0 b) - H_1(\nu_0 b)$, $a_{33} = H_1(\nu_0 b)$

$a_{32}\, a_{43} - a_{33}\, a_{42} = \{k_0 R_n(k_0 b) S_n'(k_0 b) - S_n(k_0 b) R_n'(k_0 b)\}$

$a_{11}\, a_{23} - a_{13}\, a_{21} = \{S_n(k_0 a) R_n'(k_0 b) - S_n'(k_0 a) R_n(k_0 a)\}$

where the prime denotes derivatives of function with respect to its argument.

The solution in free space is

$$h = A_3 H_1(\nu_0 \rho)$$

Inverting it we have

$$H_\phi(\rho,z) = \frac{I}{2\pi}\int_{-\infty}^{+\infty} A_3 H_I(\nu_0\rho)\, e^{j\xi z}\, d\xi \qquad (5.2.II)$$

The integrand of equation (5.2.II) is a contour integration in ξ - plane and can be solved by applying the standard method of saddle point integration (Appendix D). The solution for the radiation field in spherical coordinate system (r, θ, ϕ) can be put in the form

$$H_\phi(r,\theta) \simeq j\left(\frac{\epsilon_0}{\mu_0}\right)^{I/2} \frac{k_0\, a}{\pi}\, \epsilon_3(a) F(\theta)\, \frac{e^{jk_0 \vec{r}}}{\vec{r}}$$

where $F(\theta) = F\left[\nu_0,\ f(s,m),\ g(s,m)\right]\Big|_{\beta=\theta}$ is the transformed values of $F\left[\nu_0,\ f(s,m),\ g(s,m)\right]$ at the saddle point.

5.3 RADIATION FIELD OF A MAGNETIC RING SOURCE SURROUNDED BY AN INHOMOGENEOUS AXIALLY MAGNETIZED PLASMA COLUMN HAVING CENTRAL CONDUCTOR ALONG ITS AXIS:

5.3.I FORMULATION OF THE PROBLEM:

The geometry of the configuration analysed is shown in fig. 5.2. An infinitely long column of plasma of radius 'b' and having a central conductor of radius 'a_I' along the

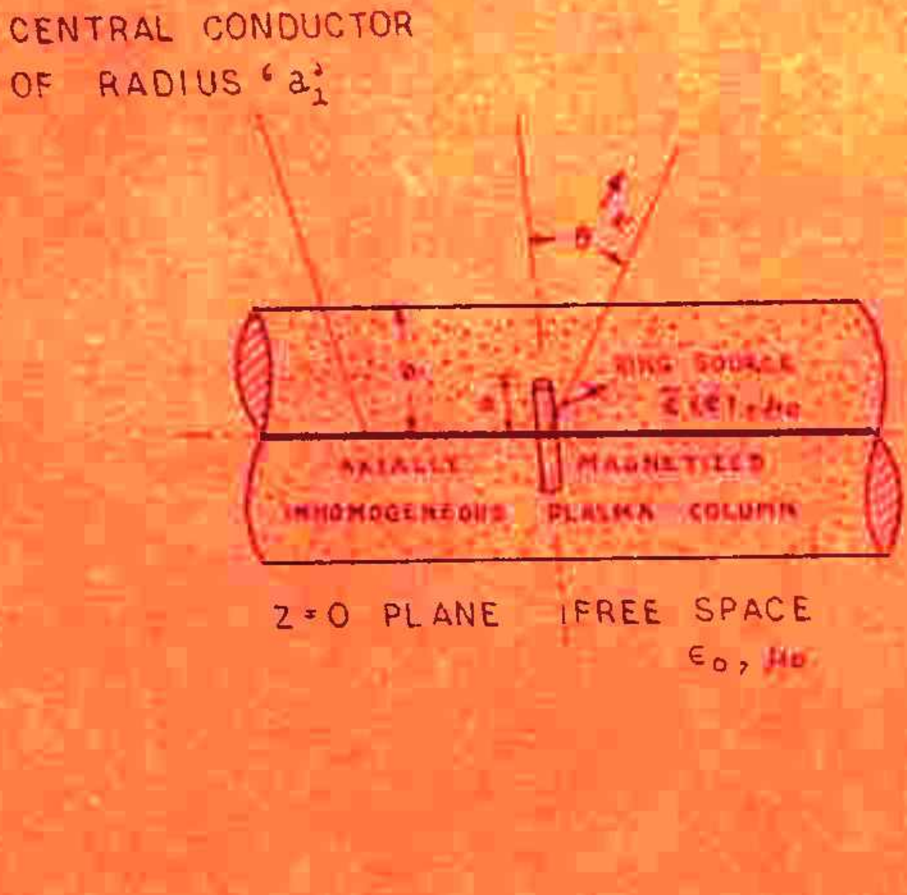
CENTRAL CONDUCTOR OF RADIUS 'a$_1$'
θ
b
a
RING SOURCE
ε(r), μ$_0$
AXIALLY MAGNETIZED INHOMOGENEOUS PLASMA COLUMN
Z = 0 PLANE
FREE SPACE
ε$_0$, μ$_0$

FIG.

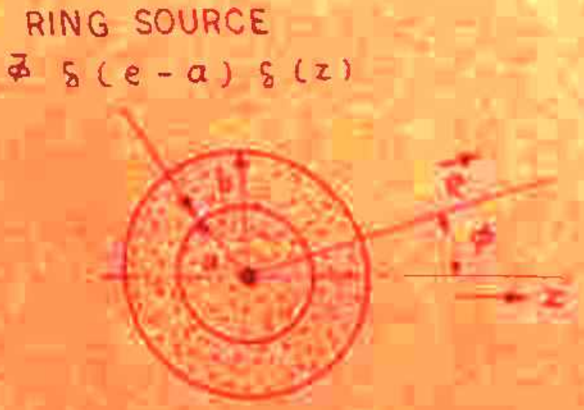
RING SOURCE
$\bar{Q}\,\delta(\rho - a)\,\delta(z)$
b
a
R
φ
z

SECTION AT Z = 0

5.2

axis is oriented with its axis along the z-axis of the cylindrical coordinate (ρ, ϕ , z) system. The source of electromagnetic radiation is a ring of magnetic current of radius 'a' (a < b), concentric with the plasma column and situated in the z = 0 plane. The source field distribution is mathematically represented as

$$\bar{K} = \bar{\phi} \quad \delta(\rho - a) \, \delta (z) \tag{5.3.I}$$

where δ represents Kronecker's delta function and $\bar{\phi}$ is a unit vector in ϕ - direction.

Due to the choice of the source of excitation, the electromagnetic fields will be independent of the coordinate ϕ (i.e. $\partial/\partial\phi = 0$). For the circular symmetric TM_{0I} mode, the inhomogeneous wave equation for H_ϕ may be written as (details in sec. 5.2.I)

$$\frac{\partial^2 H_\phi}{\partial \rho^2} + \frac{I}{\rho} \frac{\partial H_\phi}{\partial \rho} - \frac{I}{\rho^2} H_\phi + \frac{\epsilon_3(\rho)}{\epsilon_I(\rho)} \frac{\partial^2 H_\phi}{\partial z^2} + k_0^2 \, \epsilon_3(\rho) H_\phi$$
$$+ \left(\frac{H_\phi}{\rho} + \frac{\partial H_\phi}{\partial \rho} \right) \epsilon_3(\rho) \frac{\partial}{\partial \rho} \left\{ \frac{I}{\epsilon_3(\rho)} \right\} = -j\omega\epsilon_0 \, \epsilon_3(\rho) \, \delta(\rho - a) \delta(z) \tag{5.3.2}$$

In order to solve equ. (5.3.2), the method of integral transform is applied. Let the Fourier-transform $H_\phi(\rho, z)$ be defined as

$$h(\rho, \xi) = \int_{-\infty}^{+\infty} H_\phi(\rho, z)\, e^{-j\xi z}\, dz$$

and inverse transform be given by

$$H_\phi(\rho, z) = \frac{1}{2\pi} \int_{-\infty}^{+\infty} h(\rho, \xi)\, e^{j\xi z}\, d\xi$$

Now multiplying each term of equation (5.3.2) by $e^{-j\xi z}$ and integrating over the infinite range with respect to z we get

$$\frac{d^2h}{d\rho^2} + \left[\frac{1}{\rho} + \epsilon_3(\rho)\frac{\partial}{\partial\rho}\left\{\frac{1}{\epsilon_3(\rho)}\right\}\right]\frac{dh}{d\rho} +$$

$$+\left[k_0^2\,\epsilon_3(\rho) - \frac{\epsilon_3(\rho)}{\epsilon_1(\rho)}\,\xi^2 + \frac{\epsilon_3(\rho)}{\rho}\,\frac{\partial}{\partial\rho}\left\{\frac{1}{\epsilon_3(\rho)}\right\} - \frac{1}{\rho^2}\right] h =$$

$$= -j\omega\epsilon_0\,\epsilon_3(\rho)\,\delta(\rho - a) \qquad (5.3.3)$$

Equation (5.3.3) is an ordinary differential equation with ξ as a parameter constant. Boundary conditions on h follow from the boundary condition on its inverse Fourier Transform. Taking into account the appropriate boundary conditions on h and its derivative with respect to ρ, the solution for h in free space is found and then its inverse Fourier-transform gives the field in free space.

5.3.2 CALCULATION OF THE RADIATION FIELD:

The delta function is defined as follows

$$\int_{a-\Delta}^{a+\Delta} \delta(\rho-a)\, d\rho = I, \text{ and } \delta(\rho-a) = 0 \text{ for } \rho \neq a$$

Consequently for all ρ other than $\rho = a$ equation (5.3.3) reduces to differential equation

$$\frac{d^2h}{d\rho^2} + a_I(\rho)\frac{dh}{d\rho} + \left[a_2(\rho) - \frac{\epsilon_3(\rho)}{\epsilon_I(\rho)}\xi^2\right] h = 0 \qquad (5.3.4)$$

where

$$a_I(\rho) = \frac{I}{\rho} + \epsilon_3(\rho)\frac{\partial}{\partial\rho}\left\{\frac{I}{\epsilon_3(\rho)}\right\}$$

$$a_2(\rho) = k_0^2\, \epsilon_3(\rho) + \frac{\epsilon_3(\rho)}{\rho}\frac{\partial}{\partial\rho}\left\{\frac{I}{\epsilon_3(\rho)}\right\} - \frac{I}{\rho^2}$$

The solution of equation (5.3.4) have been obtained for a radially inhomogeneous plasma region within which the free electron density is given by

$$n(\rho) = n_0\left[I - (\rho/d)^2\right], \quad a_I \leq \rho \leq b, \ d \geq b \qquad (5.3.5)$$

where n_0 determines the magnitude of electron density, and d is a constant related to profile shape. Thus if d = b, the density decays monotonically to zero at the edge of the sheath ($\rho = b$), in the other limit, if d ≥ b, the electron density is essentially constant within the sheath and drops abruptly to zero at the edge. The parabolic plasma density profile of equ. (5.3.5) closely approximates the radial distribution of electron density in the plasma sheath surrounding a hypersonic re-entry vehicle[36]. The two independent series solutions are obtained,

$$R_n(k_o\rho) = (k_o\rho)^s \sum_{m=0}^{\infty} f(s,m)\,(k_o\rho)^m \qquad (5.3.6)$$

$$S_n(k_o\rho) = (k_o\rho)\ln(k_o\rho) + \sum_{m=0}^{\infty} g(s,m)\,(k_o\rho)^{m-1} \qquad (5.3.7)$$

The series coefficients f(s,m) and g(s,m) involve the parameter constant ξ. These coefficients can be evaluated by inserting equ. (5.3.6) and (5.3.7) into equation (5.3.4).

Now solution of equation (5.3.4) in region I, ($a_1 < \rho < a$), will be

$$h = A_1\, R_n(k_o\rho) + B_1\, S_n(k_o\rho)$$

In region II ($a < \rho < b$), it will be

$$h = A_2\, R_n(k_o\rho) + B_2\, S_n(k_o\rho)$$

and the solution in free space is

$$h = A_3\, H_1\,(\nu_o\,\rho)$$

where

$$\nu_o^2 = k_o^2 - \xi^2$$

Applying the appropriate boundary conditions at the junctions of different radial zones, five simultaneous equations will be obtained. By these equations the value of A_3 is found out and which in turn by inverting the Fourier-transform will give the radiation field in free space. By this procedure the calculated value of A_3 is

$$A_3 = j\omega\epsilon_0 \, \epsilon_3(a) \, F\left[\nu_0, f(s,m), g(s,m)\right]$$

$$F\left[\nu_0; f(s,m), g(s,m)\right] = \frac{(a_{43} a_{54} - a_{44} a_{53})(a_{11} a_{22} - a_{12} a_{21}}{\left[a_{11} x_1 - a_{12} x_2\right]}$$

$$x_1 = \Big\{(a_{44} a_{55} - a_{45} a_{54})(a_{22} a_{33} - a_{23} a_{32}) - (a_{43} a_{55} - a_{45} a_{53})(a_{22} a_{34} - a_{24} a_{32})\Big\}$$

$$x_2 = \Big\{(a_{44} a_{55} - a_{54} a_{45})(a_{21} a_{33} - a_{23} a_{31}) - (a_{43} a_{55} - a_{44} a_{53})(a_{21} a_{34} - a_{24} a_{31})\Big\}$$

$a_{11} = R_n(k_0 a_1) + a_1 R_n'(k_0 a_1)$, $a_{12} = S_n(k_0 a_1) + a_1 S_n'(k_0 a_1)$

$a_{21} = R_n(k_0 a)$, $a_{22} = S_n(k_0 a)$, $a_{23} = -R_n(k_0 a)$,

$a_{24} = -S_n(k_0 a)$, $a_{31} = R_n'(k_0 a)$, $a_{32} = S_n'(k_0 a)$

$a_{33} = -R_n'(k_0 a)$, $a_{34} = -S_n'(k_0 a)$, $a_{43} = R_n(k_0 b)$

$a_{44} = S_n(k_0 b)$, $a_{45} = -R_n(k_0 b)$, $a_{53} = b R_n'(k_0 b)$,

$$a_{54} = bH_n'(k_0 b), \quad a_{55} = -\varepsilon_3(\nu_0 b)H_0(\nu_0 b) - H_1(\nu_0 b)$$

where $\varepsilon_3(a)$ is the value of $\varepsilon_3(\rho)$ component of the dielectric tensor at $\rho = a$, and prime denotes derivatives of function with respect to its argument.

The solution in free space is

$$h = A_3 H_1(\nu_0 \rho)$$

inverting it we have

$$H_\phi(\rho, z) = \frac{1}{2\pi}\int_{-\infty}^{+\infty} A_3 H_1(\nu_0\rho)\, e^{j\xi z}\, d\xi \qquad (5.3.8)$$

The integrand of equation (5.3.8) is a contour integration in ξ - plane and can be solved by applying the standard method of saddle point integration (Appendix D). The solution for the radiation field in spherical coordinate system (r, θ, ϕ) can be put in the form

$$H_\phi(r,\theta) = -\frac{j\omega\varepsilon_0\, \varepsilon_3(a)}{\pi} \cdot F(\theta)\, \frac{e^{jk_0 r}}{r}$$

where $F(\theta) = F\left[\nu_0, f(a,m), g(a,m)\right]\Big|_{\rho = 0}$ is the transformed values of $F\left[\nu_0, f(a,m), g(a,m)\right]$ at the saddle point.

5.4 RADIATION FIELD IN CASE OF AN AIR CORE HAVING A CENTRAL CONDUCTOR AND SURROUNDED BY ANNULAR AXIALLY MAGNETIZED INHOMOGENEOUS PLASMA COLUMN.

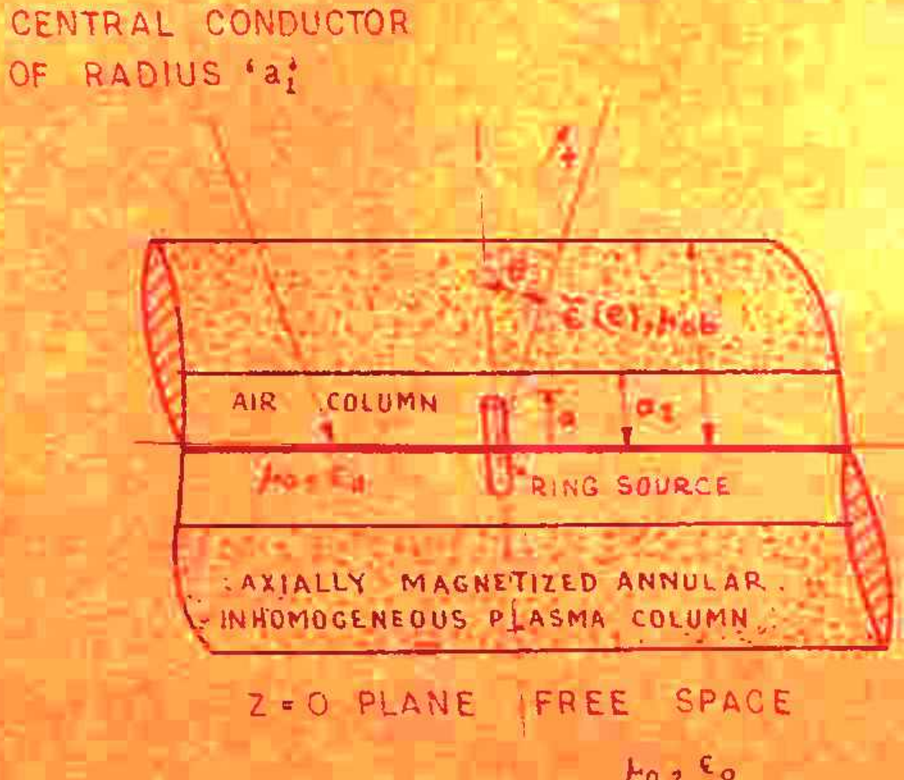
CENTRAL CONDUCTOR OF RADIUS 'a_i'
z
θ
$\epsilon(r), \mu_0 B$
AIR COLUMN
r_a
a_2
μ_0, ϵ_0
RING SOURCE
AXIALLY MAGNETIZED ANNULAR INHOMOGENEOUS PLASMA COLUMN
Z = 0 PLANE
FREE SPACE
μ_0, ϵ_0

FIG.

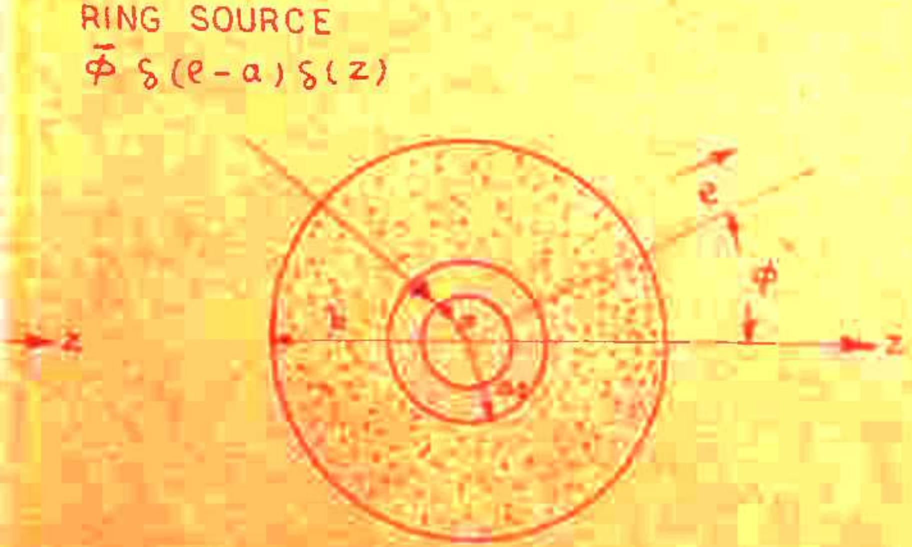
RING SOURCE
$\bar{\Phi}\,\delta(\rho-a)\,\delta(z)$
ρ
ϕ
b
a
a_0
z
z

SECTION AT Z = 0

5.3

5.4.I. FORMULATION OF THE PROBLEM:

The geometry of the configuration analysed is illustrated in fig. (5.3). An infinitely long air column of radius 'a_2' having infinitely long conductor of radius 'a_I' along the longitudinal axis and surrounded by axially magnetized annular plasma column of inner radius 'a_2' and outer radius 'b' is oriented with its axis along the z-axis of the (ρ, ϕ, z) cylindrical coordinate system. The medium surrounding the plasma column and extending to infinity is free space, with constants ϵ_0 and μ_0. The electromagnetic field source is a filamentary ring of magnetic current of radius 'a' ($a < a_2$) concentric with air column and situated at z = 0 plane. The source field distribution is presented as

$$\bar{K} = \bar{\phi}\, \delta(\rho - a)\, \delta(z) \tag{5.4.I}$$

where δ represents Kronecker's delta function and $\bar{\phi}$ is a unit vector in ϕ -direction.

Due to the choice of the source of excitation, the electromagnetic fields will be independent of the coordinate ϕ (i.e. $\partial/\partial\phi = 0$). For circular symmetric TE_{0I} mode, the inhomogeneous wave equation for H_ϕ may be written as (details in section 5.2.I)

$$\frac{\partial^2 \Pi_\phi}{\partial \rho^2} + \frac{1}{\rho}\frac{\partial \Pi_\phi}{\partial \rho} - \frac{1}{\rho^2}\Pi_\phi + \frac{\varepsilon_3(\rho)}{\varepsilon_1(\rho)}\frac{\partial^2 \Pi_\phi}{\partial z^2} +$$

$$+ k_0^2\,\varepsilon_3(\rho)\,\Pi_\phi + \left(\frac{\Pi_\phi}{\rho} + \frac{\partial \Pi_\phi}{\partial \rho}\right)\varepsilon_3(\rho)\frac{\partial}{\partial \rho}\left\{\frac{1}{\varepsilon_3(\rho)}\right\} =$$

$$= -j\omega\varepsilon_0\varepsilon_3(\rho)\,\delta(\rho-a)\,f(z) \qquad (5.4.2)$$

In order to solve equation (5.4.2), the method of integral transform is applied. Let the Fourier transform $\Pi_\phi(\rho,z)$ be defined as

$$h(\rho,\xi) = \int_{-\infty}^{+\infty} \Pi_\phi(\rho,z)\,e^{-j\xi z}\,dz.$$

and inverse transform be given by

$$\Pi_\phi(\rho,z) = \frac{1}{2\pi}\int_{-\infty}^{+\infty} h(\rho,\xi)\,e^{j\xi z}\,d\xi$$

Now multiplying each term of equation (5.4.2) by $e^{-j\xi z}$ and integrating over the infinite range with respect to z, we got

$$\frac{d^2h}{d\rho^2} + \left[\frac{1}{\rho} + \varepsilon_3(\rho)\frac{\partial}{\partial \rho}\left\{\frac{1}{\varepsilon_3(\rho)}\right\}\right]\frac{dh}{d\rho} +$$

$$+\left[k_0^2\,\varepsilon_3(\rho) - \frac{\varepsilon_3(\rho)}{\varepsilon_1(\rho)}\xi^2 + \frac{\varepsilon_3(\rho)}{\rho}\frac{\partial}{\partial \rho}\left\{\frac{1}{\varepsilon_3(\rho)}\right\} - \frac{1}{\rho^2}\right] h =$$

$$= -j\omega\varepsilon_0\,\varepsilon_3(\rho)\,\delta(\rho-a) \qquad (5.4.3)$$

Equation (5.4.3) is an ordinary differential equation with ξ as a parameter constant. Boundary conditions on h follow from the boundary condition on its inverse Fourier-transform. Taking into account the appropriate boundary conditions on h and its derivative with respect to ρ, the solution for h in free space is found and then its inverse Fourier-transform gives the field in free space.

5.4.2 CALCULATION OF THE RADIATION FIELD

The delta function is defined as follows

$$\int_{a-\Delta}^{a+\Delta} \delta(\rho-a)\,d\rho = 1, \text{and} \quad \delta(\rho-a) = 0 \text{ for } \rho \neq a.$$

consequently for all ρ other than $\rho = a$ equation (5.4.3) reduces to differential equation,

$$\frac{d^2h}{d\rho^2} + a_1(\rho)\frac{dh}{d\rho} + \left[a_2(\rho) - \frac{\epsilon_3(\rho)}{\epsilon_1(\rho)}\xi^2\right] h = 0 \qquad (5.4.4)$$

where

$$a_1(\rho) = \frac{1}{\rho} + \epsilon_3(\rho)\frac{\partial}{\partial\rho}\left\{\frac{1}{\epsilon_3(\rho)}\right\}$$

$$a_2(\rho) = k_0^2\,\epsilon_3(\rho) + \frac{\epsilon_3(\rho)}{\rho}\frac{\partial}{\partial\rho}\left\{\frac{1}{\epsilon_3(\rho)}\right\} - \frac{1}{\rho^2}$$

The solution of equation (5.4.4) have been obtained for a radially inhomogeneous plasma region within which the free electron density is given by

$$n(\rho) = n_0 \left[I - (\rho/d)^2 \right], \quad a_2 \leq \rho \leq b, \quad d \geq b. \qquad (5.4.5)$$

where n_0 determines the magnitude of electron density, and d is a constant related to profile shape. Thus if $d = b$, the density decays monotonically to zero at the edge of the sheath ($\rho = b$), in the other limit, if $d \geq b$, the electron density is essentially constant within the sheath and drops abruptly to zero at the edge. The parabolic plasma density profile of (5.4.5) closely approximates the radial distribution of electron density in the plasma sheath surrounding a hypersonic re-entry vehicle[36]. The two independent series solutions are obtained,

$$R_n(k_0\rho) = (k_0\rho)^s \sum_{m=0}^{\infty} f(s,m)\,(k_0\rho)^m \qquad (5.4.6)$$

$$S_n(k_0,\rho) = (k_0\rho)\ln(k_0\rho) + \sum_{m=0}^{\infty} g(s,m)\,(k_0\rho)^{m-I} \qquad (5.4.7)$$

The series coefficients $f(s,m)$ and $g(s,m)$ involve the parameter constant ξ . These coefficients can be evaluated by inserting equation (5.4.6) and (5.4.7) into equation (5.4.4).

Now solution of equation (5.4.4) in region $I(a_I<\rho<a)$ will be

$$h = A_I J_I(\nu_I \rho) + B_I Y_I(\nu_I \rho)$$

where $\nu_I^2 = k_I^2 - \xi^2$, and $k_I^2 = \omega^2 \mu_0 \epsilon_0 \epsilon_a$

In region II ($a < \rho < a_2$), it will be,

$$h = A_2 J_I(\nu_I \rho) \quad B_2 Y_I(\nu_I \rho)$$

In region (III) ($a_2 < \rho < b$), it is

$$h = A_3 R_n(k_0 \rho) + B_3 S_n(k_0 \rho)$$

and the solution in free space is

$$h = A_4 H_I(\nu_0 \rho)$$

where $\nu_0^2 = k_0^2 - \xi^2$

Applying the appropriate boundary conditions at the junctions of different radial zones, seven simultaneous equations will be obtained. By these equations the value of A_4 is found out and which in turn by inverting the Fourier-transform will give the radiation field in free space. By this procedure the calculated value of A_4 is

$$A_4 = -\left(\frac{2j\omega\epsilon_0\epsilon_a a}{\pi} \right) F\left[\nu_0, \nu_I, f(a,m), g(a,m)\right]$$

where

$$F\left[\nu_0, \nu_I, f(a,m), g(a,m)\right] = \frac{(a_{11}a_{22} - a_{12}a_{21})(a_{56}a_{75} - a_{55}a_{76})}{(a_{11}x_I - a_{12}x_2)}$$

$$x_I = \Big\{ (a_{56}a_{77} - a_{57}a_{76})(a_{45}a_{64} - a_{44}a_{65}) + \\ + (a_{55}a_{77} - a_{57}a_{75})(a_{44}a_{66} - a_{64}a_{46}) \Big\}$$

$$X_2 = \Big\{ (a_{55}\, a_{77} - a_{57}\, a_{75})\, (a_{43}\, a_{66} - a_{46}\, a_{63}) +$$

$$+ (a_{56}\, a_{77} - a_{57}\, a_{76})\, (a_{45}\, a_{63} - a_{43}\, a_{65}) \Big\}$$

$$a_{11} = (\nu_1\, a_1)\, J_0(\nu_0 a_1), \quad a_{12} = (\nu_1\, a_1)\, Y_0(\nu_1\, a_1),$$

$$a_{21} = J_1(\nu_1\, a), \quad a_{22} = Y_1(\nu_1\, a), \quad a_{43} = J_1(\nu_1 a_2)$$

$$a_{44} = Y_1(\nu_1 a_2), \quad a_{45} = -R_n(k_0 a_2), \quad a_{46} = -S_n(k_0 a_2),$$

$$a_{55} = R_n(k_0 b), \quad a_{56} = S_n(k_0 b),$$

$$a_{57} = -H_1(\nu_0 b), \quad a_{63} = -\Big[(\nu_1 a_2) J_0(\nu_1 a_2) - J_1(\nu_1 a_2)\Big]$$

$$a_{64} = -\Big[(\nu_1 a_2)\, Y_0(\nu_1 a_2) - Y_1(\nu_1\, a_2)\Big],$$

$$a_{65} = \left[\frac{\epsilon_a}{\epsilon_3(a_2)}\, (k_0 a_2)\, R_n'(k_0 a_2) + \left(\frac{\epsilon_a}{\epsilon_3(a_2)} - 1\right) R_n(k_0 a_2)\right]$$

$$a_{66} = \left[\frac{\epsilon_a}{\epsilon_3(a_2)}\, (k_0 a_2)\, S_n'(k_0 a_2) + \left(\frac{\epsilon_a}{\epsilon_3(a_2)} - 1\right) S_n(k_0 a_2)\right].$$

$$a_{77} = \Big[(\nu_0\, b) \quad * \quad H_0(\nu_0 b) - H_1(\nu_0\, b)\Big],$$

where ϵ_a is the dielectric constant of air, $\epsilon_3(a_2)$ and $\epsilon_3(b)$ are the value of the $\epsilon_3(\rho)$ component of the dielectric tensor at $\rho = a_2$ and b respecively . Here the prime denotes the derivatives of the function with respect to its agrument.

The solution in free space is

$$h = A_4\, H_1(\nu_0\, \rho)$$

Inverting it we have

$$H_{\phi}(\rho,z) = \frac{1}{2\pi} \int_{-\infty}^{+\infty} A_4 H_1(\nu_0 \rho)\, e^{j\xi z}\, d\xi \qquad (5.4.8)$$

The integrand in equation (5.4.8) is a contour integration in ξ - plane and can be solved by applying the standard method of saddle point integration. The solution for the radiation field in spherical coordinate system (r, θ, φ) can be put in the form,

$$H_{\phi}(r,\theta) = -\frac{j\omega\epsilon_0 \epsilon_a a}{\pi} F(\theta) \frac{e^{jk_0 \vec{r}}}{\vec{r}}$$

where $F(\theta) = F(\nu_0, \nu_I, f(s,m), g(s,m))\Big|_{\beta=\theta}$ is the transformed values of $F\left[\nu_0, \nu_I, f(s,m), g(s,m)\right]$ at the saddle point.

5.5 CONCLUSION:

The radiation field of a magnetic ring source in three plasma geometries [(i) axially magnetised plasma column with central conductor (ii) axially magnetised plasma column with central conductor (iii) an air core having a central condutor and surrounded by an annular axially magnetised plasma column] have been evaluated assuming. the plasma column to be inhomogeneous. The plasma density profile of the sheath is chosen such that it approximates the actual profile encountered for a re-entry vehicle. The radiation patterns (variation of $F(\theta)$ with θ) may be computed for various parametric values and effect of inhomogeneity and magnetic field may be studied.

* * *

CHAPTER 6.

SUMMARY, CONCLUDING REMARKS AND SUGGESTIONS FOR FURTHER WORK.

6.I Summary I58

6.2 Concluding remarks I63

6.3 Suggestions for further work I65

CHAPTER-6.

SUMMARY, CONCLUDING REMARKS AND SUGGESTIONS FOR FURTHER WORK:

6.I SUMMARY:

The radiation patterns of a magnetic ring source surrounded by axially magnetized plasma column have been studied. Plasma is considered as a lossless and anisotropic dielectric medium with the permittivity given by the permittivity tensor. The existence of a pure E-mode is assumed. It has been shown by Kislov and Bogdanov[30] that E-mode can be considered to exist independently when operating frequency is away from the cyclotron frequency. In transparent region ($w > w_p$), the radiation field is calculated by the technique of saddle point integration. The configuration gives rise to radiation peak or peaks depending upon the value of plasma density, applied magnetic field and column diameter.

The peaks are obtained when the denominator of $F(\theta)$ (equ. 2.3) is minimum which in turn is governed by the value of $J_o(k_o bv)$ or $J_I(k_o bv)$. In case of low density plasma, the value of half power beam width is large. The number of peak increases with increase in the column diameter. For very high magnetic fields, the broad radiation peak is obtained in end-fire direction. It may also be noted that source radius 'a' occurs only in the numerator of equ.(2.3). Since, the direction of peak is governed only by the denominator of equ. (2.3) , any variation in source radius will not change the direction of peak and only the amplitude will be affected. The geometry has advantage over the previously analysed isotropic geometry[9,10] because now there are two scanning functions (i.e. plasma density and applied magnetic field) instead of one scanning function (plasma density). Therefore, the beam can be scanned over a considerably wider range of angles. The presence of these radiation peaks may be attributed to the leaky waves.

The radiation patterns of a magnetic ring source surrounded by axially magnetised plasma column having a central conductor along its axis have been studied. For $\epsilon_1 < \epsilon_3$, the radiation pattern possess two radiation peaks. The first peak corresponds to the minima of denominator and second peak corresponds to the maxima of numerator. When ϵ_1 is negative or $\epsilon_1 > 1$, only shallow peaks are obtained. Thus for the values $w_c < w < w_p$, sharp peaks are obtained. For uniaxial plasma column, a sharp radiation peak at 90° corresponding to the maxima of numerator is obtained. The direction of peak depends upon the plasma density, applied magnetic field, column diameter and radiation field is obtained as a vector sum of field components due to individual rings of magnetic current. The geometry gives rise to relatively strong peaks with a smaller value of half power beam width in comparision to the geometry analysed in section 3.I. The direction of radiation peak is independent of the inner radius of the outer conductor of the coaxial line. The presence of these beams may be attributed to the leaky waves supported by the configuration.

The radiation patterns of a magnetic ring source of electromagnetic waves, in an air column having a central conductor along its axis and surrounded by an annular axially magnetised plasma column are studied. The radiation peaks or a peak is obtained in the patterns depending upon the parametric values of the configuration. When $\epsilon_I < \epsilon_3$, ϵ_I is negative or $\epsilon_I > I$, the peak corresponds to the minima of the denominator of $F(\theta)$. For $\epsilon_I = I$, a sharp peak at 90° is obtained corresponding to the maxima of numerator. The direction of the peak can be varied by changing the plasma density, applied magnetic field, diameter of annular plasma column and diameter of central conductor. The direction of the peak is independent of the diameter of ring source. For low density plasma, sharp peak is obtained in end-fire direction.

To have a practically more convenient source of excitation, the radiation patterns of an open ended coaxial line in an air core having a central conductor and surrounded by an annular axially magnetised plasma column have been studied. The direction of the beam is independent of the inner diameter of the outer conductor of the open ended coaxial line. The geometries discussed in sec. 4.1 and 4.2 give rise to most sharp peaks with the smallest value of half power beam width as compared to the previously analysed geometries (in chap. 2 and chap. 3). More over, the parametric values of the configuration are also small compared to the previously analysed geometries (in chap.2 and chap. 3). The presence of these sharp beams may be attributed to the leaky waves supported by the geometry.

The radiation field of a magnetic ring source in three plasma geometries [(i) axially magnetised plasma column (ii) axially magnetised plasma column with central conductor (iii) an air core having a central conductor and surrounded by an annular axially magnetised plasma column] have been evaluated considering the plasma column to be inhomogeneous. The plasma density profile of the sheath is chosen such that it approximates the actual profile encountered for a re-entry vehicle. The radiation patterns (variation of F(0) with 0) may be computed for various parametric values and effect of inhomogeneity and magnetic field may be studied.

6.2 CONCLUDING REMARKS:

The work reported in this thesis is mainly concerned with the radiation pattern characteristics of different sources in different geometries. It is found that radiation pattern possessing one or more sharply peaked beams may be obtained. Attempt has been made in the direction of selecting practically feasible geometries with proper parametric values, excited by practically convenient sources of electromagnetic waves so as to give well enhanced radiation peaks. The anisotropic plasma geometries analysed here,have advantage over the isotropic plasma geometries since it gives a wider range of angles over which the beam can be scanned. Since it is difficult to maintain the plasma density for the large radius of the plasma column it is also desired to choose that configuration which requires small plasma column radius.

The radiation patterns of circular symmetric sources (magnetic ring source, open ended coaxial line) in an air core having central conductor and surrounded by an annular axially magnetized plasma column give rise to most enhanced radiation peak with a very small value of half power beam width. This configuration also requires smaller column radius compared with the geometry analysed in chap. 2 and 3. But in this case, the radiation peak amplitude decreases heavily as we change the main radiation angle. The radiation peaks obtained in chap. 2 are broad and less enhanced compared with those in chap. 3. Comparing the results of these chapters, it may be noted that most promosing case from practical point of view with an eye on having sharp peak with larger scanning angle seems to be that of coaxial line excitation in an axially magnetized plasma column having central conductor along its axis.

Based upon these results it may be proposed to develop an electronically scannable antenna system. For the physical realisation of such an antenna system, the theoretically selected parameters should be within the experimental range. For the excitation frequency of 10 GHz , the value of plasma density varies approximately from $10^{12}/cm^3$ to $10^{11}/cm^3$ as the value of ϵ_3 changes from 0.1 to 0.9. The d.c. discharge can be used for producing plasma whose density can be varied by changing the plasma current. Bachyanski and Gibbs[37] has described that magnetic field can be produced by two magnetic coils arranged in a Helmholtz configuration without enclosing the plasma column. This arrangement is capable of producing magnetic fields of several kilo-Gauss . For $\epsilon_3 = 0.1100$ the magnetic field of 5000 Gauss allows the variation of ω_c/ω_p upto 1.5 and for $\epsilon_3 = .9081$, it allows the variation of ω_c/ω_p

upto 3.7. The magnetic field can be varied by changing the working area of the coil.

The field distribution $\bar{\phi}\ \delta(\rho-a)\,\delta(z)$ of the magnetic ring source can physically be approximated by a coaxial line excited in the TEM mode and tapered to a narrow annular aperture. In case of an open ended coaxial line excitation the inner conductor of the coaxial line can be made to run through the length of the column to serve as the central conduc-tor. In solids[38], the plasma state can be achieved by an injection process and the plasma density can be varied by varying the injection current. The anisotropic plasma state can also be simulated with the help of articicial dielectrics[39]. In theory, axially magnetized plasma column and air core (chap. 4) have been assumed to be infinitely long . For practical arrangement, a finite plasma column has to be taken and due to the presence of finite plasma a widening of the major lobe of radiation is expected[40-4I].

6.3 SUGGESTIONS FOR FURTHER WORK:

In all the geometries considered here, the emergence of radiation peaks may be attributed to the excitation of leaky waves on the plasma surfaces. It is proposed to do theoretical analysis of calculating radiation field from the near field consideration of properly excited leaky waves by

Kirchoff Hugen integration method. For this purpose, first the location of leaky wave poles is to be calculated. Analytic calculation for the location of leaky wave poles is difficult because of the involvement of Bessel functions with complen arguments. Numerical methods may be helpful in calculating the location of leaky wave poles.

In the present analysis, excitation of circular symmetric mode has been considered. For obtaining a radiation pattern with a limited extent in azimuthal plane, it is necessary to excite a dipolar or multipolar mode on the plasma column. Excitation of these higher modes on the plasma column should be studied. Effect of inhomogeneities of plasma column could also be studied as the summation of uniform annular plasma column of different dielectric tensor.

The temperature effect (compressibility) of plasma state should also be taken into account in all geometrics. Due to the compressibility of plasma, an excitation of electroacoustic mode in addition to electromagnetic mode is expected. The effect of glass tubing (which is normally used for containing the plasma), finite length of the plasma column and those of losses in plasma should also be taken into account.

Plasma is a gyroelectric medium whose permittivity is given by a tensor. On the other hand, there is another class of materials known as ferrites which exhibit ferromagnetic properties. In presence of a state magnetic field the permeability of a ferrite becomes anisotropic i.e. μ becomes a tensor. A number of investigations have been carried out in connection with the wave propagation in gyromagnetic medium[42-45]. These investigation mostly deals with guided waves. The radiation characteristics of the e.m. sources inside the following geometries should be studied. The suggested geometries are:

(i) Ferrite column.

(ii) Ferrite column having central conductor

(iii) A dielectric rod surrounded by an annular ferrite column.

(iv) A wave guide filled with ferrite and having holes on its surface.

The radiation field of e.m. sources for these geometries may be evaluated and the radiation pattern characteristics may be studied.

•••

APPENDICES

Appendix A. Analysis of the axially magnetized plasma column

A.I Derivation and solution of equ. 2.2 I69

A.2 Calculation of the radiation field I74

Appendix B. Analysis of the axially magnetized plasma column having central conductor I78

Appendix C. Analysis of the an air core having central conductor and surrounded by annular axially magnetized plasma column I8I

Appendix D. Saddle point integration method I84

APPENDIX-A.

[illegible] PLASMA COLUMN:

A.I DERIVATION AND SOLUTION OF THE EQUATION 2.2:

The electromagnetic field is a solution of Maxwell's equation, written in differential form for $e^{-j\omega t}$ time dependence we have

$$\nabla \times \bar{E} = j\omega\mu_0 \bar{H} - \bar{K} \qquad (A.1)$$

$$\nabla \times \bar{H} = -j\omega\tilde{\varepsilon} \cdot \bar{E} \qquad (A.2)$$

where the source distribution $\bar{K}$ of a magnetic ring source of radius 'a' is represented as a product of the dirac delta function in the ρ and z coordinate as follows

$$\bar{K} = \bar{\phi}\, \delta(\rho - a)\, \delta(z) \qquad (A.3)$$

The source distribution $\bar{K}$ is independent of $\bar{\phi}$ and is a unit source such that

$$\iint \bar{K} \cdot \bar{\phi}\, da = \int_{a-\Delta}^{a+\Delta} \int_{a-\Delta}^{a+\Delta} \delta(\rho-a)\delta(z)\, dz\, d\rho = I$$

$\bar{K}$ has the dimensions of volts per square meter. The plasma is anisotropic by virtue of an applied magnetostatic field along the z-axis of the cylindrical column. The permittivity tensor $\tilde{\varepsilon}$ for the cold, anisotropic plasma is given by

$$\tilde{\varepsilon} = \varepsilon_0 \begin{vmatrix} \varepsilon_{\rho\rho} & j\varepsilon_{\rho\theta} & 0 \\ -j\varepsilon_{\theta\rho} & \varepsilon_{\theta\theta} & 0 \\ 0 & 0 & \varepsilon_{zz} \end{vmatrix}$$

where

$$\epsilon_{\rho\rho} = \epsilon_{\theta\theta} \quad \epsilon_I = \left[I + \left(\frac{w_p^2}{w_c^2 - w^2} \right) \right]$$

$$\epsilon_{\rho\theta} = \epsilon_{\theta\rho} = \frac{w_c}{w} \left\{ \frac{w_p^2}{w_c^2 - w^2} \right\}$$

$$\epsilon_{zz} = \epsilon_3 = \left[I - \frac{w_p^2}{w^2} \right]$$

where w is the source frequency , w_p is the plasma frequency and w_c is the cyclotron resonance frequency.

The existence of a pure E-mode is considered. The magnetic current filament generates a field having component H_ϕ, E_ρ and E_z while the components E_ϕ, H_ρ and H_z are equal to zero. Due to the symmetry of the source, the field is independent of ϕ (i.e. $\frac{\partial}{\partial\phi} = 0$). For TM_{0I} mode, from equ. (A.I) and equ. (A.2), the inhomogeneous wave equation for H_ϕ may be written as;

$$\frac{\partial^2 H_\phi}{\partial\rho^2} + \frac{I}{\rho} \frac{\partial H_\phi}{\partial\rho} - \frac{I}{\rho^2} H_\phi + \frac{\epsilon_3}{\epsilon_I} \frac{\partial^2 H_\phi}{\partial z^2} + k_o^2 \epsilon_3 H_\phi =$$

$$= -jw\epsilon_o\epsilon_3 \, \delta(\rho - a) \, \delta(z) \qquad (A.5)$$

where $k_o^2 = w^2 \mu_o \epsilon_o$. In order to solve equ. (A.5), it is reduced to a non-homogeneous ordinary differential equation by method of integral transforms. We define the Fourier-transform of $H_\phi (\rho, z)$ as,

$$h(\rho, \xi) = \int_{-\infty}^{+\infty} H_\phi(\rho, z)\, e^{-j\xi z}\, dz \qquad (A.6)$$

The inverse transform is given by

$$H_\phi(\rho, z) = \frac{I}{2\pi} \int_{-\infty}^{+\infty} h(\rho, \xi)\, e^{j\xi z}\, d\xi \qquad (A.7)$$

multiplying each term of equation (A.5) by $e^{-j\xi z}$ and integrating over the infinite range with respect to z, we get,

$$\frac{d^2h}{d\rho^2} + \frac{I}{\rho}\frac{dh}{d\rho} + \left(k_o^2 \epsilon_3 - \frac{\epsilon_3}{\epsilon_I}\xi^2 - \frac{I}{\rho^2}\right) h = -j\omega\epsilon_o\epsilon_3\, \delta(\rho - a) \qquad (A.8)$$

where the source term $\delta(z)$ is no longer present. Since

$$\int_{-\infty}^{+\infty} \delta(z)\, e^{-j\xi z}\, dz = I$$

We may consider (A.8) an ordinary differential equation in which ξ is a parameter constant. The boundary condition on $h(\rho, \xi)$ follows from the boundary condition on $h(\rho, \xi)$ and its derivative with respect to ρ, the solution for $h(\rho, \xi)$ in free space is found out and then its inverse Fourier-transform gives the field in free space.

Because of the nature of delta function the equ.(A.8) may be written for all ρ other than $\rho = a$, as

$$\frac{d^2h}{d\rho^2} + \frac{I}{\rho}\frac{dh}{d\rho} + \left(k_o^2 \epsilon_3 - \frac{\epsilon_3}{\epsilon_I}\xi^2 - \frac{I}{\rho^2}\right) h = 0 \qquad (A.9)$$

The delta function $\delta(\rho - a)$ implies a boundary condition which $h(\rho, \xi)$ must satisfy at $\rho = a$. Multiplying each term of equ. (A.8) by $d\rho$, integrating over the interval from $\rho = a - \Delta$ to $\rho = a + \Delta$ and assuming $h(\rho, \xi)$ to be continuous across $\rho = a$, we have

$$\left.\frac{dh}{d\rho}\right|_{a+\Delta} - \left.\frac{dh}{d\rho}\right|_{a-\Delta} = -j\omega\epsilon_0\epsilon_3$$

The remaining boundary conditions on $h(\rho, \xi)$ follow from the boundary conditions on $H_\phi(\rho, z)$ and $E_z(\rho, z)$.

Equation (A.9) is Bessel's equation and its solution may be written as (for $0 < \rho < a$),

$$h = A_1 J_1(\nu_1 \rho)$$

for $a < \rho < b$,

$$h = A_2 J_1(\nu_1 \rho) + B_1 Y_1(\nu_1 \rho)$$

and for $\rho > b$,

$$h = A_3 H_1(\nu_0 \rho)$$

where $$\nu_1 = \sqrt{\left(k_0^2 \epsilon_3 - \frac{\epsilon_3}{\epsilon_1} \xi^2\right)}$$

$$\nu_0 = \sqrt{\left(k_0^2 - \xi^2\right)}$$

For the configuration analysed in section 2.2, the boundary conditions on h and $dh/d\rho$ at $\rho = a$ and $\rho = b$ will be

$$h\Big|_{a-\Delta} = h\Big|_{a+\Delta}$$

$$\frac{dh}{d\rho}\Big|_{a+\Delta} - \frac{dh}{d\rho}\Big|_{a-\Delta} = -\, jw\varepsilon_o\varepsilon_3$$

$$h\Big|_{b-\Delta} = h\Big|_{b+\Delta}$$

$$\varepsilon_3\frac{dh}{d\rho}\Big|_{b+\Delta} - \frac{dh}{d\rho}\Big|_{b-\Delta} + (\varepsilon_3 - I)\,\frac{h}{\rho}\Big|_{b+\Delta} = 0$$

Applying all these boundary conditions on the solutions of equ. (A.9) in different regions we have:

$$A_I J_I(\nu_I a) - A_2 J_I(\nu_I a) - B_2 Y_I(\nu_I a) = 0$$

$$A_I\,[(\nu_I a)\, J_o(\nu_I a) - J_I(\nu_I a)] - B_2\,[(\nu_I a)\, Y_o(\nu_I a) - Y_I(\nu_I a)]$$

$$- A_2[(\nu_I a)\, J_o(\nu_I a) - J_I(\nu_I a)] = jw\varepsilon_o\varepsilon_3 a$$

$$A_2 J_I(\nu_I b) + B_2\, Y_I(\nu_I b) - A_3\, H_I(\nu_o b) = 0$$

$$A_2\,[(\nu_I b)\, J_o(\nu_I b) - J_I(\nu_o b)] + B_2\,[(\nu_I b)\, Y_o(\nu_I b) - Y_I(\nu_I b)]$$

$$- A_3\,[\varepsilon_3(\nu_o b)\, H_o(\nu_o b) - H_I(\nu_o b)] = 0$$

Here we have four equations and four constant. Solving the value of A_3 from these equations we have

$$A_3 = \frac{j\omega\epsilon_0\epsilon_3\, a\, J_I(\nu_I a)}{(\nu_I b)J_0(\nu_I b)H_I(\nu_0 b) - \epsilon_3(\nu_0 b)J_I(\nu_I b)H_0(\nu_I b)}$$

The solution in free space is

$$h(\rho, \xi) = A_3 H_I(\nu_0 \rho)$$

inverting it we have

$$H_\phi(\rho, z) = \frac{I}{2\pi}\int_{-\infty}^{+\infty} A_3 H_I(\nu_0\rho)\, e^{j\xi z}\, dz \qquad (A.IO)$$

A.2 CALCULATION OF THE RADIATION FIELD:

The variables ν_I and ν_0 which appear in the integrand of equ. (A.IO) are multivalued functions in the neighbourhood of $\nu_I = 0$ and $\nu_0 = 0$ respectively. It can be shown by expanding the integrand about $\nu_I = 0$ and $\nu_0 = 0$ that integrand is an even function of ν_I and ν_0 respectively. But at $\nu_0 = 0$ the Hankel functions which appear in the integrand have logarithmetic singularity, hence $\nu_0 = 0$ gives rise the branch points of the integrand.

Consider the integrand of equ. (A.IO) as contour integral in ξ- plane and apply the method of saddle point integration to evaluate the integral. Introduce the transformation

$$\xi = k_0 \sin \beta \qquad (A.II)$$

where $\beta = \lambda + j\psi$

This transformation transforms the region of integration in ξ- plane in to a strip in the β-plane, which is bounded by two curved lines corresponding to the branch cuts at $\xi = \pm k_0$ in the β-plane. The branch cuts in β-plane are given by,

$$\sin \lambda \cos h\psi = \pm I$$

This transformation yields

$$\gamma_0 = k_0 \cos \beta$$

$$\gamma_I = k_0 \sqrt{\left(\epsilon_3 - \frac{\epsilon_3}{\epsilon_I} \sin^2 \beta \right)}$$

Now equation (A.IO) transforms to

$$H_\phi(\rho, z) = \frac{I}{2\pi} \int_c A_3(\beta)\, H_I(k_0\, \rho \cos \beta)\, e^{jk_0 \sin \beta\, z}$$

$$* \, k_0 \cos \beta \, d\beta \qquad (A.I2)$$

Shifting from cylindrical coordinate system (ρ, ϕ, z) to spherical coordinate system (r, θ, z) with the help of the transformations

$$\rho = r \cos \theta$$

$$z = r \sin \theta$$

equation (A.I2) transforms to

$$H_{\phi}(r,\theta) = \frac{I}{2\pi} \int_{C} A_3(\beta)\, H_I(r\, k_0 \cos\theta \cos\beta)$$

$$\exp(jrk_0 \sin\theta \sin\beta)\; k_0 \cos\beta \, d\beta \qquad (A.I3)$$

Taking approximate value of Hankel function of the integrand of equ. (A.I3) for large value of r, we have

$$H_{\phi}(r,\theta) = \frac{I}{\pi} \int_{C} A_3(\beta)\, e^{-j(3\pi/4)} \left(\frac{k_0}{2\pi r \cos\theta}\right)^{I/2} (\cos\beta)^{I/2}$$

$$e^{jk_0 r \cos(\beta-\theta)}\, d\beta, \text{for } k_0 r \gg I \qquad (A.I4)$$

The saddle point of this integral is given by

$$\frac{d}{d\beta} \cos(\beta - \theta) = 0$$

which gives $\beta = 0$ as saddle point. The steepest descent path (S. D. P.) is given by the constant phase of the exponential factor of the integrand of equation (A.I4) and it is to pass through the saddle point. So we have, $\operatorname{Im} j \cos(\beta - \theta) =$ constant and which is to pass through $\beta = 0$ giving

$$\cos(\beta - \theta) \cos h\psi = I$$

$$\sin\left(\beta + \frac{\pi}{2} - \theta\right) \cos h\psi = I.$$

Applying the standard method (given in Appendix D) of saddle point integration, the lowest order approximation of the integral is given as,

$$H_{\phi}(r,\theta) = -j\left(\frac{\epsilon_0}{\mu_0}\right)^{1/2} \frac{k_0 a \epsilon_3}{\pi} F(\theta) \frac{e^{jk_0 \vec{r}}}{\vec{r}} \qquad (A.16)$$

where

$$F(\theta) = \frac{J_1(k_0 a v)}{\left\{(k_0 b v)\, J_0(k_0 b v)\, H_1(k_0 b \cos\theta) - \epsilon_3 (k_0 b \cos\theta)\, J_1(k_0 b v)\, H_0(k_0 b \cos\theta)\right\}}$$

$$v = \sqrt{\left(\epsilon_3 - \frac{\epsilon_3}{\epsilon_1} \sin^2\theta\right)}$$

$H_{\phi}(r, \theta)$ gives the radiation field in free space.

* * *

APPENDIX -B.

ANALYSIS OF THE AXIALLY MAGNETIZED PLASMA COLUMN HAVING CENTRAL CONDUCTOR:

The configuration analyzed is shown in fig. 3.I. For TM_{0I} mode, the inhomogeneous wave equation for H_ϕ may be written as

$$\frac{\partial^2 H_\phi}{\partial \rho^2} + \frac{I}{\rho} \frac{\partial H_\phi}{\partial \rho} - \frac{I}{\rho^2} H_\phi + \frac{\epsilon_3}{\epsilon_I} \frac{\partial^2 H_\phi}{\partial z^2} + k_0^2 \epsilon_3 H_\phi =$$

$$= - j\omega\epsilon_0\epsilon_3 \, \delta(\rho - a) \, \delta(z)$$

The method of Fourier Transforms as described in Appendix A is used. The solution of the Bessel's equation (A.8) in different regions will be as follows,

$$h = A_I J_I(\nu_I \rho) + B_I Y_I(\nu_I \rho), \quad \text{for } a_I < \rho < a$$

and for $a < \rho < b$

$$h = A_2 J_I(\nu_I \rho) + B_2 Y_I(\nu_I \rho)$$

and for $\rho > b$

$$h = A_3 H_I(\nu_0 \rho)$$

where $\nu_I = \sqrt{(k_0^2 \epsilon_3 - \frac{\epsilon_3}{\epsilon_I} \xi^2)}$

$$\nu_0 = \sqrt{(k_0^2 - \xi^2)}$$

For this configuration, the boundary conditions on h and $dh/d\rho$ at $\rho = a_I$, a and b will be,

$$-\frac{I}{j\omega\epsilon_0\epsilon_3}\left(\frac{dh}{d\rho}+\frac{h}{\rho}\right)\Bigg|_{a_I+\Delta} = 0$$

$$h\Bigg|_{a-\Delta} = h\Bigg|_{a+\Delta}$$

$$\frac{dh}{d\rho}\Bigg|_{a-\Delta}^{a+\Delta} = -j\omega\epsilon_0\epsilon_3$$

$$h\Bigg|_{b-\Delta} = h\Bigg|_{b+\Delta}$$

$$\epsilon_3\frac{dh}{d\rho}\Bigg|_{b+\Delta} - \frac{dh}{d\rho}\Bigg|_{b-\Delta} + (\epsilon_3 - I)\frac{h}{\rho}\Bigg|_{b+\Delta} = 0$$

Applying all these boundary conditions on the solution of equ. (A.9) in different regions, we will have five equations with five constants. Solving the value of A_3 from these equations, we have

$$A_3 = \frac{j\omega\epsilon_0\epsilon_3\, a * A}{\left[(\nu_I b)\, H_I(\nu_o b)\, B - \epsilon_3\,(\nu_o b)\, H_0(\nu_o b)\, C\right]}$$

where

$$A = \left[J_0(\nu_I a_I)\, Y_I(\nu_I a) - Y_0(\nu_I a_I)\, J_I(\nu_I\, a) \right]$$

$$B = \left[J_0(\nu_I a_I)\, Y_0(\nu_I b) - Y_0(\nu_I a_I)\, J_0(\nu_I\, b) \right]$$

$$C = \left[J_0(\nu_I a_I)\, Y_I(\nu_I b) - Y_0(\nu_I a_I)\, J_I(\nu_I\, b) \right]$$

The solution in free space is

$$h\,(\,\rho, \xi\,) = A_3\, H_I(\nu_0\, \rho)$$

inverting it, we have

$$H_\phi\,(\rho,\ z) = \frac{I}{2\pi} \int_{-\infty}^{+\infty} A_3\, H_I(\nu_0\, \rho)\, e^{j\xi z}\ \ dz$$

Now calculating the radiation field (as in Appendix A), the expression for H_ϕ (r, 0) will be as given by equ. (3.I.3).

* * *

APPENDIX -C.

ANALYSIS OF AN AIR GUIDE HAVING CENTRAL CONDUCTOR AND SURROUNDED BY ANNULAR AXIALLY MAGNETISED PLASMA COLUMN:

The configuration analysed is shown in fig. 4.I. For TM_{oI} mode, the inhomogeneous wave equation for H_ϕ may be written as

$$\frac{\partial^2 H_\phi}{\partial \rho^2} + \frac{I}{\rho} \frac{\partial H_\phi}{\partial \rho} - \frac{I}{\rho^2} H_\phi + \frac{\epsilon_3}{\epsilon_I} \frac{\partial^2 H_\phi}{\partial z^2} + k_o^2 \epsilon_3 H_\phi =$$

$$= -j\omega\epsilon_o\epsilon_3 \, \delta(\rho - a) \, \delta(z)$$

Method of Fourier-Transforms as described in Appendix A is used. Now as shown in fig. 4.I region between $\rho = a_I$ to $\rho = a$, is denoted as region I, between $\rho = a$ to $\rho = a_2$, as region II, between $\rho = a_2$ to $\rho = b$, as region III and the region for which $\rho > b$ as region IV. The solution of equ. (A.9) in region I is given as

$$h = A_I \, J_I(\nu_a \rho) + B_I \, Y_I(\nu_a \rho)$$

where $\nu_a^2 = k_I^2 - \xi^2$, and $k_I^2 = w^2 \mu_o \epsilon_o \epsilon_a$

In region II is given as

$$h = A_2 J_I(\nu_a \rho) + B_2 \, Y_I(\nu_a \rho)$$

In region III is as given as

$$h = A_3 \, J_I(\nu_I \rho) + B_3 \, Y_I(\nu_I \rho)$$

where $\nu_I^2 = k_o^2 \, \epsilon_3 - \left(\frac{\epsilon_3}{\epsilon_I}\right) \xi^2$

and for $\rho > b$

$$h = A_4 H_1(\nu_0 \rho)$$

where $\nu_0^2 = k_0^2 - \xi^2$

For this configuration, the boundary conditions on h and $dh/d\rho$ at $\rho = a_1$, a, a_2 and b will be

$$-\frac{1}{j\omega\epsilon_0\epsilon_a}\left(\frac{dh}{d\rho} + \frac{h}{\rho}\right)\Bigg|_{a_1+\Delta} = 0.$$

$$h\Big|_{a-\Delta} = h\Big|_{a+\Delta}$$

$$\frac{dh}{d\rho}\Bigg|_{a+\Delta} - \frac{dh}{d\rho}\Bigg|_{a-\Delta} = -j\omega\epsilon_0\epsilon_a$$

$$h\Big|_{a_2-\Delta} = h\Big|_{a_2+\Delta}$$

$$\frac{\epsilon_a}{\epsilon_3}\frac{dh}{d\rho}\Bigg|_{a_2+\Delta} - \frac{dh}{d\rho}\Bigg|_{a_2-\Delta} + \left(\frac{\epsilon_a}{\epsilon_3} - 1\right)\frac{h}{\rho}\Bigg|_{a_2+\Delta} = 0$$

$$h \Big|_{b-\Delta} = h \Big|_{b+\Delta}$$

$$\varepsilon_3 \frac{dh}{d\rho} \Big|_{b+\Delta} - \frac{dh}{d\rho} \Big|_{b-\Delta} + (\varepsilon_3 - I) \frac{h}{\rho} \Big|_{b+\Delta} = 0$$

Applying all these boundary conditions on the solutions in different regions , we will have seven equations with seven constants. The value of A_4 can be calculated in a similar way as in Appendix A. The solution in free space is

$$h (\rho, \xi) = A_4 H_I(\nu_0 \rho)$$

inverting it we have

$$H_\phi(\rho, z) = \frac{I}{2\pi} \int_{-\infty}^{+\infty} A_4 H_I(\nu_0 \rho) e^{j\xi z} dz$$

Now calculating the radiation field (as in Appendix A), the expression for H_ϕ (r, θ) will be as given by equ. (4.I.3)

…

APPENDIX -D.

SADDLE POINT INTEGRATION METHOD:

Representation in the steepest descent plane involves a transformation

$$\xi = k_0 \sin \beta \qquad (D.I)$$

with

$$\beta = \lambda + j\psi \qquad (D.2)$$

This transformation will map the two-sheated ξ - plane into a connected strip of the β-plane as shown in fig. D.2. It is noticed that each of the eight quardants in ξ - plane (fig. D.I) transforms into a half strip identified by means of T(top) or B (bottom), and the quadrant number . The path of integration about the branch cut in ξ - plane then maps into path in the β-plane. The path of integration is next deformed into the path of steepest descent, shown as SDP in fig. D.2, its equation is given by

$$\operatorname{Re} \cos (\beta-\theta) = \cos (\lambda - \theta) \cos \psi = I \qquad (D.3)$$

The latter path goes through the 'saddle-point' at $\beta = \theta$, θ being a polar angle as shown in fig. 2.I. For integration over the SDP, the integral (equ. A. IO) may be written as

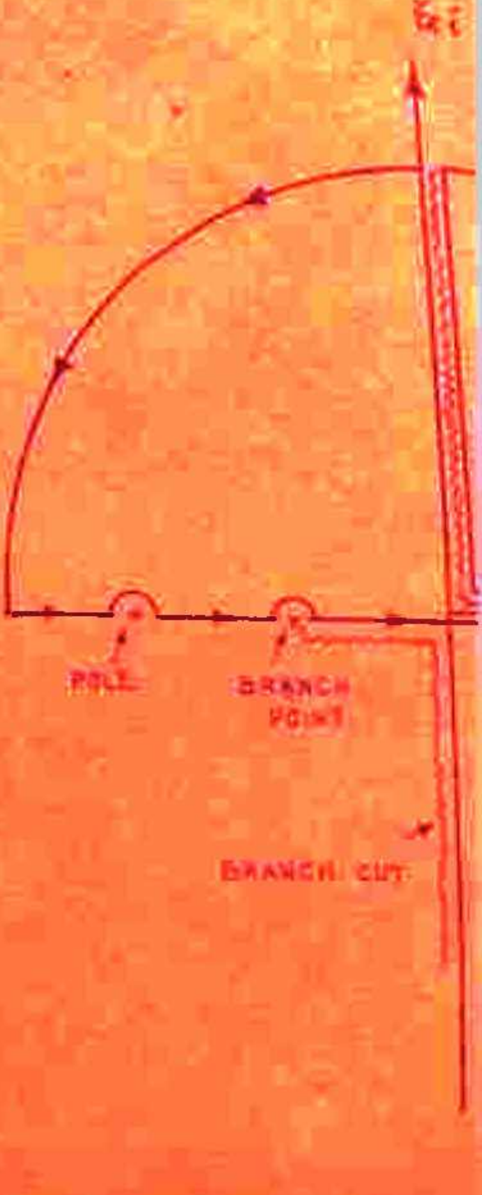
POLE
BRANCH POINT
BRANCH CUT

FIG. D

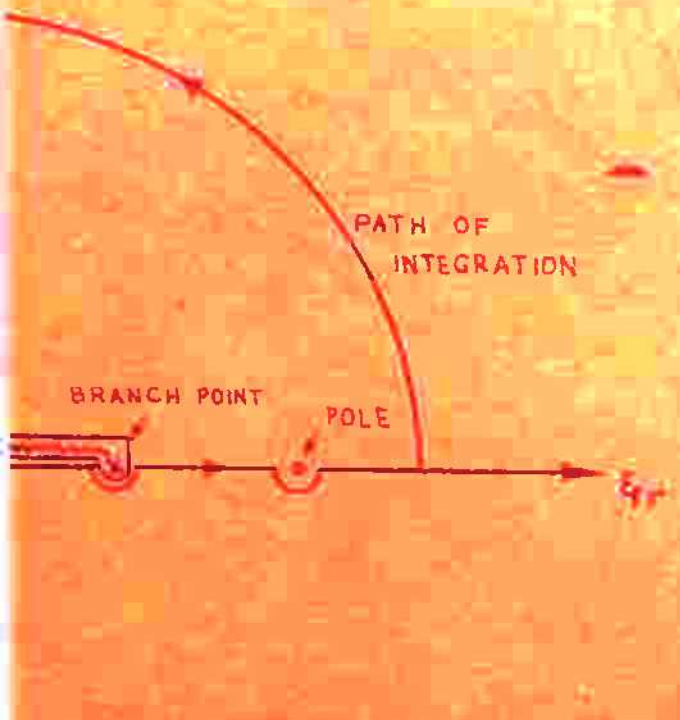
PATH OF INTEGRATION
BRANCH POINT
POLE
ξr

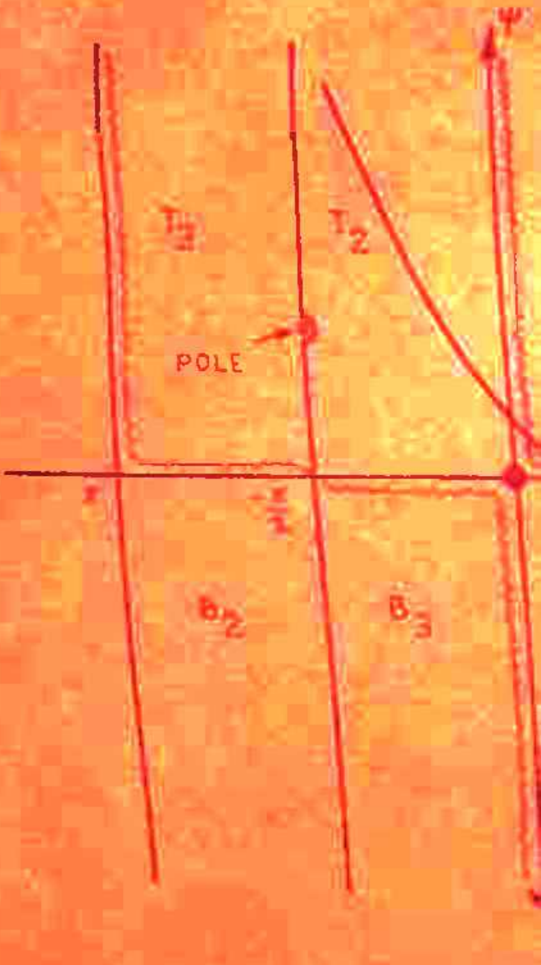

ψ
T_3
T_2
POLE
π
$\frac{\pi}{2}$
B_2
B_3

FIG D.2

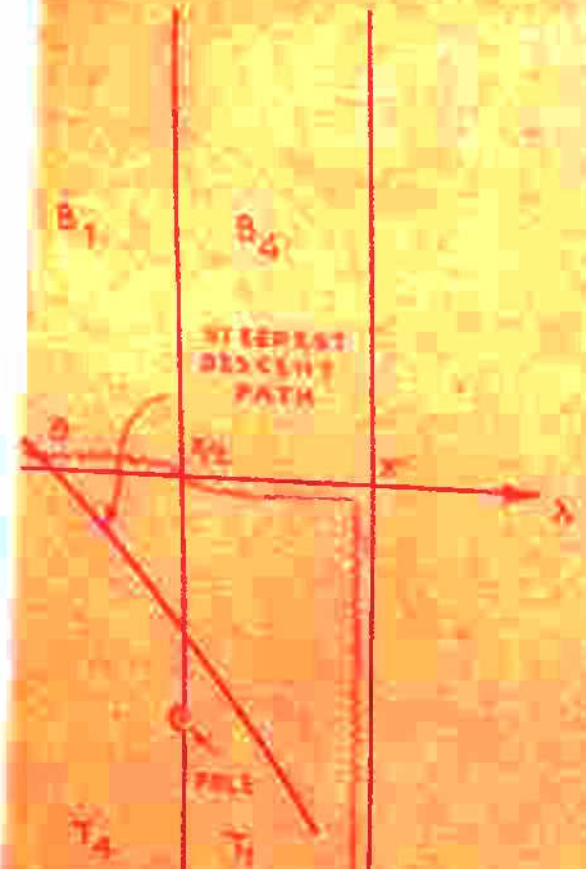
B1
B4
STEEPEST
DESCENT
PATH
θ
π/2
x'
x
POLE
T4
T1
BRANCH
CUTS

$$F_s(r,\theta) = \int_{SDP} F(\beta) \exp\left\{ jk_o r \cos(\beta-\theta) \right\} d\beta \qquad (D.4)$$

To evaluate the integral we choose a transformation

$$\cos(\beta - \theta) = I + ju^2 \qquad (D.5)$$

where u is purely real. The integration will now run along the real values of u ($-\infty < u < \infty$) and equation (D.4) is transformed as

$$F_s(r,\theta) = \int_{-\infty}^{+\infty} L(u) \exp(-k_o r u^2)\, du \qquad (D.6)$$

where

$$L(u) = F(\beta) \exp(jk_o r) \frac{d\beta}{du}$$

For $k_o r >> I$, assuming that $L(u)$ is a well behaved and slowly varying function, the integral is given by the asymptotic approximation as

$$F_s(r,\theta) \simeq \sqrt{\frac{\pi}{k_o r}} \quad L(u) \Big|_{u=0}$$

At $u = 0$, $\beta = \theta$, we have

$$\frac{d\beta}{du}\Big|_{u=0} = -\frac{2ju}{\sin(\beta-\theta)}\Big|_{u=0} = -\frac{2j}{\frac{d\beta}{du}}\Big|_{u=0}$$

hence

$$\frac{d\beta}{du}\Big|_{u=0} = \sqrt{(-2j)}$$

making these substitutions,

$$F_s(r,\theta) \simeq \sqrt{\left(\frac{2\pi}{k_0 r}\right)}\; F(\theta) \exp\left\{j\left(k_0 r - \frac{\pi}{4}\right)\right\}, \quad F(\theta) \neq 0 \qquad (D.7)$$

If however, $F(\theta) = 0$ at $\theta = \theta_0$, $L(u)$ is expanded first in Taylor's series in the neighbourhood of $u = 0$,

$$L(u) = uL'(0) + \frac{u^2}{2} L''(0) + \ldots.$$

$$F_s(r,\theta) = \frac{L''(0)}{4} \sqrt{\frac{\pi}{(k_0 r)^3}} + O(k_0 r)^{-5/2}$$

Evaluating the second derivative of $L(u)$

$$L''(u) = \exp(jk_0 r) \left[F''(\beta) \left(\frac{d\beta}{du}\right)^3 + 3\, F'(\beta) \frac{d\beta}{du} \cdot \frac{d^2\beta}{du^2} + \right.$$
$$\left. + F(\beta) \frac{d^3\beta}{du^3} \right]$$

At $u = 0$, $\beta = \theta_0$, $F(\theta_0) = 0$ and $\frac{d^2\beta}{du^2} = 0$, only the first terms remains. Substituting of $\frac{d\beta}{du} = \sqrt{-2j}$. yields,

$$F_s(r,\theta) \simeq \frac{1}{2} \sqrt{\frac{2\pi}{(k_0 r)^3}}\; F''(\theta_0) \exp\left\{j(k_0 r + \pi/4)\right\}, F(\theta_0) = 0.$$

The method of saddle point integration is given in detail in standard texts[46-48]. The analysis carried out here is valid when poles are not very close to the saddle point. If poles are located very close to the saddle point t on the saddle point integration method is to be modified to include their effect[49-50].

• • •

LIST OF REFERENCES

I. Hodara, H. and Cohn, G.I. (I962), Radiation from a gyro-plasma coated magnetic line source, IRE Trans. Ant. Prop., AP- IO, No. 5, 58I- 593.

2. Hodara, H. (I963), Radiation from a gyro-plasma sheathed aperture, IEEE Trans. Ant. Prop., AP-II, No. I, 2-I2.

3. Shore, R. and Meltz, G. (I962), Anisotropic plasma covered magnetic line source, IRE Trans. Ant. Prop., AP- IO, No. I, 78- 82.

4. Chen, H. C. and Cheng, D. K. (I965), Radiation from axially slotted anisotropic plasma clad cylinder, IEEE Trans. Ant. Prop., AP-I3, No. 3, 395- 40I.

5. Meltz, G. and Shore, R. A. (I965), Leaky waves supported by uniaxial plasma layers, IEEE Trans. Ant. Prop., AP- I3, No. I, 94- I05.

6. Pachyanski, M. P. and Gibbs, G. W. (I968), Antenna radiation properties in presence of anisotropic plasmas, Radio Science, 3, No. 9, 920- 935.

7. Harris, J. H. (I963), Radiation through cylindrical plasma sheaths, J. Res. NBS 67D (Radio Prop.), No. 6, 7I7 - 733.

8. Harris, J. H., A. T., Villeneuve and Rypoca, L. A. (I965), Radiation patterns from plasma enclosed cylindrical hypersonic vehicles, Radio Science, J. Res. NBS 69D, No. IO, I335 - I343.

9. Gupta, K. C. (I97), A multiple narrow beam antenna system using a column of isotropic plasma, Int. J. Electronics, 29, No. I, 45 - 53.

IO. Gupta, K. C. and Garg, R. K. (I97I), Antenna using cylindrical columns of isotropic plasma, Research report I.I.T., Kanpur/[illegible]/7I, 3 - I2.

II. Dhani Ram and Verma, J. S. (I972), Electronically scannable narrow beam antenna system using isotropic plasma column having central conductor along the axis and excited by magnetic ring source, Ind. J. of Pure and Applied Physics, IO, No. IO, 716 - 720.

I2. Dhani Ram and Verma, J. S. (I973), Electronically scannable narrow beam plasma antenna system, Int. J. Electronics, 34, No. 6, 83I - 836.

I3. Bunkin, F. V. (I957), On radiation in anisotropic media, Soviet Physics JETP (Eng. Trans.), 5, No. 2, 277 - 283.

I4. Kogelnik, H. (I960), On electromagnetic radiation in magneto-ionic media, J. Res. Nat. Bureau Stds 64D, No. 5, 5I5 - 523.

I5. Kuehl, H. (I962), Electromagnetic radiation from an electric dipole in a cold anisotropic plasma, J. Phys. Fluids, 5, No. 9, I095 - II03.

I6. Arbel, E. and Felsen, L. B. (I963), Electromagnetic waves Pt. I Edited by E. C. Jordan (Pergamon Press, New York), pp. 39I- 459.

I7. Felsen, L. B. (I964), Radiation from plasmas, J. Res. NBS 68D, No. 4, 480 - 485.

I8. Bachynski, M. P. (I967), Sources in plasma, RCA review, 28, III - I52.

I9. Wait, J. R. and Brackett, E. A. (I967), Bibliography on waves in plasma, ESSA Tech. Rept. IER3I - ITSA 39.

20. Newstin, M. and Lurye, J. (I956), The fields of a magnetic line source in the presence of a layer of complex refractive index, Tech. Res. Group Scientific Rept. No. I .

2I. Tamir, T. and Oliner, A. A. (I962), The influence of complex waves on the radiation field of a slot excited plasma layer, IRE Trans. Ant. Prop, AP-I0, No. I, 55-65.

22. Harris, J. H. (I968), Leaky wave beam of multiply layered plasma media, Radio Science, 3, No. 2, I8I-I89.

23. Wait, J. R. (I96I), The electromagnetic field of dipole in the presence of thin plasma sheet, Appl. Sci. Res. Sec. B, 8, 307- 417.

24. Yip, G. L. and Seshadari, S. R. (I967), Surface wave along an axially magnetized plasma column - Symmetric modes, Can. J. Phys., 45, No. 9, 2889- 2907.

25. Yip, G. L. and Seshadari, S. R. (I967), Radiation from an electric dipole in an axially magnetized plasma column- Dipolar modes, Can. J. Phys., 45, No. II, 3627- 3648.

26. Gupta, K. C. and Singh, A. (I967), Excitation of electromagnetic waves on a plasma column by a ring source outside the plasma, Int. Jour. Electronics, 23, No. 4, 323 - 328.

27. Gupta, K. C. and Singh, A. (I967), Excitation of bulk-wave on columns of magnetized plasma, Int. Jour. Electronics, 23, No. 5, 433 - 44I.

28. Samaddar, S. N. and Yildiz, M. (I964), Excitation of coupled electro-acoustic waves by a ring source in a compressible plasma cylinder, Can. J. Phys., 42, No. 4, 638 - 656.

29. Samaddar, S. N. (1964), Wave propagation in an anisotropic column with a ring source excitation Part I, Jour. Electronics and Control, 16, No. 3, 273-303.

30. Kislov, V. J. and Bogdanov, E. V. (1961), Proc. Symp. Electromagnetic and Fluid dynamics of Gaseous plasma, Polytechnic Institute of Brooklyn, 249 - 268.

31. Duncan, J. W. (1959), The efficiency of excitation of a surface wave on a dielectric cylinder, IRE Trans. MTT- 7, No. 4, 257 - 268.

32. Yeh, C. and Rusch, W. V. T. (1965), Interaction of microwaves with an inhomogeneous and anisotropic plasma medium, J. Appl. Phys., 36, No. 7, 2302-2306.

33. Samaddar, S. N. (1963), Wave propagation in a cylindrical wave guide containing inhomogeneous plasma involving a turning point, Can. J. Phys., 41, No. 1, 113-131.

34. Samaddar, S. N., (1965), An approach to improve re-entry communications by suitable orientation of antenna and static magnetic field, Radio Science 69D, No. 6, 851- 863.

35. Swift, C. T. (1964), Radiation patterns of a slotted cylinder antenna in the presence of an inhomogeneous lossy plasma, IEEE Trans. Ant. Prop., AP-12, No. 6, 728- 738.

36. Rotman, [illegible]. and Meltz, G. (1961), Experimental investigation of the electromagnetic effects of re-entry, USAF Cambridge Research Center, Bedford, Mass, Tech. Rept. AFCRL 67.

37. Bachynski, M. P. and Gibbs, [illegible]. (1966), Propagation in plasma along the magnetic field I- Circular polarization, Phys. Fluids, 9, 3, 520- 531.

38. Chynoweth, A. G. and Buchsbaum, [illegible]. J. (1965), Solid state plasma, Physics Today, 18, No. 11, 26-36.

39. Collin, R. E. (1958), A simple artificial anisotropic dielectric medium, IRE Trans. MTT-6, No. 4, 206-209.

40. Bachynski, M. P. and Graf, K. A. (1964), RCA Review, 25, 3 - 54.

41. Smith, T. H. and Golden, K. E. (1965), Radiation patterns from a slotted cylinder surrounded by a plasma sheath, IEEE Trans. Ant. Prop., AP-13, No. 5, 775 - 781.

42. Vantrier, A. A. Th. M. (1953), Guided electromagnetic waves in anisotropic media, Appl. Sci. Research B, 3, 4 - 5, 305 - 309.

43. Suhl, H. and Walker, L. R. (1954), Topics in guided wave propagation through gyromagnetic media, B.S.T.J., 33, Part I 579-639, Part II 939-986, Part III 1133-1194.

44. Epstein, Paul S. (I956), Theory of wave propagation in a gyromagnetic medium, Rev. Mod. Phys., 28, No. I, 3 - I7.

45. Gurevich, A. G. (I963), Ferrites at microwave frequencies, (Heywood and Company Ltd., London).

46. Collins, R. E. (I960), Field theory of guided waves, (Mc Graw-Hill, New York), 485-490.

47. Morse, M. P. and Feshbach, H. (I953), Methods of theoretical physics, (Mc Graw-Hill, New York), 437-443.

48. Tyras, G. (I969), Radiation and propagation of electromagnetic waves, (Academic Press, New York), II8-I29.

49. Vander Waerden, B. L. (I95I), On method of saddle points, Appl. Sci. Res. B, 2, 33 - 40.

50. Oberhettinger, F. (I959), On modification of watson's lemma, Nat. Bur. Std. J. Res. 64B, I5 - I7.

***

LIST OF PUBLICATIONS

I. Joshi, N. K. and Verma, J. S., 'A narrow beam antenna system using an air column having a central conductor and surrounded by an anisotropic plasma column', to be published in Radio Science (U. S. A.), January, 1975.

2. Joshi, N. K. and Verma, J. S., 'Radiation from axially magnetized plasma column', presented in Indian Rocket Society Symposium on Space Science and Technology (from 24th Sept. 1973 to 26th Sept. 1973 in Trivandrum).

3. Joshi, N. K. and Verma, J. S., 'Electronically scannable narrow beam plasma antenna system', accepted for publication in NTZ Communication Journal (West Germany).

4. Joshi, N. K. and Verma, J. S., 'Scattering of a plane electromagnetic wave from a conducting cylinder coated with three annular anisotropic plasma columns of different densities', to be published in JIETE (New Delhi), February 1974.

5. Joshi, N. K. and Verma, J. S., 'Radiation from an annular axially magnetized inhomogeneous plasma column', presented in Indian Science Congress Session (from 3.I.74 to 9.I.74 in Nagpur).

6. Joshi, N. K. and Verma, J. S., 'Radiation field of a magnetic ring source surrounded by an inhomogeneous axially magnetized plasma column', Communicated to Journal of Applied Scientific Research, The Netherlands.

7. Joshi, N. K. and Verma, J. S., 'Radiation from a magnetic ring source surrounded by axially magnetized plasma column', Communicated to International Journal of Electronics, London.

8. Joshi, N. K. and Verma, J. S., 'Enhanced radiation from axially magnetized plasma column having central conductor and excited by magnetic ring source', Communicated to Indian Journal of Pure and Applied Physics(New Delhi).

9. Joshi, N. K. and Verma, J. S., 'Enhanced radiation from axially magnetized plasma column having central conductor and excited by open ended coaxial line, Communicated to Indian Journal of Pure and Applied Physics (New Delhi).